THE CALIBRATION OF A PARABOLIC ANTENNA WITH THE AID OF CLOSE-RANGE PHOTOGRAMMETRY AND SURVEYING

S. J. JODOIN

August 1987

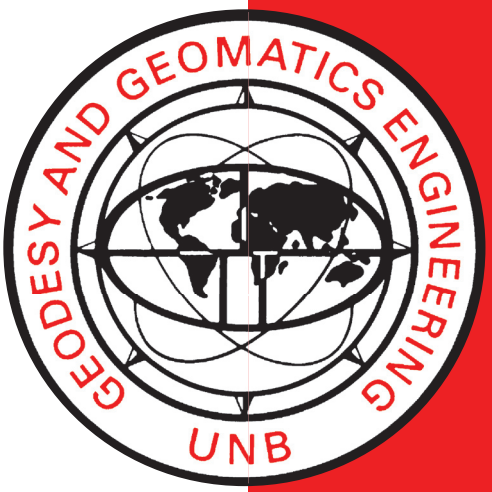

TECHNICAL REPORT
NO. 130

PREFACE

In order to make our extensive series of technical reports more readily available, we have scanned the old master copies and produced electronic versions in Portable Document Format. The quality of the images varies depending on the quality of the originals. The images have not been converted to searchable text.

THE CALIBRATION OF A PARABOLIC ANTENNA WITH THE AID OF CLOSE-RANGE PHOTOGRAMMETRY AND SURVEYING

by

Captain Steven John Jodoin

Department of Surveying Engineering
University of New Brunswick
P.O. Box 4400
Fredericton, N.B., Canada E3B 5A3

August 1987

PREFACE

This report is an unaltered version of the author's M.Eng. report submitted to the Department of Surveying Engineering under the same title in August of 1987.

The advisor of this work was Dr. Wolfgang Faig, whose assistance was highly appreciated. The Department of National Defence is also acknowledged for providing the author with the necessary time to complete studies at U.N.B.

The assistance rendered by others is given in detail in the acknowledgements of the author's M.Eng. report.

ABSTRACT

In recent years, close-range photogrammetry and surveying have been applied in many industrial applications to analyse complex shapes. In particular, these two mensuration techniques have been applied to antenna reflector calibration, receiving widespread acceptance. The purpose of this report is to investigate the suitability of non-metric analytical photogrammetry for reflector antenna calibration through the comparison of results with those obtained using precision surveying with electronic theodolites.

This study begins with an examination of the requirements for the calibration of reflector antennas. A one-metre parabolic weather satellite reflector was evaluated in this investigation. The planning and preanalysis considerations for both photogrammetry and surveying are discussed. Since the data acquisition and reduction techniques differ for each method, analytical close-range photogrammetry is further examined.

With the assistance of three software packages designed for non-metric photography, object space coordinates were determined on the reflector antenna. The bundle adjustment programs UNBASC2 and GEBAT-V as well as the Direct Linear Transformation with Data Snooping were evaluated and compared.

The computed object coordinates were used to determine, using the method of least squares, the best fitting paraboloid which defines the parabolic reflector under consideration. An evaluation of the surface

parameters and deviations from the ideal paraboloid are considered in the final calibration. SAS/GRAPH software was used to provide a 3-dimensional representation of the surface and detected deviations.

The results of this investigation illustrate that close-range photogrammetry can be used to accurately determine spatial coordinates for the purpose of calibrating reflector antennas. Furthermore, the potentials and limitations of non-metric imagery have been observed and recommendations for its use in industrial applications are proposed.

TABLE OF CONTENTS

PAGE

LIST OF FIGURES

LIST OF FIGURES (Cont'd)

LIST OF TABLES

LIST OF NOTATIONS

A	: First Design Matrix
$\bar{A}$	: Coefficient Matrix of Quadratic Form
α_A, α_B	: Horizontal Angles used in Base Angular Intersection
B	: Second Design Matrix
b	: Theodolite Base Distance
β_A, β_B	: Vertical Angles Used in Base Angular Intersection
C	: Critical Value for a Specific Confidence Level in Data Snooping Test.
c	: Camera Constant or Calibrated Focal Length
D	: Diameter of Aperture of Antenna
D_{min}	: Minimum Diameter of Photogrammetric Target Dot
DOF	: Depth of Field
d	: Size of Measuring Mark (e.g. Zeiss PSK Stereo Comparator 20 μm)
Δh	: Height Difference Between Two Theodolites
Δx_p	: x Compensation Term for Systematic Errors
Δy_p	: y Compensation Term for Systematic Errors
δ	: Vector of Corrections
FFL	: Far Field Limit
FOD	: First-Order Design
f	: Focal Length of Paraboloid Reflector Surface
G	: Antenna Gain (db)
G_{max}	: Maximum Gain (db)
G_0	: No error Gain
η	: Antenna Aperture Efficiency

k_1, k_2, k_3 : Parameters of Radial Symmetric Lens Distortion

$L_1 - L_{11}$: The Eleven Direct Linear Transformation Parameters

$\lambda_1, \lambda_2, \lambda_3$: Eigenvalues or Characteristic Roots of Coefficient Matrix A

λ : Operational Wavelength (mm)

λ_{max} : Wavelength at Which Gain Reaches a Maximum

M : Magnification of Theodolite Telescope

M_{ij} : Elements of Rotation Matrix R

NFL : Near Field Limit

n : Number of Sets of Angular Measurements

P_ℓ : Weight Matrix of Observations

P_x : Weight Matrix of Parameters

π : 3.141 592...(Ratio of the Circumference of a Circle to its Diameter)

q : Antenna Index of Smoothness

P : Matrix of Eigenvalues, U_1, U_2, U_3

W : Misclosure Vector

ρ" : 206265" (Number of Seconds in One Radian)

R : The Rotation Matrix of the Image With Respect to the Object

S : Photo Scale

SOD : Second-Order Design

σ_c : Theodolite Centering Error

σ_ℓ : Theodolite Levelling Error

σ_p : Theodolite Pointing Error

σ_r : Theodolite Reading Error

σ_s : RMS of Effective Surface Deviations

σ_θ	: Combined Standard Deviation for an Observed Angle
$\sigma_{\theta c}$	: Influence of Centering Errors on an Angle Measurement
$\sigma_{\theta \ell}$	: Influence of Levelling Errors on an Angle Measurement
$\sigma_{\theta p}$	: Influence of Pointing Errors on an Angle Measurement
$\sigma_{\theta r}$	: Influence of Reading Errors on an Angle Measurement
σ_x, σ_y, σ_z	: Estimated Standard Deviations of Object Point Coordinates.
T	: Temperature
TOD	: Third-Order Design
V	: Vector of Residuals
w_i	: Standardized Residual at Point i
X_c, Y_c, Z_c	: Coordinates of the Camera Station in the Object Space
X_o, Y_o, Z_o	: Coordinates for Centroid of Best Fitting Paraboloid
X_p, Y_p, Z_p	: Object Space Coordinates of the Point with Photo Coordinates x_p, y_p
x_p, y_p	: Image Coordinates in Image Plane
x_o, y_o	: Image Coordinates of the Principal Point
ZOD	: Zero-Order Design

ACKNOWLEDGEMENTS

I would like to express my gratitude to Dr. Wolfgang Faig for having been my primary advisor for this report. The many hours Dr. Faig spent throughout this investigation providing guidance, constructive criticism and wise counsel have been the sole reason for its timely completion. In particular I wish to thank Dr. Faig for making available many excellent references in close-range photogrammetry.

I am also appreciative of Dr. E. Derenyi and Dr. S.E. Masry for their lectures which stimulated my interest in the many potentials of photogrammetry. I must acknowledge Dr. A. Chrzanowski whose lectures in engineering surveying have provided many insights into the particular requirements of deformation surveys.

Without reservation I am appreciative for having been able to become involved with the Photogrammetry and Engineering Surveying Groups at UNB. Many fruitful discussions with the graduate students of these groups have proven invaluable in the completion of this report.

Finally, I express my deepest thanks to my wife Susan for her constant encouragement and understanding. Susan not only typed the manuscript but helped keep our home (and myself) together during the writing of this report.

CHAPTER 1

INTRODUCTION

Reflector antennas have been used since the radio pioneering era of Hertz, Lodge and Marconi in the latter part of the 19th century when electromagnetic wave theory, first predicted theoretically by James Maxwell, was demonstrated experimentally. While an antenna can be any conducting structure which efficiently converts electromagnetic energy from a guided wave (voltages and currents along a transmission line) to an unguided or free space wave (radiating electric and magnetic fields), a reflector antenna belongs to that group of antenna structures which is derived from conic sections. The surfaces of reflector antennas are usually generated by rotating a conic section around a focal axis to produce a surface of revolution. Such surfaces are utilized in various operating environments, ranging from radio to optical frequencies.

The primary development of reflector antennas blossomed with the advent of radar during the Second World War. In the late 1940's and early 1950's design principles were refined and prime focus feed systems were established. Cassegrain, or secondary focus systems, and horn reflectors came into prominence in the early 1960's with the advent of satellite tracking and space communication networks.

Reflector antennas come in various sizes ranging from one-metre in diameter for satellite communications to large radio telescopes of hundreds of metres in diameter used for radio astronomy and space communications. The Arecibo radar-radio telescope located in Puerto Rico is the world's largest reflector at 305 metres in diameter.

In recent years, studies in reflector antenna theory have centered

around the desire to maximize the gain, or gain/temperature ratio (G/T), particularly for large, expensive reflectors. In order to do this, it is necessary to increase aperture efficiency. Surface deviations adversely affect gain and therefore surface accuracy requirements in the manufacture of antennas has become correspondingly more constrained. In the past twenty years there has been an evergrowing need to address the problem of measuring the surface of reflector antennas. This process is known as "reflector calibration" and can be envisioned as a form of deformation analysis of reflector surfaces.

Numerous techniques have been developed to precisely measure antenna surfaces. These include various forms of direct measurement (Anderson and Groth, 1963), the use of conventional surveying techniques, and the utilization of laser equipment in the alignment of antenna surface components. Analytical photogrammetry has been found particularly suitable for the mensuration of antennas of all sizes and under all operational circumstances. In this report, the use of analytical close-range photogrammetry for the calibration of reflector surfaces is considered together with modern precision surveying.

1.1 Close-Range Precision Photogrammetry

The application of analytical photogrammetry to various precision engineering mensuration tasks has received widespread acceptance in the past two decades. Although often overlooked as a data acquisition source, applications in close-range photogrammetry are now practical for many diversified studies (eg. Architecture, Medicine, Archaeology and Industry). With possible sources of imagery ranging from electron

microscopes in a laboratory setting to metric cameras used in outer space, any object can be considered provided it is capable of being photographed. Subsequent point mensuration and analysis can then be performed to arrive at 3-dimensional object coordinates.

The analytical reconstruction of the bundles of rays from image coordinate readings in comparators or analytical plotters make close-range photogrammetry viable for many applications. Photogrammetric instrumental developments and the general automation of the data reduction process, sponsored by digital computer advances and ever-increasing availability, have resulted in more rapid problem-solving packages for engineering problems.

As there are no longer any restrictions to the central projection, any camera type with any orientation in space can be used with the newest analytical reduction techniques. This clears the way for increased utilization of non-metric imagery which is inexpensive and readily available. Analytical methods have also opened vast avenues for the integration of photogrammetric and geodetic observations during the analysis of results.

Close-range photogrammetry (CRP) is commonly referred to in conjunction with object-to-camera distances of not more than 300 metres (Karara, 1979). The outcome of such mensuration processes is the same as for close-range surveys of all types, that being the determination of unique quantities which are derived from three dimensional spatial coordinates, e.g. areas, volumes or distances. In the realm of reflector antenna calibration, surface fitting techniques are employed to suitably describe complex shapes and reveal surface deformations.

1.2 Close-Range Precision Surveying with Electronic Theodolites

In recent years, virtually every major manufacturer of surveying instruments has produced a theodolite featuring automatic digital display and readout of angles. These instruments lend themselves to rapid data acquisition. Although developed to enhance geodetic surveys, these instruments are increasingly being employed in industrial and engineering applications. In these applications, electronic theodolites are generally employed in coordinated pairs coupled directly to a portable microcomputer.

In order to reduce the costs of data acquisition, smaller and less expensive microcomputers are being sought to coordinate the measurement of object points. In addition, sophisticated software is being developed to provide greater operational flexibility to this measurement approach.

Electronic theodolites can act as stand-alone measurement devices or serve the photogrammetrist in acquiring rapidly the necessary control for a photogrammetric evaluation. In the industrial setting the combination of surveying and photogrammetry is proving to be the most efficient and rapid way of analysing an object, for quality control purposes, while minimizing interruptions in the manufacturing process.

1.3 Objectives and Scope of this Study

Given that the calibration of reflector antennas has become an increasingly important task, the use of close-range photogrammetry has been selected as the primary measurement technique in this study of reflector surfaces. Recent analytical photogrammetric developments will be utilized. Theoretically the bundle adjustment method yields the

highest accuracy and therefore will provide the primary point densification method for this study. The following objectives have been identified for this report:

a. Literature search:

To conduct a literature review of the techniques and design considerations for analytical, non-metric, close-range photogrammetric evaluations. The Photogrammetric preanalysis and planning considerations will encompass a review of antenna tolerance theory to permit a surface deformation analysis of the antenna under study.

b. Measurements and data acquisition:

This includes close-range surveying and the use of a non-metric camera to acquire convergent photography of an antenna reflector surface. Coordinates of image points will subsequently be measured on a Zeiss PSK-2 Stereocomparator.

c. Data reduction and analytical evaluation:

To this end, two analytical, self-calibrating bundle adjustment solutions will be evaluated; namely UNBASC2 (Moniwa, 1976) and GEBAT-V (El-Hakim, 1979 and 1982). The Direct Linear Transformation Solution with Data Snooping (Chen, 1985) will also be investigated.

d. Evaluation of results:

A two-phase comparison of results will be possible. First a comparison of results using the three photogrammetric program packages. Secondly, a comparison of results obtained by close-range photogrammetry and surveying.

e. Data analysis:

This phase of the project involves the calibration of the antenna reflector. The determination of the surface shape and regularity by a least squares fit of the paraboloid surface to the coordinates will also provide the position of the center of the surface of best fit and the focal length of the reflector. A maximum operational frequency for the antenna can be proposed based on an understanding of surface roughness.

f. Presentation of results:

The utilization of computer graphics to represent the shape and regularity of the reflector. This involves the representation of the measured surface via a 3-dimensional plot and by contours.

An evaluation of the potentials and limitations of both close-range photogrammetry and close-range surveying for the precision surveying demands of reflector antenna calibration will then be possible.

CHAPTER 2

CLOSE-RANGE PHOTOGRAMMETRY IN INDUSTRIAL APPLICATIONS

Industrial photogrammetry involves the use of photogrammetric techniques in an industrial setting. According to Meyer (1973) the potential fields of industrial photogrammetry include

> "building construction, civil engineering, mining, vehicle and machine construction, metallurgy, ship-building and traffic, with their fundamentals and border subjects, manufacture, testing, monitoring, repair and reconstruction. Objects measured by photogrammetric techniques may be solid, liquid, or gaseous bodies or physical phenomena, whether stationary or moving, that allow of being photographed".

This is in no way an all encompassing definition, and one is hardly plausible in such a diverse realm of activity. It should however provide a signal to industry of the potentials of photogrammetry for rapid, flexible, non-contact, spatial measurement. Concerning reflector antennas, whether photogrammetry is used as a quality control approach during manufacture (El-Hakim, 1984) or as a calibration technique for existing reflector antenna surfaces, its use as proposed in this study underscores the potentials for its application in the industrial setting.

2.1 Requirements of Close-Range Industrial Surveys

Although the industrial setting presents a wealth of new applications for both close-range photogrammetry and surveying, it remains that both techniques will not gain general acceptance unless they prove cost effective. Factors vary with each application, however

for each project the measurement process must be defined, the achievable accuracy investigated, direct costs analyzed, and the labour and time requirements carefully considered. Even if photogrammetric techniques are deemed cost effective, the manufacturer must still weigh the delicate balance of performing the photogrammetric analysis "in-house" (and accept the equipment and training costs) or utilize the services of a consulting photogrammetric engineer.

For photogrammetric techniques to be feasible for industrial measurement and inspection tasks a number of data acquisition and reduction considerations must be improved. Karara (1975) points out that point measurement time should be reduced when compared with traditional methods by as much as 90%. In addition, there is a need to develop large format focusable metric cameras and analytical data reduction techniques to provide accurate results quickly. Over the past decade, with the focus primarily on computer technology, attempts have been made to overcome these problems. The Simultaneous Triangulation And Resection System (STARS) developed by Geodetic Services Inc. (Brown, 1982) is an example of a highly accurate, fast processing system for industry requiring little photogrammetric expertise. STARS consists of three major elements: (1) a large format terrestrial camera, (2) a powerful desktop computer system, and (3) a bundle adjustment program with self-calibration optimized for the diverse applications encountered in close-range photogrammetry. Similar systems have been developed specifically for larger automobile and aircraft industries with the impetus being placed on near real-time systems in response to every day industrial measurements.

In this project, due to the nature of the evaluation procedure, a

near real-time response as required in day-to-day industrial applications is hardly expected. However, the same principles are applied and it is important to keep in mind the eventual industrial application of reflector antenna calibration and various ways to optimize the techniques used.

2.2 Review of Antenna Tolerance Theory

The deviations of an antenna reflector from its ideal shape cause, in general, loss of gain and pattern degradation (Zarghamee, 1967). The causes of such deviations may originate from manufacturing and rigging tolerances or they may be temporal in nature and due to causes such as gravity, wind and thermal effects. Just as the development of reflector antenna theory has occurred in a progressive fashion, so has the investigation of tolerance theory and the effects of aperture phase errors on the gain. Tolerance theory probably had its earliest beginnings in the work of such researchers as Spencer and Ruze. (Zarqhamee, 1967)

The gain of an antenna is defined as the difference observed at some distant point between the power radiated isotropically and the same original power radiated by a directive antenna (Love, 1976). This is also referred to as the "effect factor" of the antenna. Mathematically, gain for a parabolic antenna is expressed as:

$$G = \eta \left[\frac{\pi D^2}{\lambda}\right]^2 \cdot \exp\left[-\left(\frac{4\pi\sigma_s}{D}\right)^2 \cdot \left(\frac{D}{\lambda}\right)^2\right] \qquad (2.1)$$

where

G = Gain [db]
η = aperture efficiency
λ = wavelength
D = aperture diameter
σ_s = the RMS deviation of the reflector surface from the ideal paraboloid

The effects of surface deviations on the radiation pattern and gain may be predicted from the actual distribution of surface deviations over the aperture. Ruze (1966) provides a simple approximate method for computing these effects whereby the tolerance of the reflector sets a limit on the highest frequency of operation and therefore on the D/λ (Diameter to Wavelength) ratio.

Figure 2.1 illustrates the important result that for any reflector antenna, there is a wavelength at which the gain reaches a maximum. This wavelength depends on σ_s and is expressed as:

$$\lambda_{max} = 4 \pi \sigma_s \tag{2.2}$$

The provision here is that roughness is randomly distributed in a Gaussian (normal) fashion. Substituting equation 2.2 into equation 2.1, the maximum gain is given by:

$$G_{max} = 20q - 16.3 + 10\log_{10}\eta \quad [db] \tag{2.3}$$

or approximated as:

$$G_{max} \simeq \frac{\eta}{43} \left(\frac{D}{\sigma_s}\right)^2 \tag{2.4}$$

where q is defined as an index of smoothness, defined by:

$$\frac{\sigma_s}{D} = 10^{-q} \tag{2.5}$$

According to Ruze (1966) a similar expression can be derived to express the loss in gain resulting from surface roughness:

$$\frac{G}{G_0} = e^{-(4\pi\sigma s/\lambda^2)} e^{\frac{1}{4}(4\pi\eta o/\lambda^4)} \tag{2.6}$$

where

G_0 = no-error gain
G = gain with phase error
σ_s = RMS of effective surface deviations

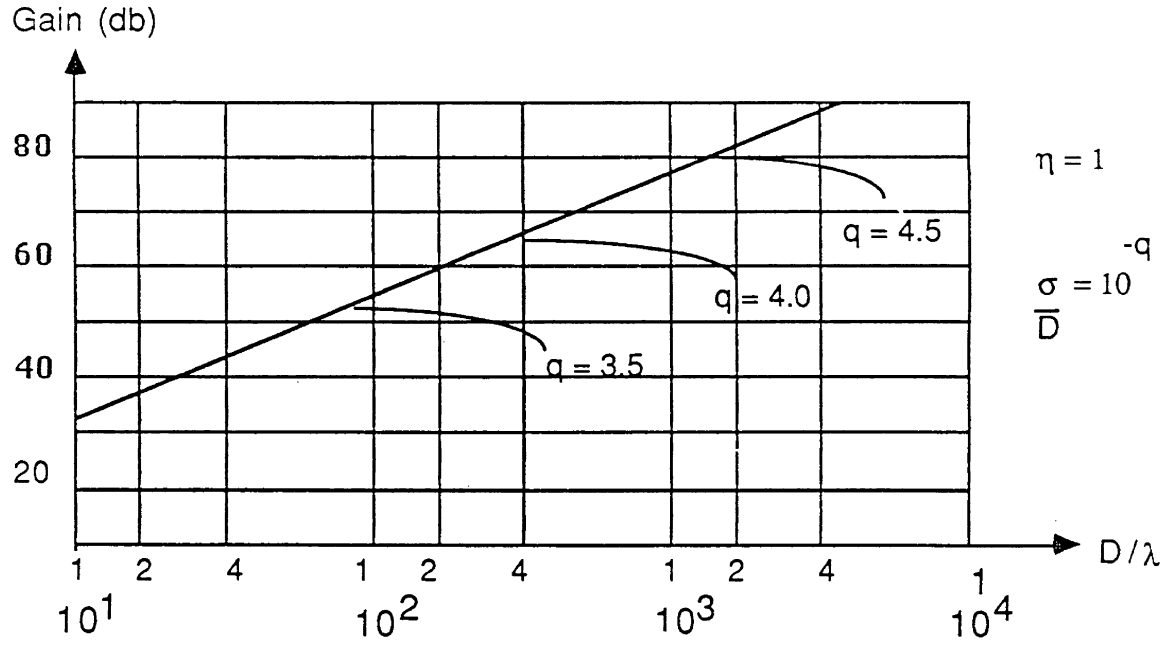

Figure 2.1: The Effect of Reflector Roughness on Antenna Gain (from Love, 1976)

Diagrammatically one could classify the problem as shown in Figure 2.2. In (a) a plane wave front is propagated from a perfect paraboloid while in (b) a grossly exaggerated, distorted wavefront results from an imperfect paraboloid surface.

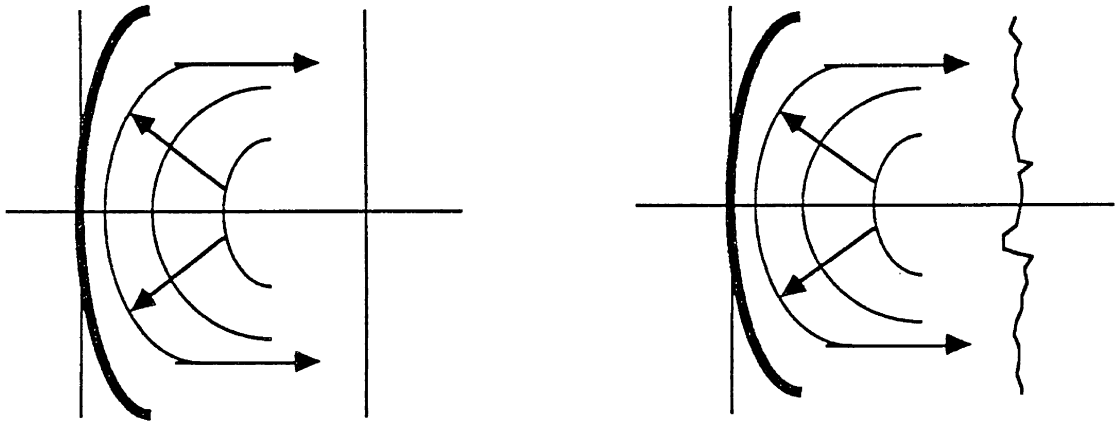

(a) Perfect Paraboloid (b) Imperfect Paraboloid

Figure 2.2: The Problem of Diffraction from an Imperfect Paraboloid (after Ruze, 1966)

It has been estimated that for antenna reflector deformations a one db loss in gain results from the rms phase variation about the mean phase plane of $\lambda/14$. This corresponds in shallow reflectors to surface errors which are greater than $\lambda/28$. For antennas which operate at wavelengths of 10 GHz (3cm), this means the maximum allowable RMS surface errors are 1.07 mm. For the basic spectrum of electromagnetic waves the reader is referred to Appendix I.

2.3 Antenna Mensuration Techniques

In order to verify the antenna surface tolerances, a number of techniques have been attempted in the past two decades. In all methods, however, the procedure involves the verification of some form of measured data with a predicted conic section or quadratic surface in keeping with the fundamentals of antenna tolerance theory. In addition, a linear regression analysis of the experimental data to establish confidence limits provides a convenient and accurate method of determining the surface precision (Ruze, 1966).

One method of measuring reflector surfaces is by means of electrical measurements. Here, the temperature measured on an extended astronomical source (e.g. the moon) is equal to the product of the fractional enclosed power and the source brightness temperature. With no surface errors, practically all the radiated power is enclosed by the source if it is at least several beamwidths in extent. With reflector errors some of the scattered energy is outside of the source and the measured temperature is decreased. This reduction depends on both the RMS surface error and the size of the correlation region of these errors. Using this technique RMS surface errors of 1.5 mm were

found to be detectable (Ruze, 1966).

Another technique which provides rapid and very accurate measurement of distortions on the reflector surface is microwave holography. Holography is unique in that it provides information about the antenna that cannot be measured by any other technique. This technique utilizes the Fourier transform relation between the far-field beam pattern of the antenna and the currents in the aperture of the antenna. Microwave holography determines surface errors proportional to the wavelength of the radiation used for the measurements with an accuracy of about 0.01λ. The complete antenna surface can be evaluated at once and the measurement and presentation of results usually are completed in a few hours. This facilitates the possibility of conducting a series of measurements to rapidly monitor thermal-, gravitational-, and wind-induced deformations. Microwave holography also provides information about errors in the location of the antenna feed and allows for its optimum positioning. The feed is that part of an antenna at which signals transit from guided propagation in wire or waveguide to unguided propagation in free space (Shaffer, 1986). Further discussion of this technique is beyond the scope of this report. Interested readers may find results of practical applications using microwave holography in Bennet et al. (1976), Mayer et al. (1983) and Shaffer (1986).

Two non-contact measurement techniques for reflector antenna studies are more within the realm of surveying engineering and this report, namely close-range photogrammetry and conventional surveying. The remainder of this chapter will deal with the former while Chapter 3 deals with the latter. In summary, Figure 2.3 illustrates the various

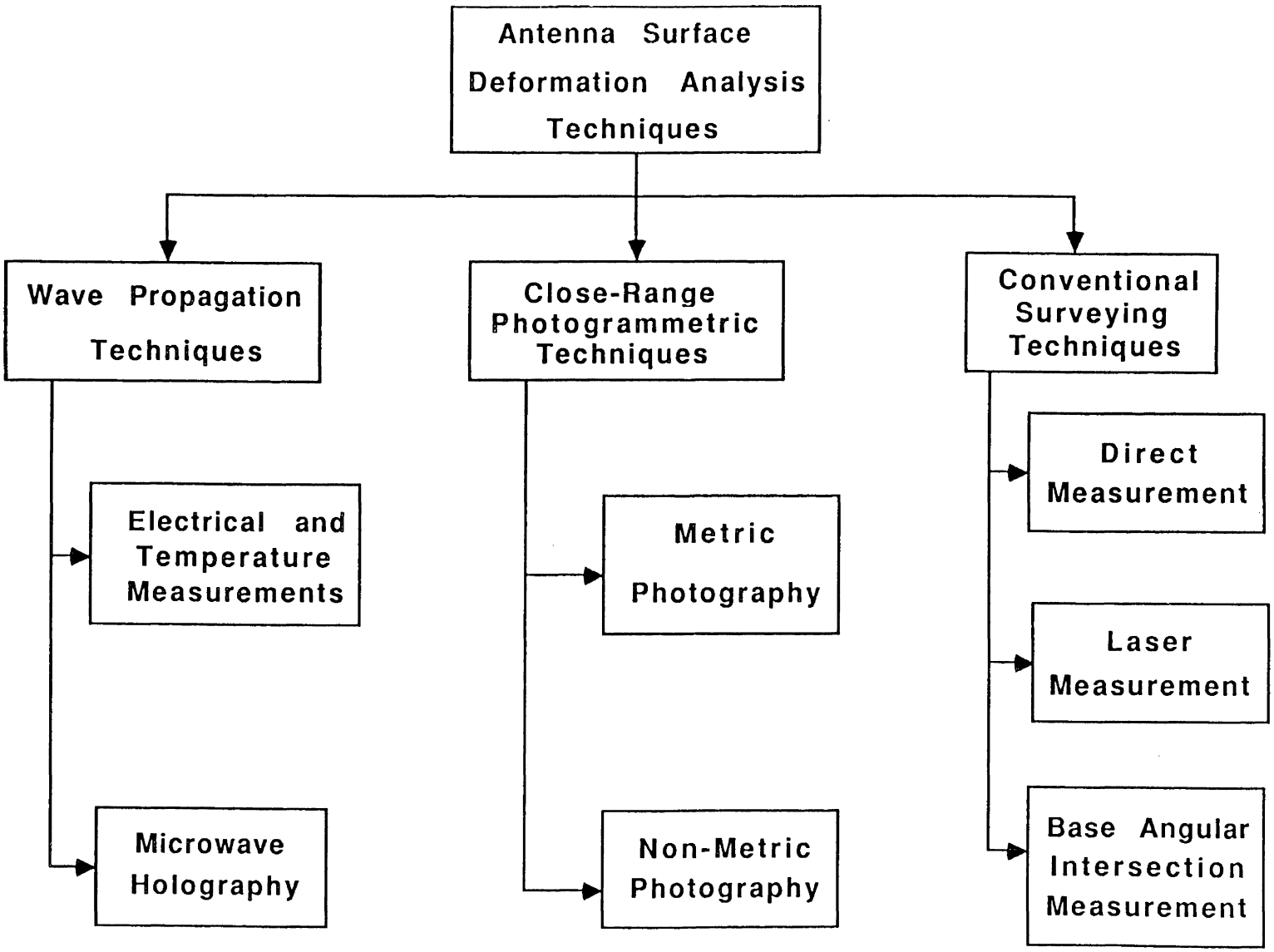

Figure 2.3: Antenna Surface Deformation Data Acquisition and Analysis Techniques

possible techniques available for Antenna Surface Deformation Analysis. Factors influencing the methodology best suited for a given mensuration project, such as required accuracy, time constraints, cost, available equipment and technological competence, must all be considered before any one specific method is selected.

2.4 Review of Photogrammetric Evaluations of Reflector Antenna Surfaces

Close-range photogrammetry has been used extensively to date to study reflector antenna surfaces of various shapes and sizes and in a multitude of operational situations. Its capability of being employed with a minimum of antenna downtime renders close-range photogrammetry superior to other non-contact techniques. With the onset of concerns over the reduction in gain due to surface deformations, studies using photogrammetry were investigated as early as the late 1950's to determine if structural design tolerances were achieved during construction. Ockert (1959) studied a 40-foot radio telescope at Ohio State University using a Wild P-30 Phototheodolite and a Wild A-7 Autograph. This analogue evaluation proved successful in point positioning with standard deviations of ±3 mm. Another early study by Marks (1963) utilized photogrammetry to calibrate an antenna under arctic conditions. De Vengoechea (1965) proposed antenna calibration using half-base convergent photography. At the world's largest reflector antenna in Arecibo, Puerto Rico, Forrest (1966) utilized an aerial mapping camera mounted to the feed support structure plus Brown's analytical aerotriangulation solution to perform the calibration of this 305-metre antenna. Surface deviations of the reflector were determined

with standard deviations of ±12 mm.

Considering the newest developments in photogrammetry, particularly analytical methods in photogrammetry, antenna mensuration in the past ten years has become more versatile and accurate. Analytical self-calibrating bundle adjustment programs are at the heart of these advances and have been employed in antenna manufacture and calibration by El-Hakim (1984) and Oldfield (1985). Perhaps the world's leader in promoting analytical photogrammetry in antenna calibration commercially is Geodetic Services, Inc. (GSI) (Brown, 1982, Fraser, 1986). The most significant contributions of GSI's technological developments are the use of specially designed large format cameras, retro-targetting technology, automatic video-scanning monocomparators, and personal computer-based network design and data reduction systems. These advances are described by Brown (1982) and Fraser (1982B) and lead to a definite potential of real-time industrial applications of close-range photogrammetry in antenna reflector calibration.

2.5 Basic Concepts of Close-Range Photogrammetric Evaluations

For any photogrammetric evaluation there are five basic phases which must be fulfilled in order to ensure satisfactory results. These include:

(1) Planning and Preanalysis;

(2) Data Acquisition;

(3) Data Reduction and Evaluation;

(4) Data Analysis; and

(5) The Presentation of Results.

In close-range photogrammetry the first three phases contain distinct

characteristics, which set it apart from any other evaluation method. However, it is the choice of data acquisition, reduction and evaluation techniques which establishes the fundamental project limitations such as accuracy, time, cost, and type of data output. This section will deal with the various preliminary considerations of photogrammetric evaluations. Closely tied to these considerations is an analysis of the various error sources which are inherent to the particular technique employed.

2.5.1 Attributes and Limitations of Close-Range Photogrammetry

There are distinct advantages in using CRP as a method of solving a measurement problem:

a. the object is not touched during measurement;

b. data capture (acquisition) is rapid;

c. the photographs store both metric and semantic data with very high density;

d. not only rigid and fixed objects, but also deformation and movement can be measured;

e. evaluation of metric and non-metric imagery can be done at any time in the office, and repetition and amendment of observations are always possible to provide a computer compatible data base;

f. photography and evaluation are flexible and as a result the optimization of accuracy to fit project requirements can easily be achieved;

g. complicated shapes and movements are easily measured; and

h. analytical methods allow a means of integration of re-measured photos into succeeding calculations.

All of these advantages make CRP clearly suitable for reflector antenna calibration. However, the success of any mensuration technique depends on a number of factors such as cost, accuracy, effectiveness, and availability. Therefore, a number of drawbacks of close-range photogrammetry must be considered as well, namely:

a. the results of the measurements are not available in real time because of the time needed for photographic processing and for photogrammetric evaluation;

b. the need for specialized and expensive equipment, such as comparators, plotters, and computers, makes photogrammetric evaluations expensive;

c. errors during photography and film development can adversely affect the results;

d. data acquisition, reduction and analysis requires trained personnel who understand photogrammetric concepts; and

e. it must be possible to photograph the object.

In some applications, the use of photogrammetry may have to be ruled out altogether in favour of an alternate precision surveying method. However, continuing developments in computer hardware and software technology have enabled industry to recognize close-range photogrammetry as an important tool for object mensuration.

2.5.2 Error Sources in Close-Range Photogrammetry

Depending on the data acquisition method used in close-range photogrammetry, decisions must be made concerning the minimization of

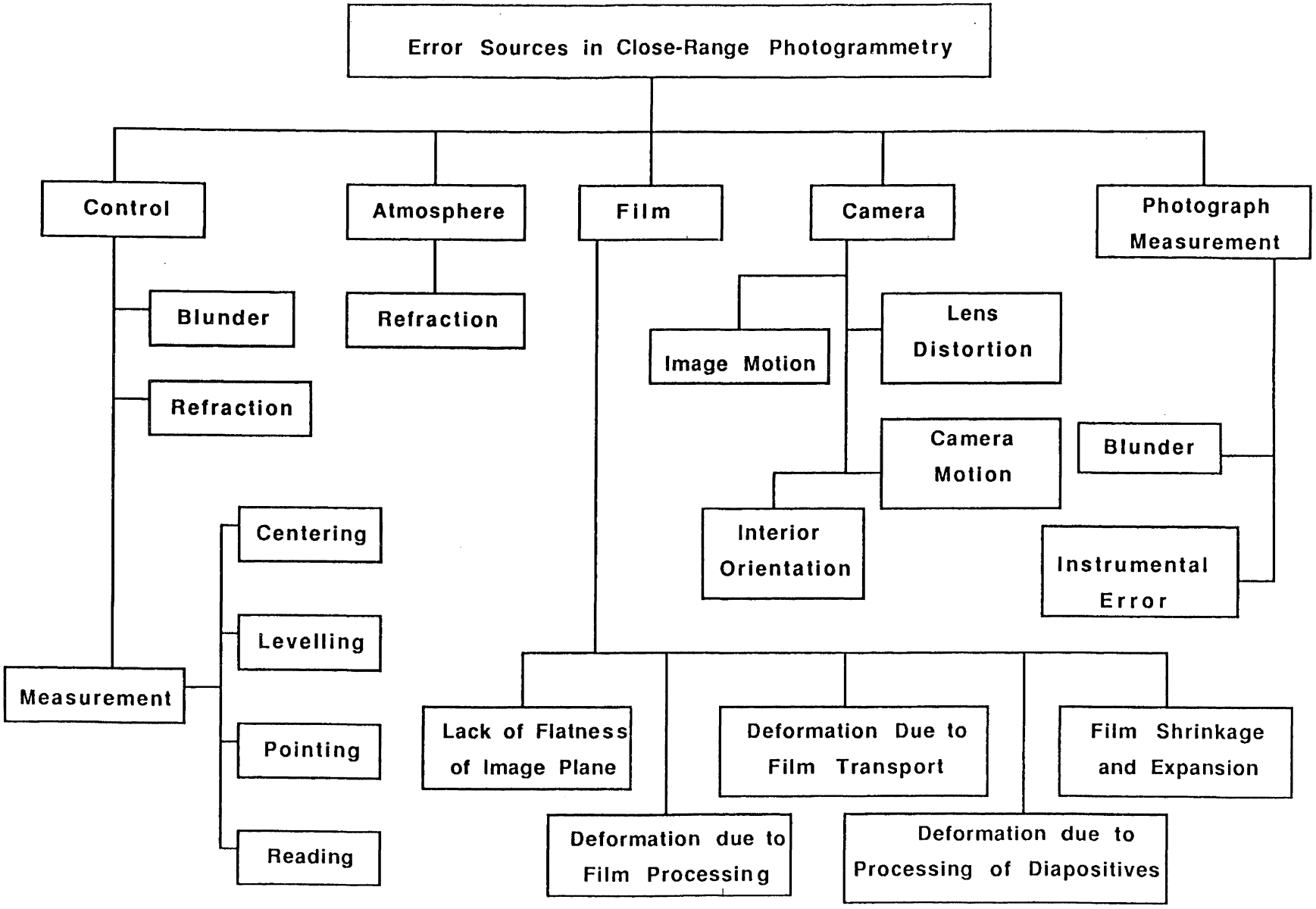

Figure 2.4: Error Sources in Close-Range Photogrammetry
(after Ayeni, 1982)

numerous potential sources of errors. Basically, error sources can be classified as five major types. These include (1) Control Acquisition Errors; (2) Atmospheric Errors; (3) Camera Errors; (4) Film Errors; and (5) Photograph Measurement Errors. Figure 2.4 illustrates these error sources and their causes.

The criterion for optimizing these error sources begins with the choice between the use of metric or non-metric imagery for the evaluation. Traditionally, photogrammetric data reduction and evaluation procedures were based on the assumption that a photogrammetric camera with known and stable interior orientation was used at the data acquisition stage. This implied the use of metric cameras. An important factor to be emphasized here, however, is that metric characteristics of photogrammetric cameras are only valid up to a specific accuracy threshold, beyond which it is prudent to utilize a more general evaluation approach. Therefore, non-metric cameras on the basis of experimental results are gradually gaining acceptance as data acquisition tools for numerous special industrial applications.

2.5.3 Potentials and Limitations of Non-Metric Imagery

A non-metric camera is a camera whose interior orientation is completely or partially unknown and frequently unstable (Faig, 1976B). Recent advances in analytical data reduction methods have helped non-metric cameras become viable data acquisition systems in close-range photogrammetry. In comparison with metric cameras, non-metric cameras have the following obvious advantages:

a. general availability of both camera and film;

b. considerably less costly than metric cameras;

c. smaller and lighter than metric cameras;

d. can be hand-held and therefore oriented in any direction; and

e. flexible focusing range.

However, coupled with these advantages are a number of disadvantages which must be addressed:

a. lack of definition of interior orientation;

b. instability of interior orientation;

c. large and irregular distortions which are complicated by variable focusing;

d. film deformations caused by a lack of film flattening device; and

e. inability to repeat camera settings.

Due to these difficulties it becomes obvious that the conventional approach of thoroughly calibrating a camera (pre-calibration) and then using the resultant parameters in the evaluation procedure is no longer valid. In response to these difficulties camera calibration must be applied to each individual photograph in the evaluation stage, either through the use of on-the-job-calibration or self-calibration. In summary, three possible camera calibration methods are possible.

Pre-calibration represents the more conventional calibration approach in a laboratory (using goniometers or collimator banks) or through the use of a photogrammetric test field (Faig, 1972A), and can be useful for non-metric cameras by providing partial calibration of camera parameters.

On-the-job-calibration involves the complete determination of individual camera parameters using the actual object photography. Here, however, a sufficient number of known object space control points are needed in each photograph to perform a simultaneous calibration and evaluation. This procedure can also be performed sequentially in a manner similar to a metric evaluation with the advantage that image coordinates are used as the input for the camera calibration.

Of more interest for non-metric photography is the self-calibration approach where the geometrical strength of overlapping photographs is used to determine interior orientation parameters, distortions, and the object evaluation simultaneously. This is especially the case where highly convergent imagery is used in a non-metric analysis. In the self-calibration approach there is no need for additional object space control beyond the requirement for absolute orientation, even when interior orientation parameters and distortions are included as unknowns in the mathematical model.

2.5.4 Analogue Solutions

Analogue solutions are generally recommended for medium accuracy output in the form of a contour map. The analogue approach is suitable for data reduction from metric photographs but not recommended for precision evaluation of non-metric imageries. Most universal precision plotters do not have sufficient principal distance ranges to evaluate photography taken with close-range photogrammetric cameras. Therefore, analogue approaches in close-range photogrammetry are not suitable for precision industrial applications.

2.5.5 Semi-Analytical Solutions

In the semi-analytical approach, the requirement for near normal case photography for photocoordinate measurement reduces the flexibility which convergent photography enables in close-range work. However, the analytical adjustment phases of this approach are quite flexible and can take one of three forms, making it an attractive alternative:

a. planimetric adjustment only (the "Anblock" method);

b. alternating iteration between planimetric and height adjustments; or

c. simultaneous three-dimensional adjustment.

In the semi-analytical approach, independent block adjustment relies on the basic unit of the model. A stereoplotter is used to form the stereomodel of the object. Models are then connected together analytically through the use of pass points, tie points, and perspective centres. To do this a three-dimensional similarity transformation equation is used:

$$\begin{bmatrix} X_p \\ Y_p \\ Z_p \end{bmatrix} - \begin{bmatrix} X_o \\ Y_o \\ Z_o \end{bmatrix} = \lambda . R \begin{bmatrix} x_p \\ y_p \\ z_p \end{bmatrix} \qquad (2.7)$$

where

$(X_p, Y_p, Z_p)^T$ are the object space coordinates of the point p

$(X_o, Y_o, Z_o)^T$ are the object space coordinates of the origin of the model coordinate system

λ is the scale factor between model and ground coordinate systems

R is a (3x3) rotational matrix, defining the space rotation of the model system with respect to the ground system

$(x_p, y_p, z_p)^T$ are the model coordinates of point p

In the semi-analytical method, consecutive pairs of overlapping photographs are relatively oriented on a stereoplotter and the resulting model coordinates are measured. The observation equations (2.7) are linearized and object coordinates are computed in a least-squares adjustment which transforms the whole block of models from the model coordinate system to the object coordinate system using control points. The semi-analytical approach to block adjustment has become popular mainly due to Ackermann's development of the computer program PAT-M-4-3 (Ackermann et al., 1973).

2.5.6 Analytical Solutions

In analytical photogrammetry, the basic computational unit is the bundle of rays which originates at the exposure station and passes through the image points. This is joined by the simultaneous accomplishment of the resection of all photos and the adjustment of the object control points.

Two methods have been developed using this principle, namely bundle adjustment approaches and the direct linear transformation approach. These analytical approaches can be used in the simplest evaluation case where interior and exterior orientations are known, but their main advantage and versatility become more obvious in the most general case of close-range photogrammetry. Here, the simultaneous solution is incorporated to solve for exterior orientation elements of all photographs with the space coordinates of object points as unknowns, as well as interior orientation elements and various additional parameters (AP's). In analytical solutions, image coordinate readings are made on various precision instruments including comparators, analytical or

analogue plotters, and cartographic digitizers depending on accuracy requirements of the project. In order to produce graphical output, computer graphic techniques can be used subsequent to the computation of final object space coordinates.

2.5.6.1 Bundle Adjustment Approaches

Theoretically, the bundle approach should be expected to yield the highest accuracies due to its mathematical completeness. The condition fulfilled in the bundle approach is the collinearity condition illustrated in Figure 2.5. The mathematical model is the collinearity equation:

$$\frac{x_p - x_o}{-c} = \frac{(X_p - X_c)m_{11} + (Y_p - Y_c)m_{12} + (Z_p - Z_c)m_{13}}{(X_p - X_c)m_{31} + (Y_p - Y_c)m_{32} + (Z_p - Z_c)m_{33}}$$

$$\frac{y_p - y_o}{-c} = \frac{(X_p - X_c)m_{21} + (Y_p - Y_c)m_{22} + (Z_p - Z_c)m_{23}}{(X_p - X_c)m_{31} + (Y_p - Y_c)m_{32} + (Z_p - Z_c)m_{33}} \qquad (2.8)$$

where:

(x_p, y_p) are image coordinates in the image plane;

(x_o, y_o) are image coordinates of the principal point;

(X_c, Y_c, Z_c) are the coordinates of the camera station in the object space;

(X_p, Y_p, Z_p) are the coordinates in object space of the point with photo coordinates x_p, y_p;

c is the camera constant or calibrated focal length; and

m_{ij} are the elements of R, an orthogonal rotation matrix of the image with respect to the object, in terms of the rotations ω, ϕ, κ.

In the basic bundle adjustment approach the three interior orientation parameters (x_o, y_o, c) are generally considered to be known

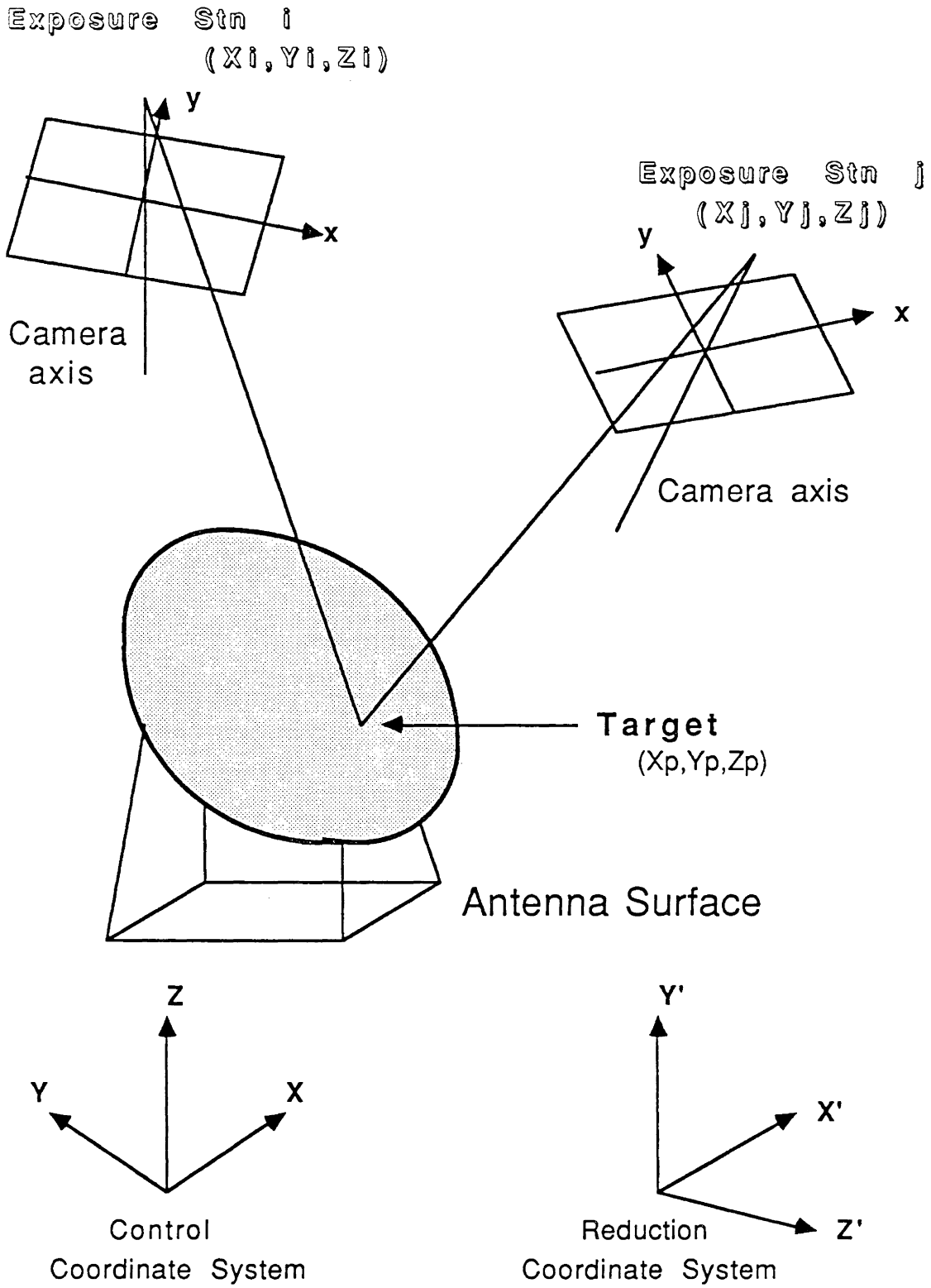

Figure 2.5: Photogrammetric Triangulation

from camera calibration. Therefore, in the most general case it is assumed that the image coordinates have been adequately corrected for all significant sources of systematic errors and that the only remaining errors are random in nature. Of course this is not the case, and numerous investigations in the 1970's pointed to such systematic errors as the main drawback for the bundle approach from yielding better results than the semi-analytical approaches. It has been the successful incorporation of additional parameters to model these systematic errors which allows the bundle adjustment method to be the most accurate.

2.5.6.2 The Direct Linear Transformation Approach

A second analytical approach which is particularly suitable for non-metric imagery is the Direct Linear Transformation (DLT) developed at the University of Illinois (Abdel-Aziz and Karara, 1971). The solution here is based on the concept of the direct transformation from comparator coordinates into object-space coordinates. The usefulness of this analytical method is that it bypasses the traditional intermediate step of transforming image coordinates from a comparator system to a photo system. As a result the solution requires no fiducial marks. The method is based on the following pairs of equations:

$$x_p = \frac{L_1X_p + L_2Y_p + L_3Z_p + L_4}{L_9X_p + L_{10}Y_p + L_{11}Z_p + 1}$$

$$y_p = \frac{L_5X_p + L_6Y_p + L_7Z_p + L_8}{L_9X_p + L_{10}Y_p + L_{11}Z_p + 1} \qquad (2.9)$$

where

(x_p, y_p)	are the coordinates of the point p
(x_p, Y_p, Z_p)	are the object space coordinates of the point p
L_1-L_{11}	are the eleven direct linear transformation parameters

When originally presented in 1971 the basic DLT equations, as with the bundle adjustment at the time, did not involve any additional parameters to compensate for systematic errors. However, in time both methods have been expanded to include additional parameters (see Section 5.7). The DLT, although yielding slightly less accurate results than the bundle solution, is capable of a quick and efficient calculation of exterior orientation parameters for use as initial approximations in those bundle adjustment programs which require them.

CHAPTER 3

PRECISION SURVEYING WITH ELECTRONIC THEODOLITES

As is the case with photogrammetric instruments, recent developments in surveying instruments have made them useful tools for close-range measurements. This is true both for establishing control points for photogrammetric analytical methods and for separate, stand-alone, close-range measurements. Today, theodolites are equipped with computers so that point positioning (the determination of x-, y- and z-coordinates) can be carried out in either "real-time" or "pseudo real-time" modes, while data acquisition is in process. This permits real-time "cause and effect" study of an object where external influences such as stresses can be observed as they are applied. The purpose of this chapter then is to examine the various potentials and limitations of close-range precision surveying with electronic theodolites in industrial applications.

3.1 Precision Engineering Surveying for Industrial Applications

As described in Chapter 2, an important activity in the industrial manufacturing process is that of performing measurements of workpieces, assembly jigs, or machine components during the assembly process to confirm that the prescribed tolerances are being met. Traditional techniques in industry involve the construction of various measuring instruments such as component assembly jigs to perform these tasks. In certain applications however, such as shipbuilding, aeronautical engineering and antenna construction, this method is not practical due to the magnitude of some of the components and the costs involved.

In addition, many undesirable effects occur when objects under manufacture are measured directly. These include deformations, interference with components, and time delays in the manufacturing process.

Therefore, an attractive alternative involves the use of electronic theodolites for precise intersection. This method involves using two or more theodolites interfaced to a computer in what is known as a multiple theodolite system. Besides the necessary computer hardware components needed, elaborate software is required to compute the 3-D coordinates of a simultaneously intersected point.

3.2 Attributes and Limitations of Close-Range Surveying with Electronic Theodolites

The use of electronic theodolites in a close-range environment has proven successful for a number of reasons:

a. The object is not touched during measurement. In addition, for truly inaccessible objects, laser eyepieces can be used for establishing target points;

b. Data capture (acquisition) is rapid once initial set-up and orientation is completed;

c. Objects of any kind, shape and made from any material can be measured;

d. Data acquisition and reduction are performed concurrently for "pseudo real-time" point positioning;

e. Point positioning of extremely high accuracy is possible. For object distances of under 10-metres, accuracies of 0.05 mm are possible using only two theodolites (Lardelli, 1984).

f. In case of blunders or poor observations, re-measurements can be performed before the instruments are disassembled;

g. A computer compatible data base can be established from automatic recordings for future evaluation or for use as photogrammetric control; and

h. The measurement procedure is simplified to the point where expert surveyors are no longer needed for precise data acquisition.

Just as in the case of close-range photogrammetry, there are a number of drawbacks which must be considered when using electronic theodolites:

a. Data capture or recapture once the instrument set-up is disassembled requires the transformation of all newly acquired points to the original coordinate system;

b. Once measurement is in process both object and theodolites cannot be moved. Hence, the technique is susceptible to unstable objects and to local vibrations;

c. Although data capture is achieved in "pseudo real-time", complex objects requiring a large number of points need a long time for evaluation;

d. Because of the large capital investment (hardware and software), numerous applications are needed to ensure an adequate payback period;

e. Object mensuration is limited to ground based data acquisition of discrete points only;

f. It must be possible to sight onto the object; and

g. Due to the length of time needed for theodolite set-up this method is only practical for a large number of object points.

These limitations make close-range precision surveying unsuitable for certain industrial engineering mensuration tasks such as applications in space and the study of moving objects. However, precise point mensuration using electronic theodolites has proven to be an attractive technique in a variety of applications.

3.3 Point Measuring Procedure

The spatial coordinates of specific points are measured using the traditional base angle method of intersection. Figure 3.1 illustrates

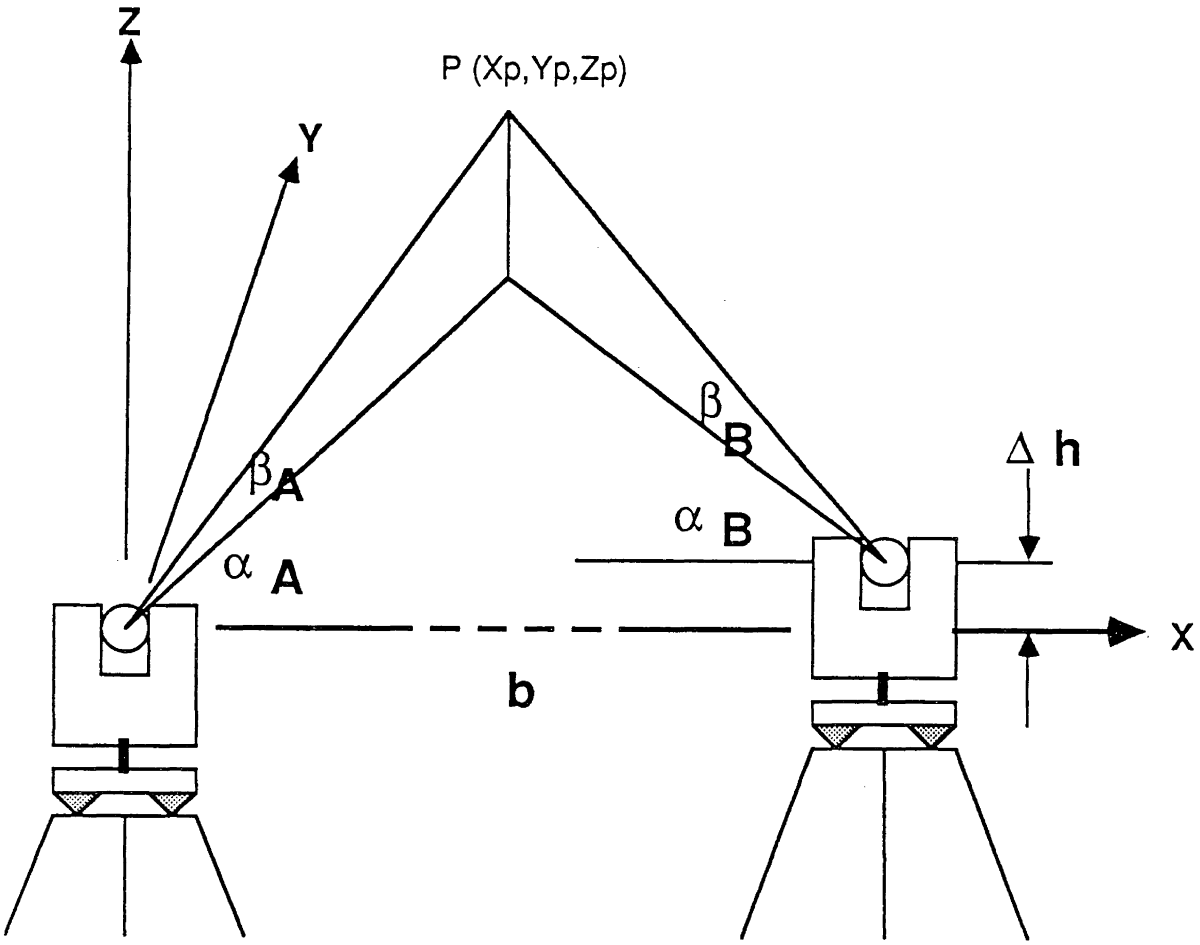

Figure 3.1 Base Angle Method of Intersection

the geometry of this technique.

In order to compute coordinates of object points, a local 3-dimensional rectangular coordinate system whose origin is at the point of intersection of the theodolite vertical and trunion axes of the left station (Stn A) is often used. The x-axis is chosen as a horizontal line parallel to the base direction, while the y-axis is a horizontal line perpendicular to the base direction positive in the direction towards the object. Finally, the z-axis is a vertical line determined by the vertical axis of the theodolite at the left station. Thus, a right-handed coordinate axis system is chosen for data acquisition.

In order to compute the position and height of any new point P, the baseline data must first be determined, which includes the calculation of the horizontal base length b and height difference Δh. This can be found using, for instance, a subtense bar or an invar levelling rod. The fundamental angular intersection and trigonometric heighting formulae are well known and their derivation can be found in any surveying text. These include:

$$X_p = \frac{(Y_A - Y_B) + X_A \operatorname{Cot} \alpha_B + X_B \operatorname{Cot} \alpha_A}{\operatorname{Cot} \alpha_A + \operatorname{Cot} \alpha_B}$$

$$Y_p = \frac{(X_B - X_A) + Y_A \operatorname{Cot} \alpha_B + Y_B \operatorname{Cot} \alpha_A}{\operatorname{Cot} \alpha_A + \operatorname{Cot} \alpha_B} \qquad (3.1)$$

$$Z_p = 0.5\,\Delta h + \frac{b}{2 \sin (\alpha_A + \alpha_B)} (\operatorname{Sin} \alpha_B \operatorname{Tan} \beta_A + \operatorname{Sin} \alpha_A \operatorname{Tan} \beta_B)$$

where:

(X_A, Y_A, Z_A) = Coordinates of Theodolite at Stn A

(X_B, Y_B, Z_B) = Coordinates of Theodolite at Stn B

Naturally the above intersection formulae can be expanded to encompass more than two electronic theodolites and the resulting overdetermination in positioning enhances the accuracy of the final results. The advantage of this measurement approach is that the positioning of electronic theodolites can be established so that the instrument and observer do not interfere with the object provided all desired object points can be directly sighted from all stations.

3.4 Multiple Electronic Theodolite Systems

With the advent of cheaper, smaller and more powerful computers, the interfacing of electronic theodolites has led to a broadening of applications in engineering, production-control and quality assurance. The implementation of this technology, however, has only been possible since the mid 1970's when the 3-D intersection method was first widely employed in industry by Keuffel and Esser (Brown, 1985). Since this time, various manufacturers of electronic theodolites have introduced systems for industrial applications. A partial list includes:

a. the Kern ECDS1 system;

b. the Wild CAT system;

c. the K&E AIMS - R/T system;

d. the Zeiss Industrial Measuring System; and

e. the AGA IMS 1600.

In principle, the fundamental unit behind all of these systems is still the electronic theodolite and so it is appropriate to examine the special characteristics of this instrument.

3.4.1 The Electronic Theodolite

Theodolites are standard measuring instruments in surveying for the measurement of horizontal and vertical angles. Traditionally, the optical theodolite has been used to measure angles needed in surveying tasks. However, electronic theodolites are now surpassing these analogue systems because of their convenient continuous electronic output and automatic data flow. An electronic theodolite is one with optoelectronic scanning of the circles. Most are based on an incremental measuring procedure which is characterized by high accuracy and stability. This accuracy is not reduced when turning the theodolite about its vertical or trunion axes. The majority of electronic theodolites need no activating prior to measurement as a continous readout of current circle readings is available to the user through electronic digital displays. This proves advantageous as the measured values can be stored or transmitted directly to a computer for further processing. In addition to saving time this procedure enables blunder-free data transfer to a secondary computer system for analysis and adjustment.

Although most electronic theodolites are different in design, the circle reading system is generally of the type where a photoelectric detector system counts the graduation in the circle as the instrument is rotated about its vertical or trunion axis (Paiva, 1987). Various ingeneous methods have been utilized in interpolating between marks on the circle. It must be remembered that interpolation errors are similar to the types of errors encountered with optical theodolites and therefore readings must be distributed throughout the circle. Errors such as circle or telescope eccentricities are compensated for by

measuring in the direct and reverse senses.

A key feature found in electronic theodolites is an electronic compensator for standing axis tilt. Here an electronic tilt sensor is used for the purpose of compensating the observed horizontal and vertical angles for the tilt of the standing axis. The most common type of compensator is a liquid-based device with the associated electronics for converting into digital signals the movement of a bubble in a tube. Other liquid based devices utilize variations in the angle of reflection or refraction of the top surface of the liquid caused by standing axis tilts. Readings from the compensator - although often displayed - are rarely used directly by the user, since the output from this electronic device directly affects the horizontal and vertical circle readings which are displayed. The external display of the compensator reading enables the surveyor to monitor the compensator's accuracy.

3.4.2 Computer Interfacing

The interfacing of two or more electronic theodolites to a computer system forms the basic design of every multiple electronic theodolite system. Generally, a system will require a computer, data transmission cables (usually RS-232), a comprehensive software package and perhaps a printer for hardcopy listing of data. Figure 3.2 illustrates the configuration of a multiple electronic theodolite system. The software for such a system consists of essentially five sub-program packages:

a. Operating System Software: Since most multiple electronic theodolite systems run on various personal computers, the inherent operating system software is required for system operation.

b. Scaling Software: This package enables the baseline calibration to be performed prior to actual object mensuration.

c. Data Capture Software: This subprogram allows the spatial coordinates of points on the object to be computed and displayed.

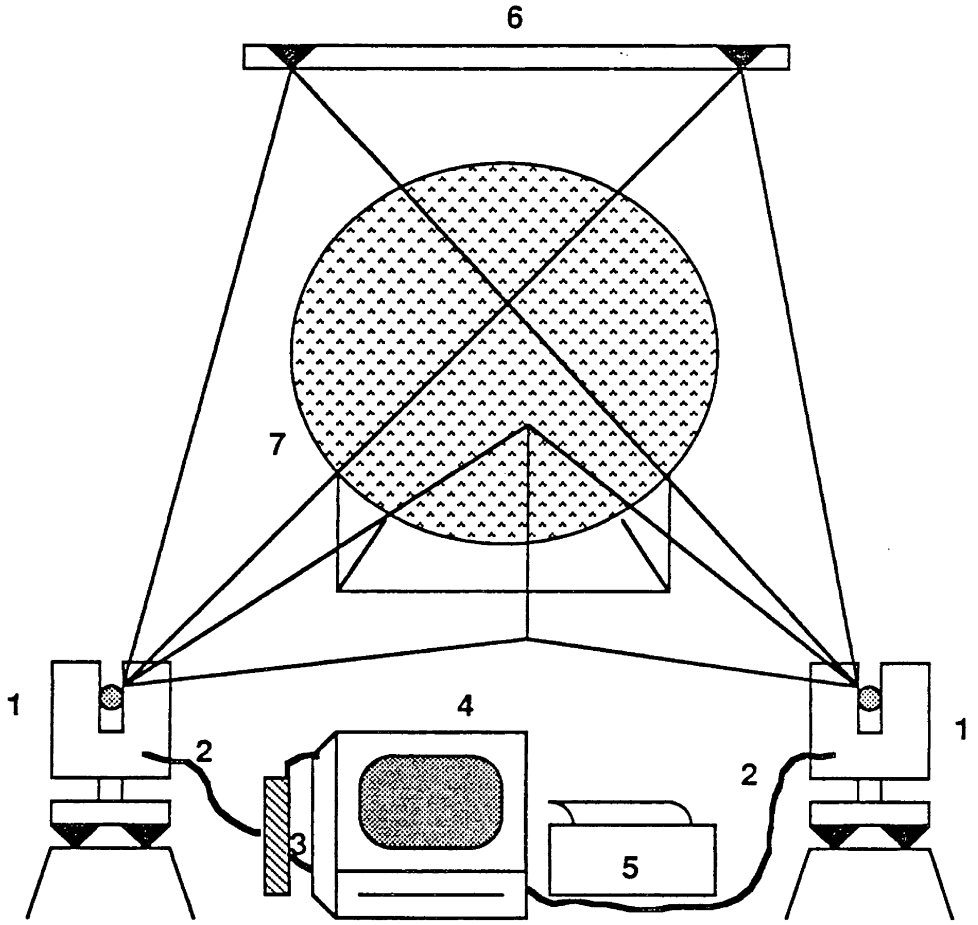

(1) Two or more Electronic Theodolites
(2) Data Transmission Cables (RS-232)
(3) Junction Box for Theodolite - Computer Interface
(4) Computer Terminal for Graphic Display
(5) Parallel Printer for Hardcopy Output
(6) Subtense Bar for Baseline Calibration
(7) Object under Consideration (Antenna)

Figure 3.2: Multiple Electronic Theodolite System

d. Data Manipulation Software: This utility package allows the recording of object points onto files and the performance of other utility functions such as sorting and printing.

e. Specialized Function Software: Depending on the system, various specialized functions are available for such operations as coordinate transformations, geometric computations, and laying-out functions for various manufacturing procedures.

3.4.3 Data Flow

The flow of data begins at each individual theodolite used. Usually one operator is in charge of the measurement procedure and will

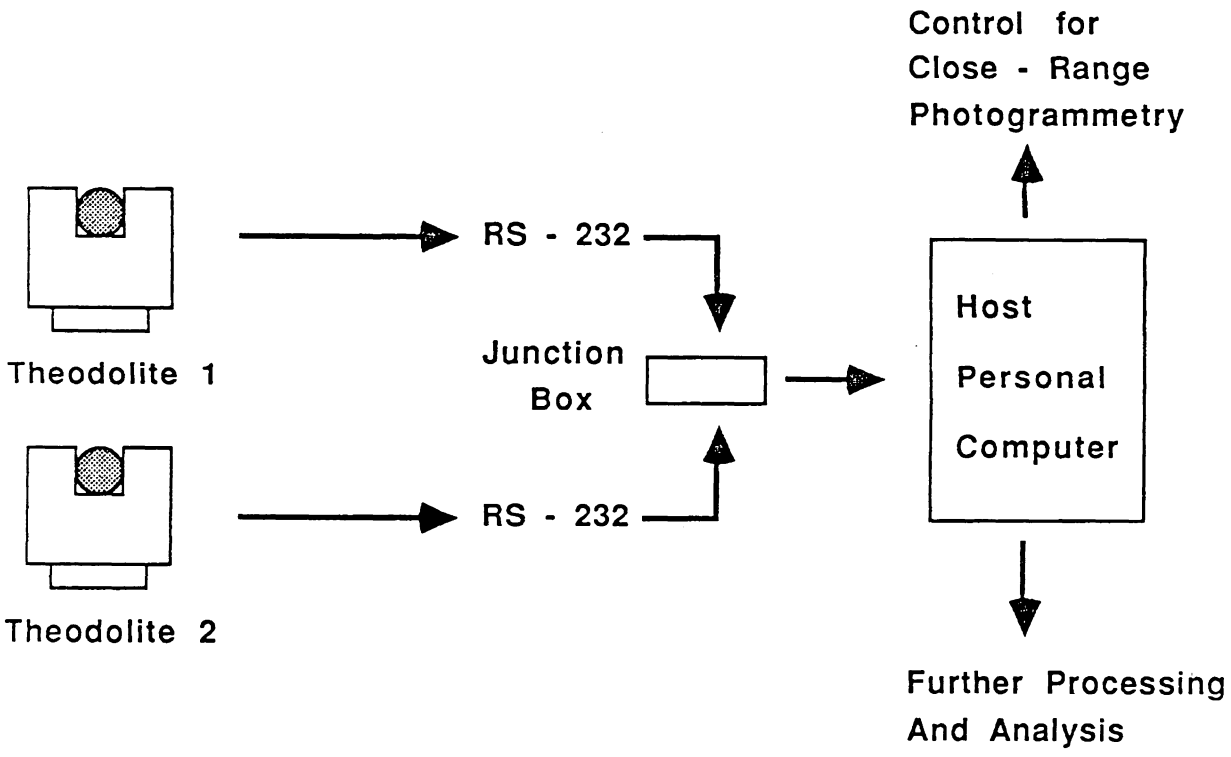

Figure 3.3 Data Flow Using a Multiple Theodolite System

control point selection and data capture. Referring to Figure 3.3, the flow of data originates at each theodolite and is automatically fed to the theodolite-computer interface junction box via RS-232 communication cables. The operator then controls data capture at the terminal, checking for blunders, and sending the results to a coordinate file or printing out a hardcopy listing of coordinates.

3.5 Recent Advances in Electronic Theodolite Coordinate Determination Systems

Although electronic precision theodolites have established themselves as instruments for surveying industrial objects, recent advances in automated 3-D coordinate determination make this technology even more convenient and economical. For example, the Kern ECDS1 system has incorporated a bundle adjustment package into its software for the determination of the spatial positions of the two theodolites prior to data acquisition. In this system all that is needed is an external scale and a number of reference targets for simultaneous pointing. Then, the simultaneous resection problem is solved for the geometry of the layout using the familiar bundle adjustment solution. This technique does not require the two theodolites to sight onto one another, thus avoiding expensive optical axis targets and external theodolite reference marks for pointing.

Perhaps the most significant development in recent years is the construction of the Kern Servo-Theodolite E2-SE, and the System for Positioning and Automated Coordinate Evaluation (Gottwald et al., 1987). Here the introduction of photogrammetric techniques combined with the on-line connection of up to eight theodolites enables truly real-time

object mensuration. The Kern Servo-Theodolite E2-SE introduces a telescope integrated CCD-camera for real-time image acquisition. A CCD (Charged-Coupled Device) array format of 576 (vertical) to 384 (horizontal) pixels with a pixel size of 23x23 μm enables the operator to control remotely the movement of all electronic theodolites in the system. With this new system a semi-automated or fully automated survey of industrial objects becomes possible with accuracies similar to existing multiple electronic theodolite systems (Gottwald et al., 1987). The calibration of this CCD-camera is described by Zhou and Roberts (1987).

3.6 Electronic Theodolites and Reflector Antenna Calibrations

Electronic theodolites have been used in various reflector antenna calibration studies since their introduction in the last half of the 1970's. Particularly useful in truly static installations, electronic theodolites provide a versatile measurement technique for small and large reflectors alike. In one study on electrostatically formed antennas conducted at NASA's Langley Research Centre, a multiple electronic theodolite system was used to measure the membrane of a new Kapton reflector surface (Goslee et al., 1984). Since the reflector surface was formed by a deformable Kapton membrane by applying electrostatic forces, the use of theodolites was found to be too time consuming to accurately study the surface. However, in most reflector antenna studies, this measurement technique is extremely suitable.

CHAPTER 4

PLANNING AND PREANALYSIS

When planning a multi-station photogrammetric or surveying project, due consideration must be given to project planning and preanalysis to ensure accurate results. Perhaps this is more critical when using non-metric cameras in a photogrammetric survey since these data capturing systems are more versatile and require special considerations before engaging in data acquisition. When performing a preliminary preanalysis the basic project requirements must be considered. Limiting factors such as accuracy specifications, time constraints, accessibility of the object, cost of the analysis and the required form of data output must also be optimized for successful results. This may preclude various techniques from being feasible at the start. In this chapter a number of preliminary preanalysis and planning considerations for the reflector antenna under study shall be discussed.

4.1 Description of Antenna Under Consideration

A fairly flat parabolic microwave reflector antenna of approximately one-metre in diameter is currently operated by the Electrical Engineering Department at the University of New Brunswick. The reflector surface was designed to be a paraboloid of revolution with a design focal length of approximately 40 cm. The complete reflector was fabricated from one piece of approximately 2.5 mm thick aluminum, whose surface is painted white. The antenna, shown in Figure 4.1, comes complete with its own support base which enables quick orientation and the ability for multiple elevation angles reconciled from the horizon.

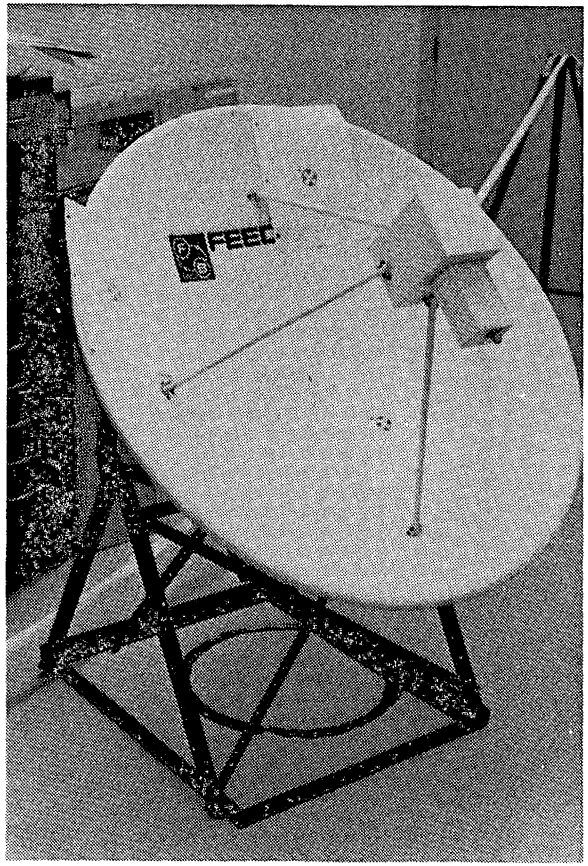

Figure 4.1: Antenna with Horn Structure and test targets

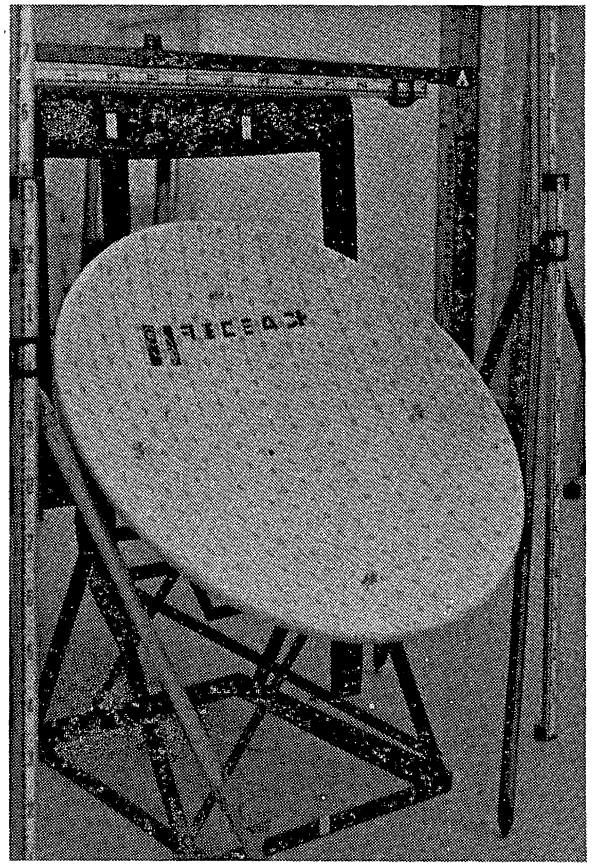

Figure 4.2: Targetted Antenna

The antenna currently supports an S-band satellite weather receiver and is mounted on the roof of Head Hall at the University of New Brunswick.

The feed structure for the antenna consists of a horn, mounted on four supports which attach to the face of the parabolic reflector. This support structure, including the horn itself, was under repair for the duration of the project. Since the reflector was quite mobile it was moved to the geodetic surveying laboratory in room A-17 of Head Hall for the purpose of studying its surface characteristics. With the feed support structure unavailable, an analysis of surface shape and deformations became the main goal of this study.

Originally this work was defined as a task for the Engineering Surveying research group at UNB. As part of the group's research efforts in interfacing electronic theodolites with various personal computers for close-range precision surveying applications, the antenna served as an object which demanded precision positioning and therefore could be a suitable application of this research. The author subsequently undertook the task of performing a calibration of the reflector surface using photogrammetric techniques. Therefore, reflector surface deformation studies should prove ideal in testing the capabilities of both close-range photogrammetry and close-range surveying, and thereby in evaluating surveying engineering methods of antenna calibration concurrently.

4.2 Surface Deformation Accuracy Requirements

The designed operational range of the reflector antenna is between 2 and 4 GHz or within the S-band range of microwave frequencies (see Appendix I). The antenna is commonly used at a frequency of 2 GHz

(λ = 15 cm) and it is speculated that it is capable of operational frequencies of up to 10 GHz (λ = 3 cm). Therefore, the goal of this research is to measure the surface roughness and thereby propose a maximum operational frequency range for the antenna based on antenna tolerance theory as described in Chapter 2. To meet this goal a mensuration procedure must be utilized so that the accuracy of the measured points on the surface of the reflector is sufficient to illustrate how well the structure conforms to design specifications. Should the design focal length not be available then the data measured must be suitable to predict the shape of the antenna, using a surface fitting technique, and a method must be established to separate deviations of the antenna surface from errors in the evaluation technique used.

For the project at hand, the design accuracy specification for measurement has been set at 0.5 mm (mean standard error for X, Y and Z coordinates). In arriving at this value it was anticipated that along with close-range surveying using precision electronic theodolites, an analytical non-metric close-range photogrammetric evaluation would be completed. Naturally, the data acquisition and evaluation procedure selected will dictate the final accuracy for the resulting coordinates. If the design accuracy is met, predictions of operational wavelengths to within 14 GHz (λ = 1.4 cm) based on surface deviations should be possible.

4.3 Project Planning

It is perhaps a secondary goal of this study to investigate the feasibility of performing a non-metric photogrammetric analysis of the antenna in question. In particular, it will be interesting to see if a

non-metric analysis of the antenna will yield the desired results. The obvious advantage in using non-metric imagery would be a reduction in cost required to perform the study, at least in the data acquisition stage. Therefore in the project planning stage it is desirable to delineate the required steps for such an evaluation. First however, it will be useful to summarize the objectives and tasks of this antenna calibration survey. These are:

a. Determine the coordinates of points on the surface of the reflector by close-range photogrammetry using non-metric imagery and close-range surveying;

b. Determine the shape and regularity of the surface of the reflector by performing a least squares fit of the paraboloidal surface to the coordinates;

c. Compute the focal length and centroid of the paraboloid from the reduction to standard form of the best fitting paraboloid;

d. Display the shape and regularity of the reflector surface along with deviations using a 3-dimensional plotting and contouring package; and

e. Propose the maximum operational frequency range for the antenna with the desired understanding of surface roughness.

In proposing techniques to meet these objectives, the overall evaluation is best represented diagrammatically. Figure 4.2 illustrates in block diagram form, the project planning considerations.

4.4 Geodetic Preanalysis Considerations

In any project the surveyor's choice of instrumentation and measurement techniques must be based on a thorough preanalysis, so

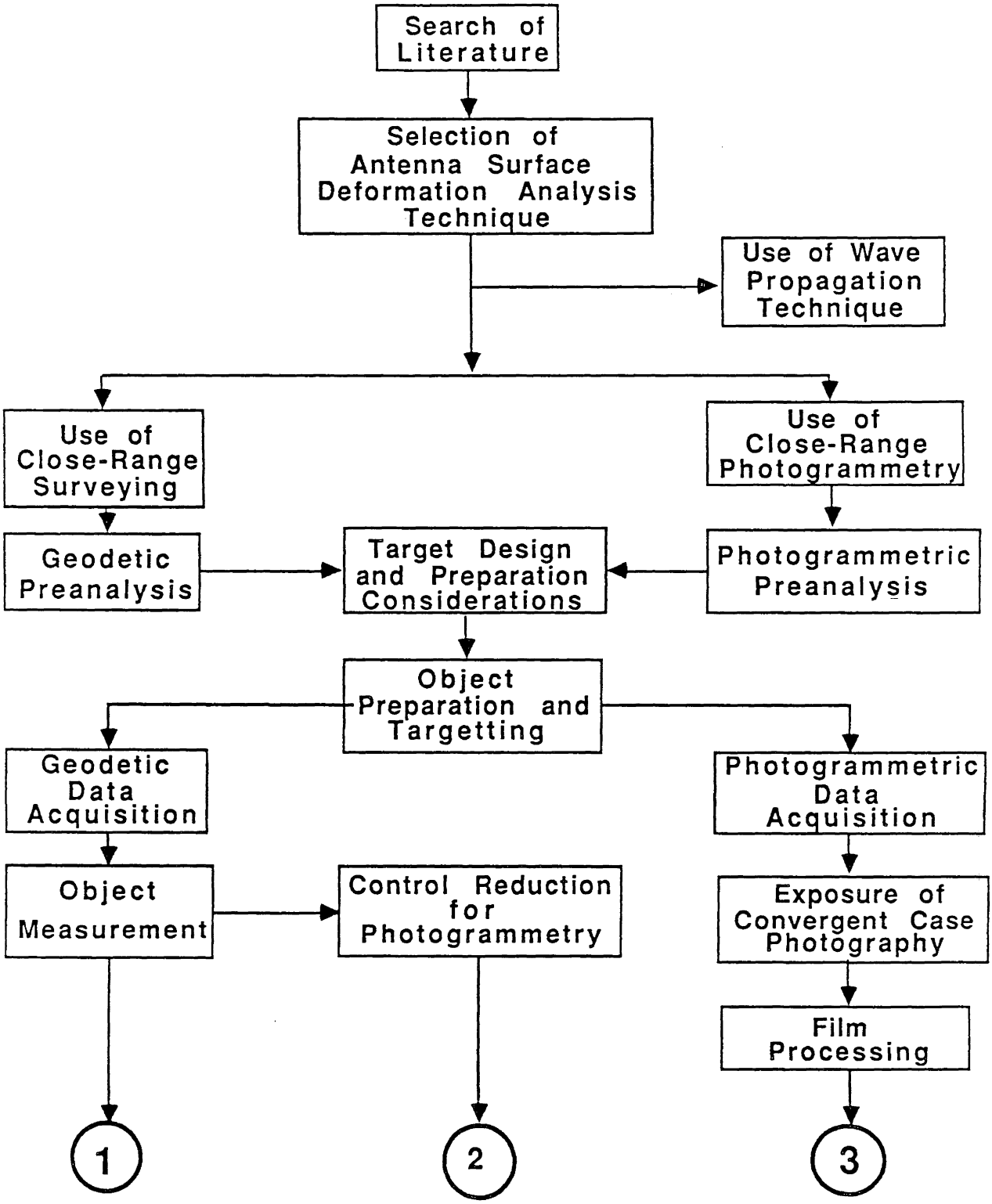
Search of Literature
Selection of Antenna Surface Deformation Analysis Technique
Use of Wave Propagation Technique
Use of Close-Range Surveying
Use of Close-Range Photogrammetry
Geodetic Preanalysis
Target Design and Preparation Considerations
Photogrammetric Preanalysis
Object Preparation and Targetting
Geodetic Data Acquisition
Photogrammetric Data Acquisition
Object Measurement
Control Reduction for Photogrammetry
Exposure of Convergent Case Photography
Film Processing
1
2
3

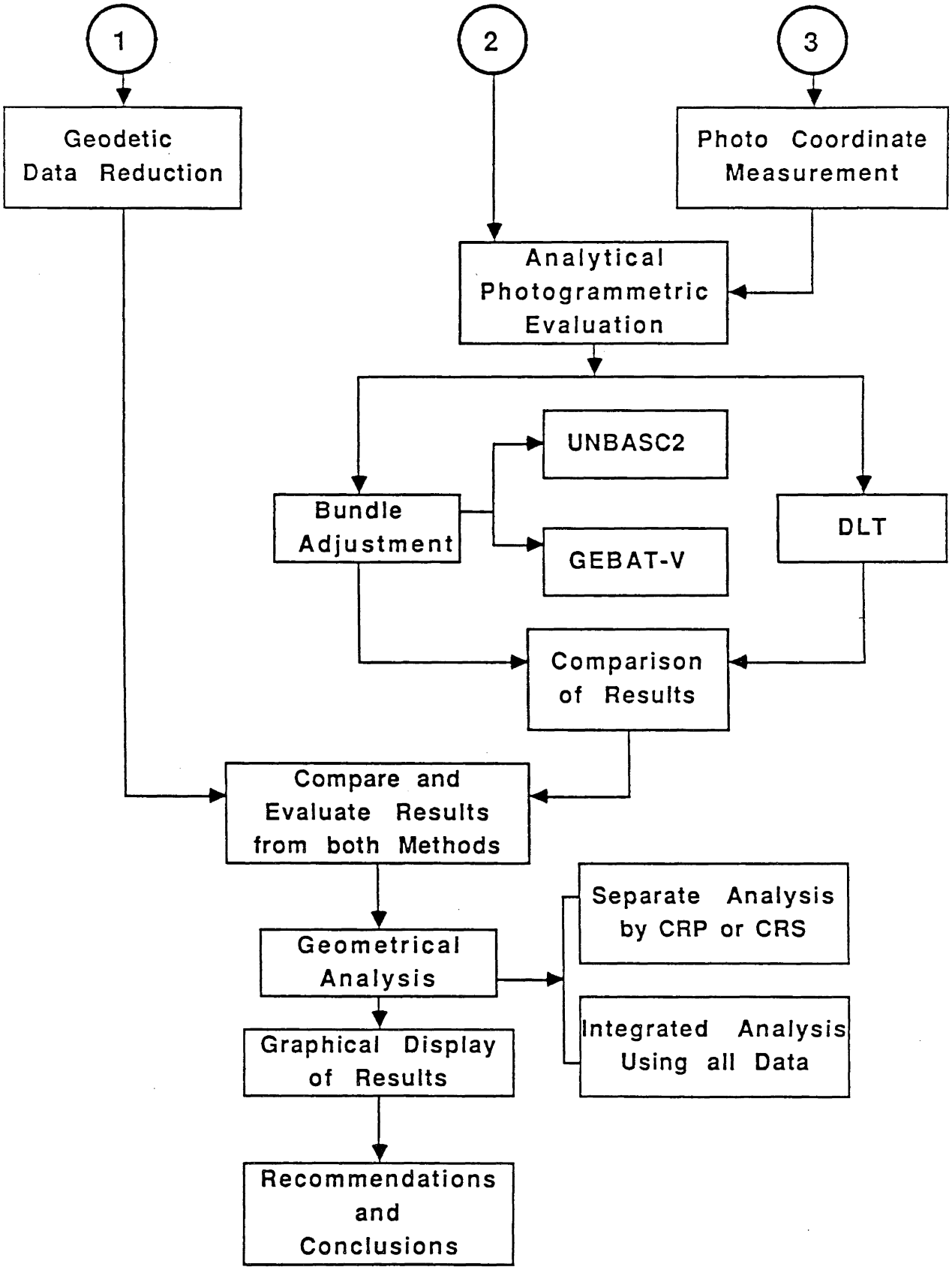

Figure 4.3: Block Diagram Layout of Study

that the accuracy requirements are achieved. In performing a preanalysis there is generally a compromise between instrumentation selection and methods, time constraints and accuracy for the task. As illustrated in Chapter 3, the base angle method of intersection is perhaps the most expedient and accurate for use in close-range 3-D point positioning. Prior to commencing a geodetic preanalysis based on this technique, it is prudent to examine the capabilities and limitations of the various available instruments.

4.4.1 Instrumentation

The Department of Surveying Engineering at UNB has one Kern E-2 precision electronic theodolite which was used in this work. This instrument was used to gather control data for use in the photogrammetric adjustment. Auxiliary instruments used in control acquisition included a Wild 2 m subtense bar, a Kern close-range target and the necessary tripods, levelling rods and centering trivets. The characteristics of the Kern E-2 are illustrated in Appendix II.

4.4.2 Surveying Accuracy Considerations

In a project of this nature, where essentially the highest possible accuracy in point determination is the goal, there is no need to differentiate between procedures for close-range surveying and procedures for control point positioning for close-range photogrammetry. Therefore, whether an electronic theodolite is used for photogrammetric control acquisition or object evaluation, the same preanalysis considerations apply when using the base angle method of intersection. To minimize various systematic errors multiple theodolites are utilized

simultaneously for point mensuration. Since the expected accuracy of the calculated coordinates is within the magnitude of the measurement errors, it is difficult to allow for a margin of safety when performing a preanalysis.

The total error in the positioning of spatial points at close-range is still influenced by errors such as:

a. Centering Errors (σ_c);

b. Pointing Errors (σ_p);

c. Levelling Errors (σ_ℓ);

d. Reading Errors (σ_r).

Observational errors such as refraction and blunders also play in the uncertainty of the observed points and these effects must also be minimized. For the four basic systematic components of horizontal and vertical angle errors, it is generally assumed, a-priori, that they contribute equally to the total error. Since all of these errors are additive, when measuring a horizontal angle the combined standard deviation σ_θ is usually expressed as:

$$\sigma_\theta = \sqrt{\sigma_{\theta c}^2 + \sigma_{\theta p}^2 + \sigma_{\theta \ell}^2 + \sigma_{\theta r}^2} \qquad (4.1)$$

with:

a. Centering Error:

$$\sigma_{\theta c} = 1.6 \frac{\sigma_c}{D} \rho'' \qquad (4.2)$$

for $\theta \simeq 45°$ as is the case for optimum intersection geometry.

where ρ'' = 206265"
D = Distance to targets
σ_c = Centering errors of targets

b. Pointing Error

$$\sigma_{\theta p} = \frac{45''}{M} \tag{4.3}$$

where M = Telescope Magnification

c. Levelling Error

$$\sigma_{\theta \ell} = \sigma_{\ell}\sqrt{\tan^2\gamma_1 + \tan^2\gamma_2} \tag{4.4}$$

where γ_1, γ_2 are vertical angles to targets

σ_{ℓ} = Levelling error to targets

d. Reading Error

$$\sigma_{\theta r} = \frac{\sigma_r}{\sqrt{n}} = \frac{2.5d''}{\sqrt{n}} \tag{4.5}$$

where d" = nominal angular value of the smallest subdivision

n = number of sets of readings

Further discussion of preanalysis considerations for angular observations can be found in Chrzanowski (1974-1977 and 1977), Nickerson (1978), and Blachut et al. (1979). Since the evaluation of the antenna was performed in a laboratory setting, a number of these systematic errors can be considered negligible. Fixed concrete pillars are available and there is no need to replace the theodolites during observation so centering errors are virtually eliminated. The antenna itself is portable and can be moved into position at approximately 3.5 metres from each instrument station to achieve optimum intersection angles and therefore errors due to levelling and refraction will also become negligible. This of course would not be the case in all antenna mensuration projects. However, here the primary contribution to error in the observed spatial coordinates comes from theodolite pointing and reading. With the use of electonic theodolites the reading error component can be considered negligibly small.

4.4.3 Photogrammetric Control

Control points are needed in close-range photogrammetry for the orientation of the photographed object and for camera calibration. Quite simply, the final accuracy of object space coordinates determined from a photogrammetric analysis depends on the accuracy of the control points provided. Abdel-Aziz (1982) studied the optimum positioning of theodolite stations when using the base angle method of intersection to provide the photographed object with the necessary control points. The recommended theodolite elevation based on these findings is at the average height of the object. In close-range photogrammetry under laboratory conditions, test-fields can be useful for the study of smaller objects which can be incorporated into the existing control (Faig, 1972A).

The provision of control by conventional means can be both expensive and time consuming. Another option investigated here is to incorporate observation equations into the photogrammetric evaluation to handle spatial distances and height differences, and perform the geodetic and photogrammetric evaluations simultaneously. (Faig and El-Hakim, 1982).

4.5 Photogrammetric Preanalysis

In order to optimize a network of camera stations in a close-range photogrammetric project, a number of design considerations must be examined. Fraser (1984, 1987) in considering this problem of CRP network analysis and design classifies the problem using a scheme proposed by Grafarend (1974). Simply stated, this scheme deals with the problem of optimization of network design in four stages:

a. Zero-Order Design (ZOD): the datum problem;

b. First-Order Design (FOD): the configuration problem;

c. Second-Order Design (SOD): the weight problem; and

d. Third-Order Design (TOD): the densification problem.

The difficulty in network design for photogrammetric projects is that for a network of over one hundred points and four to six camera stations, the required covariance matrix is obtained through the formation of normal equations and subsequent inversion of matrices of rank in the range of 350 to 400. Networks of 100 object points are considered small in photogrammetry. The implementation of interactive network design in close-range photogrammetry has found successful results in a number of studies (Gustafson and Brown, 1985) and (Krolikowsky, 1986). Although the use of simulation software packages and interactive computer graphics enables networks to be designed and analyzed in a relatively short period of time, more research is needed in this area. For this study the four stages of network design are considered without the assistance of interactive computer graphics.

4.5.1 Zero-Order Design (ZOD)

ZOD primarily deals with the datum problem. The datum is optimized by selecting an appropriate reference coordinate system for the object space coordinates. Constraints are generally imposed to define the datum (i.e. origin, orientation, scale of XYZ reference coordinate system). The control point acquisition coordinate system, shown in Figure 2.5, normally defines the XYZ object space coordinate system for control acquisition. However, for the sake of simplification of subsequent photogrammetric evaluation these coordinates were transformed

to the X'Y'Z' system shown in the same figure.

4.5.2 First-Order Design (FOD)

The purpose of first-order design is to select an appropriate imaging geometry for a given array of object target points. This includes the number of camera stations, camera type, image scale, focal length, additional parameters, and number of exposures per station. In this study the camera system to be used for imaging the antenna is a non-metric Canon T-50 35 mm camera. Thus the imaging format is restricted to 35 mm by 24 mm. As a result of the decision to use a non-metric camera a number of additional considerations are imposed if the demanded accuracy is to be met. Additional papers which deal with the optimization of FOD include Fraser (1981, 1982B), Karara and Abdel-Aziz (1974), and Papo (1982). Various other considerations must be optimized in the successful application of convergent multi-station photography. These are discussed in Abdel-Aziz (1974), and Faig and Moniwa (1973).

4.5.2.1 Selection and Targetting of Points

Since the eventual goal of this study is to compare the results of the analyses completed by both close-range photogrammetry and close-range precision surveying, the target design and distribution density should be the same for both evaluations. Numerous examples can be found in the literature of studies of complex surface targetting, particularly for reflector antennas [Ockert (1959), Marks (1963), De Vengoechea (1965), Forrest (1966), Bopp et al. (1977), El-Hakim (1984), Oldfield (1985), and Fraser (1986)]. However, variation in project

requirements for the above examples leads to an inadequate general rationalization for the distribution and density of points. The criterion for point density and distribution should then rest with the eventual goal of this study. For example, the often used radial distribution of points on the antenna is adequate for the computation of a number of best fitting parabolas which can be subsequently combined to provide a best fitting paraboloid for the surface. However, the global determination of surface deviations is missed due to the large gaps between points near the outer edges of the antenna. It has been shown (Zarghamee, 1967) that surface deviations tend to be more significant on the outer surface of a reflector. Conversely, a grid pattern provides a more uniform surface survey for deformations but presents some problems in surface fitting. These will be examined in Chapter 7.

After much consideration, it was decided that a grid system for the targetted points would provide the maximum information about surface deviations and thus was adopted. A uniform grid was selected with nodal spacing of 5 mm accepted as a maximum. At this spacing, approximately 320 separate targets should be placed on the antenna, representing a density of one target per 24.5 cm^2. In a similar study (Fraser, 1986) on a 2.9 m diameter antenna, a total of 930 targets were placed on the reflector surface. There is a tradeoff between the time needed to measure these targets in a multi-convergent photogrammetric analysis and the desired accuracy of the results. Naturally an infinite number of targets would provide the most informative results but is hardly practical.

To attain the best possible accuracy, targets must be designed so

that the measuring mark of the instrument can be placed on the target with consistent accuracy. Targets must have five fundamental characteristics to achieve this goal:

a. High contrast;

b. No variation due to illumination (phase);

c. Symmetry;

d. Proper area of reference;

e. Freedom from errors of orientation.

This project demanded the optimization of a target which would serve successfully for both the geodetic and photogrammetric instrumentation to be used. In optical tooling a target of concentric circles is often used to achieve the above properties. Black concentric circles on white or yellow backing are perhaps the best for photogrammetric projects demanding high accuracy requirements (Erlandson and Veress, 1975). For photogrammetric purposes the minimum diameter of the target dot, D_{min}, is:

$$D_{min} = d \cdot \frac{S}{f} \qquad (4.6)$$

where d = size of the measuring mark
S = photo scale
f = focal length

An illustration of the targets used in this work is given in Figure 4.3. The target designator was placed vertically below the actual target to simplify its generation on a MacIntosh microcomputer.

The material upon which the targets were printed was a mild adhesive white strip of paper, designed to blank out material prior to photocopying. This commercially available product was inexpensive and adhered well to the antenna surface without any cleaning of the

reflector prior to application.

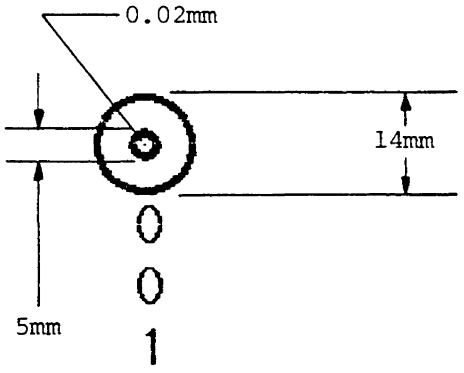

Figure 4.4: Target Used in Study

4.5.2.2 Control Point Selection

The amount of object space control needed in a photogrammetric evaluation is directly related to the data reduction approach selected including the number of additional parameters contained in the mathematical model. The selection of the number and geometry of these control points is critical. In recent studies, several factors have been pointed out for consideration when selecting object space control points (MacRitchie, 1977; Moniwa, 1977; Abdel-Aziz, 1982; Fraser, 1984; Chen, 1985; and Faig and Shih, 1986). These can be summarized as:

a. The optimum solution of bundle adjustments is obtained when the object is surrounded by the control points;

b. The final accuracy of the computed object coordinates will not exceed the accuracy of the established control points;

c. The control must be three dimensional to avoid ill-conditioning in the adjustment whether a DLT solution or bundle solution is attempted;

d. The number of iterations required to obtain convergency is sensitive to the amount, type, and location of the object control available; and

e. If the number of control points is not sufficient, the accumulation of errors in the orientation elements will cause significant errors in the adjusted coordinates.

4.5.2.3 Imaging System and Geometry

Of all the cameras considered for this project, the non-metric amateur camera was most flexible and readily available. This also holds true in an industrial setting. Accepting increased project costs due to more elaborate computations to account for additional parameters, an imaging scheme of four photographs in a fully convergent mode was used. This imaging geometry is illustrated in Figure 4.3.

It has been shown that the use of additional camera stations can be expected to not only improve precision, but also significantly enhance the network reliability (Fraser, 1984). An optimum balance, however, must be sought between the highest possible precision and the economics of performing numerous image coordinate measurements on the comparator.

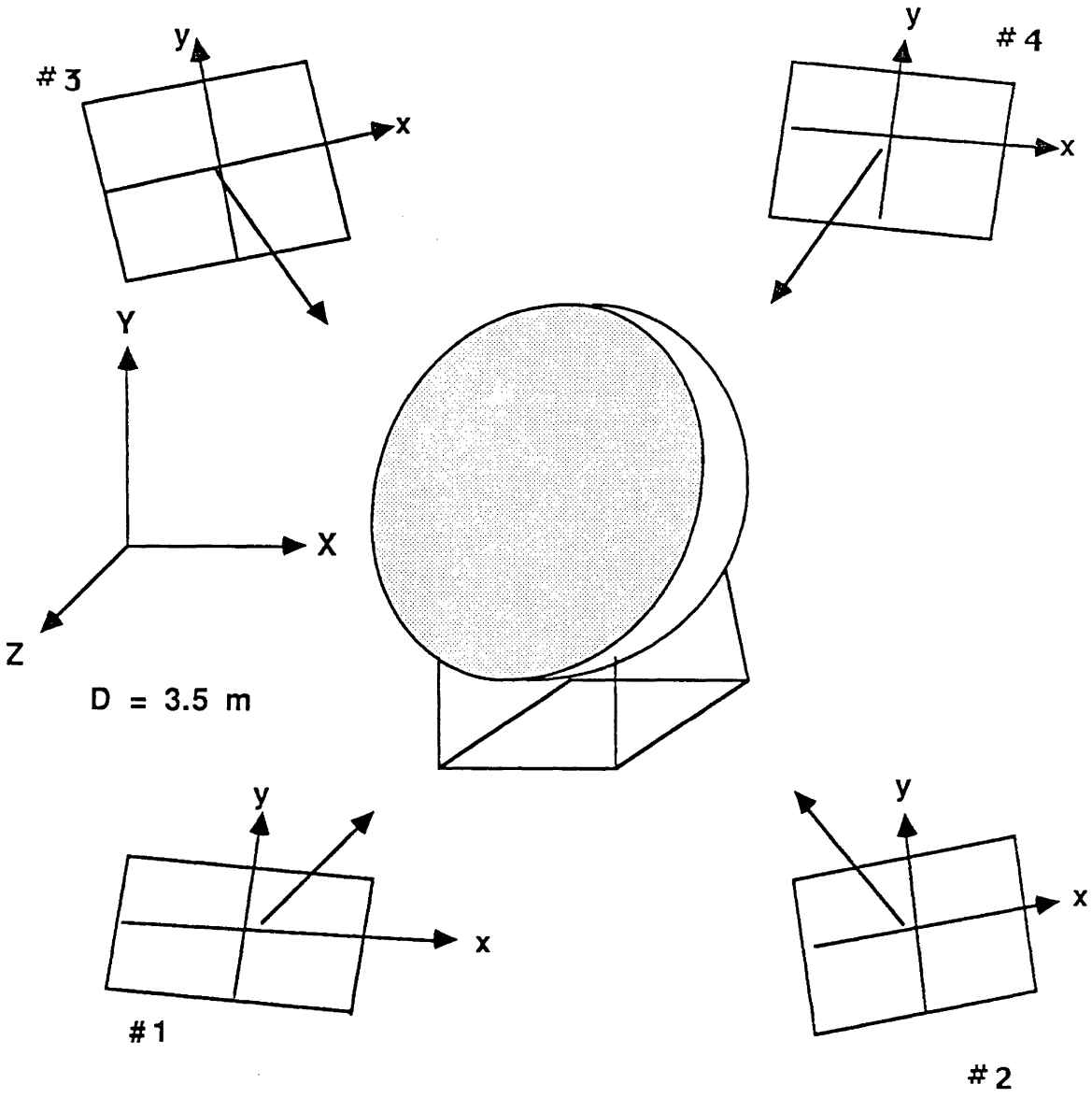

Figure 4.5: Imaging Geometry

By the same token, multiple exposures at one camera station have been shown as a simple way of enhancing accuracy (Fraser, 1982A; Barnard, 1983). In this project two photographs were taken at each camera station as a safety measure only.

The Canon T-50 has an approximate focal length of 53 mm. To ensure high contrast in the imagery, the film used was black-and-white Pan

Plus-X. A film speed of 125 was selected to attempt to optimize contrast and reduce image blur. It has been shown in various studies (Karara and Abdel-Aziz, 1974, Fraser, 1984) that optimum base/distance ratios for close-range photogrammetry vary from 0.8 to 1.2. In this project a base/distance ratio of 1.0 was attempted. The optimum photo scale is closely related to this ratio with scales of 1:25 to 1:30 being most desirable, especially for objects with little depth variation. However, in order to include spatial distances from levelling rods in the photography, it was found that the largest possible scale was 1:70.

4.5.2.4 Depth of Field

The depth of field is an important consideration in order to avoid poorly focused image points. Derived by Faig, (1972A) are the following formulas for near field limit (NFL), far field limit (FFL), and depth of field (DOF):

$$NFL = \frac{bdf}{bd+cf-df} \tag{4.7}$$

$$FFL = \frac{bdf}{bd-cf-df} \tag{4.8}$$

$$DOF = \frac{2acdf(a-f)}{d^2f^2-c^2(a-f)^2} \tag{4.9}$$

where

a = object distance
b = image distance
c = diameter of circle of confusion
d = diameter of diaphragm opening
f = focal length

For each camera the parameters b,c,d and f are fixed and a can be easily approximated to provide the user with an estimation of the depth of field.

4.5.2.5 Additional Parameters

Since non-metric photography was used in this project self-calibration is required as part of the data reduction process. Most additional parameter formulations suffer from high intercorrelations (see Chapter 6). Also, in order to determine statistically significant additional parameters a strong imaging scheme and adequate distribution of control points and object points is needed.

4.5.3 Second-Order Design (SOD)

SOD refers to the global variance of the coordinate measurements of image points (Chen, 1985). The three conditions which will affect precision in image point measurement include:

a. the use of higher-precision comparator;

b. multiple image coordinate measurements;

c. multiple exposures.

These three factors will now be considered.

4.5.3.1 Comparator Considerations

At the University of New Brunswick the instrumentation available for coordinate measurements is listed in Table 4.2. The Zeiss PSK-2 Stereocomparator was used for the measurement of image coordinates for this work due to its inherent higher accuracy. At UNB the PSK-2 is presently interfaced with an Altek digitizer and subsequently the IBM 3090 mainframe computer. Recent developments with the OMI AP-2C analytical plotter on-line data acquisition capabilities (Armenakis and Faig, 1986) reduces the time needed to measure each photograph. However, this system is not currently interfaced with the IBM 3090

mainframe and the additional step of data transfer through with magnetic tapes slows data acquisition.

Instrument	Least Count	Accuracy (RMS)
1. Wild A-10 Autograph	10 μm	20 μm
2. AP-2C Analytical Plotter	1 μm	5 μm
3. Zeiss PSK-2 Stereocomparator	1 μm	3-5 μm
4. 2-D Cartographic Digitizer	10 μm	20 μm

Table 4.2: Photogrammetric Point Measurement Instrumentation at UNB (Source: Manual of Photogrammetry, 1980)

4.5.3.2 Multiple Image Coordinate Measurements and Multiple Exposures

Theoretically, the precision improvement for coordinates of image points is proportional to the square root of the number of measurements. In this aspect of the SOD problem it is possible either to measure a point n times or the same point in each of the n images. The latter approach averages the systematic errors over n images. For this project, each image coordinate was measured three times. With such a large number of photocoordinates to measure (340/photo x 4 photos = 1360) it was felt that multiple pointings beyond this number would not be economical. MacRitchie (1977) points out that accuracy improvement after ten repetitions is minimal. From a reliability point of view three repetitions, rather than two, allowed for easier detection of blunders.

4.5.4 Third-Order Design (TOD)

The Third-Order Design problem is described by Grafarend (1974) as the densification problem. Effectively, TOD is solved at the FOD stage, and TOD generally need not be separately considered in a photogrammetric network optimization (Fraser, 1986).

CHAPTER 5

DATA ACQUISITION AND REDUCTION

The acquisition and reduction of data in industrial surveys requires the 3-dimensional point positioning of either pre-targetted or readily identifiable object points. Using the two survey techniques discussed, slightly different steps are needed to complete the data acquisition and reduction phases. Using precision surveying, data acquisition merely involves angular measurements of object points and the data reduction is completed with the computation of spatial coordinates for these points. For close-range photogrammetry data acquisition involves the determination of control points in a similar fashion, plus the exposure and development of photographs followed by photo-coordinate measurement of object and control points. Data reduction involves the further analytical processing of control point and image coordinates to densify the object space coordinates.

5.1 Object Preparation

The convenience and comfort of a laboratory environment with controlled external influences, e.g. temperature, wind, heat, etc., was available to study the antenna. Also, due to the relatively stable and undisturbed location of the laboratory in Head Hall, a prolonged investigation of the antenna was possible.

To prepare the antenna for angular observation and photography, it was simply moved into position approximately 3.5 metres away from each of the two theodolite stations. The antenna was left at an arbitrary angle to the horizon for measurement purposes. The necessary

photogrammetric control devices were positioned around the antenna. These external objects included a subtense bar which was mounted on a table above the antenna, and three levelling rods positioned around the antenna so that they would appear near the edges of the photography.

Since the antenna horn was not to be measured and its assembly and the four supporting struts only obstructed observation of the entire paraboloid surface, this assembly was removed for the data acquisition phase of the project. The final phase of the object preparation involved the positioning of computer generated targets onto the surface. To cope with the large number of targets, they were established in numerical sequence from 1 to 320 in vertical rows on the antenna (see Figure 4.2). The five centimetre target spacing specified in the preanalysis was adhered to as best as possible, but due to the concaveness of the antenna this was not always possible. However, a random scattering of object points in a quasi-grid fashion was envisioned from the outset.

5.2 Antenna Positioning

It is important to mention that in most reflector antenna calibration studies the antenna positioning would not be as flexible as in this project. Often, antennas are permanently mounted on structures and their operation cannot be interrupted for long periods of time. This would exemplify one of the advantages of using photogrammetry in reflector antenna calibration studies. After the targets are placed and minimal control requirements are met, numerous epochs of photography could be acquired with subsequent analysis by the photogrammetrist away from the antenna installation.

5.3 Acquisition of Geodetic Control

Before control point acquisition can begin, certain aspects of optimal control point selection must be understood. Although three object-space control points in a bundle solution and six object-space control points in the direct linear transformation provide a unique solution, the incorporation of more control will improve the reliability of the solution by increasing the overdetermination. In tests on both methods, optimum numbers of control points have been established beyond which it is not worth the time and effort to provide more for the solution. For the direct linear transformation the optimum number of full control points is 20 to 25 [Karara and Abdel-Aziz (1974), Chen (1985)]. For the various bundle adjustment solutions used, the optimum number of control points will of course vary, however 7 to 10 usually yields the best results (Chen 1985). The only stipulation for control point selection is that as much variation from the planar configuration as possible is needed, especially in the DLT solution (Faig and Shih, 1986).

For this study the Kern E-2 theodolite was used to measure the base distance and observe 25 preselected control points by intersection. In order to achieve the required high order of accuracy on such a short base distance, the double resection method, using a subtense bar was found to be most suitable. Observations included three sets of directions with both faces of the theodolite to the two targets of the subtense bar. The estimated standard deviation of the base distance was computed as σ_B = 0.01mm. To determine the coordinates of the control points the same theodolite and observer were used at both stations, and vertical and horizontal directions to the points were observed with one

face of the theodolite. The collimation and index errors were estimated by siting ten times to a fixed target in both faces of the theodolite. Corrections for these errors were made in a program (CONTROL) developed by the author to compute the final object coordinates.

In order to maintain the imposed accuracy by trigonometric levelling, the elevation difference between the theodolite set-ups was determined by measuring the height difference from each theodolite station to several targetted points. The average of the height differences to each point was then used as the difference in elevation between the two theodolite stations. This height difference was also computed in the program CONTROL and amounted to 24.388 mm with a standard deviation of 0.015 mm.

Now, applying a post control acquisition error propagation using the estimated errors for the observations and the derived formulae, the standard deviations of the control coordinates were estimated to be:

$$\sigma_x = 0.04 \text{ mm}$$

$$\sigma_y = 0.04 \text{ mm}$$

$$\sigma_z = 0.05 \text{ mm}.$$

The program CONTROL was also adopted to produce listings of the control points in formats compatible with the data reduction programs UNBASC2, GEBAT-V and DLT, for ease of subsequent execution. This included the transformation of the control acquisition data into a system compatible with the collinearity condition.

5.4 Acquisition of Photography

In close-range photogrammetric projects it is essential that

geodetic control acquisition and photography be performed concurrently if there is any fear of object movement. Four convergent photographs were considered sufficient with camera stations being located such that few points on the antenna surface would be lost due to the shape of the parabolic reflector.

Kodak black-and-white Pan Plus-X film (speed 125) was used to maximize image contrast. The lighting in the laboratory consisted of two rows of fluorescent fixtures which make the laboratory extremely bright. Therefore, additional artificial illumination was not needed for the project. In addition, reflection from the surface of the antenna could have posed problems had a flash unit been used. The photos were taken in a hand-held fashion due to the short exposure time used. The shutter speed was selected at 1/11. Figure 5.1 shows the four photographs used in this study.

Immediately after photographing the antenna, the film was developed using standard 35 mm darkroom techniques. The negatives were allowed time to dry and were placed in the Zeiss PSK-2 comparator immediately to check image contrast for subsequent photo-coordinate measurement. A good contrast and pointing to each target was found. Using approximate calculations it was determined that a photo scale of 1:70 was obtained. A larger scale (e.g. 1:30) would have provided better pointing accuracy at the targets on the antenna, however it was necessary for subsequent evaluation to include the levelling rods which surround the antenna in the images.

5.5 Measurement of Image Coordinates

In this study all the object points appeared on each photograph.

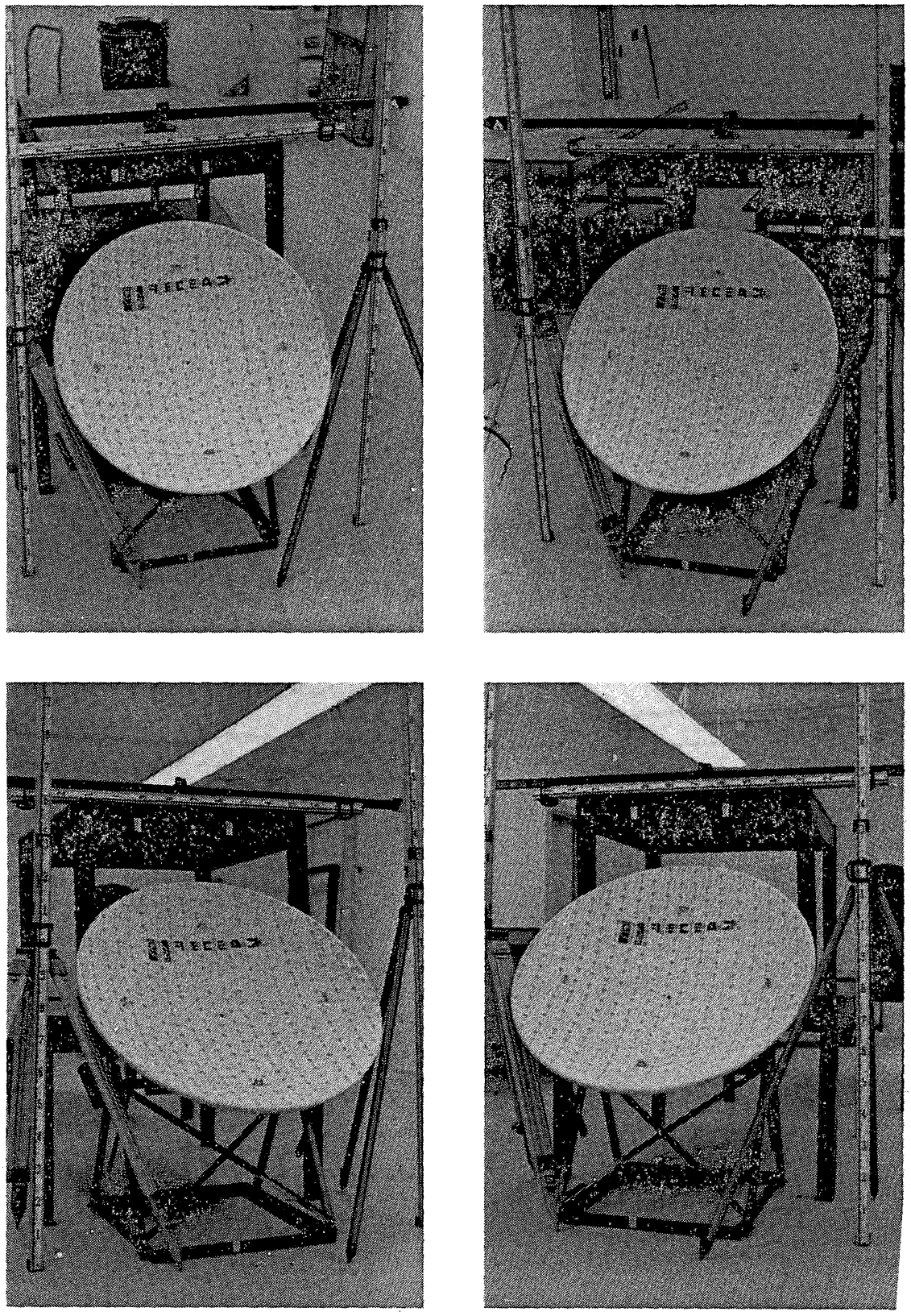

Figure 5.1: Photographs used in Antenna Evaluation

For each of the four negatives, the following points were identified and observed:

a. Three control points external to the antenna surface (points 318,319 and 320); These points appear in Figure 5.1. Points 318 and 319 were mounted above the antenna on the side of a table and point 320 is located on the base of the Antenna support stand;

b. 317 object points on the antenna surface (points 1 to 317);

c. 20 control points on three levelling rods surrounding the antenna (points 400 to 419).

The Zeiss PSK-2 stereocomparator was used for these measurements. The four negatives were placed in the right stage plate of the comparator, with the emulsion side facing the optical system. This prevents distortions of the measurements due to refraction of the ray path through the film material. As pointed out by Trinder (1972), systematic errors in pointing can be reduced if the measuring mark is placed on the target from opposite directions. This practice was employed in the three repetitions decided upon in the preanalysis. The raw comparator coordinates were stored on files in the IBM 3090 mainframe computer. Post acquisition sorting and comparison of coordinates were achieved using a utility program (PHOTOAV3) developed by the author for this purpose. The final coordinates were then printed in formats compatible with the subsequent adjustment programs and saved on separate files.

5.6 Photogrammetric Software for Non-Metric Photography

Since non-metric imagery is not usually equipped with fiducial

marks, a number of unique data reduction algorithms have been developed which do not require the transformation from comparator coordinates to image coordinates prior to subsequent computations. These include:

(i) the Direct Linear Transformation (DLT) approach (Abdel-Aziz and Karara, 1971; Marzan and Karara, 1975).

(ii) the 11 parameter solution (Bopp and Kraus, 1977, 1978).

(iii) The University of New Brunswick Analytical Self-Calibration method (Faig, 1975; Moniwa, 1972; Moniwa, 1977; El-Hakim et al., 1979).

If initial approximations are available for the principal point and various other parameters, a number of additional bundle solutions can be used with non-metric imagery. The concern here is that the particular algorithm be capable of solution in the photo-variant mode of computing additional parameters (AP's).

At the University of New Brunswick, several bundle solutions are available for use with non-metric photography. These are:

i. UNBASC2 (University of New Brunswick Analytical Self-Calibration - Moniwa, 1977);

ii. GEBAT-V (General Bundle Adjustment Triangulation Photo-Variant - El-Hakim, 1982).

As part of this research an additional program has been incorporated on the IBM 3090 at UNB. This is the Direct Linear Transformation with Data Snooping (Chen, 1985). There are other algorithms which are suitable for reduction of non-metric photography, such as:

i. BINGO (Bundelausgleichung for INGenieur Objekte - Kruck, 1984);

ii. CRABS (Close Range Analytical Bundle Solution - Kenefick, 1977);

iii. CRISP (Close Range Image Set-up Program - Fuchs and Leberl, 1984).

iv. GENTRI (GENeral TRIangulation System - Larsson, 1983);

v. MOR (Mehrbid ORientierung - Multiple Image Orientation - Wester-Ebbinghaus, 1985);

vi. SAPOCR (Simultaneous Adjustment of Photogrammetric Observations for Close Range Applications - Wong and Elphingstone, 1972).

This sample of additional software systems is further described in Faig (1987) and illustrates that numerous data reduction schemes are available for industrial close-range applications.

5.7 Compensation of Systematic Image Errors

In bundle adjustments and the direct linear transformation, systematic image errors have been compensated for with the introduction of additional parameters to model their influences. This is done by improving the mathematical model (collinearity equations) to include the compensation parameters Δx_p and Δy_p as follows:

(i) Bundle Adjustment with additional parameters:

$$\frac{x_p - x_o + \Delta x_p}{-c} = \frac{(X_p-X_c)m_{11} + (Y_p-Y_c)m_{12} + (Z_p-Z_c)m_{13}}{(X_p-X_c)m_{31} + (Y_p-Y_c)m_{32} + (Z_p-Z_c)m_{33}} \qquad (5.1)$$

$$\frac{y_p - y_o + \Delta y_p}{-c} = \frac{(X_p-X_c)m_{21} + (Y_p-Y_c)m_{22} + (Z_p-Z_c)m_{23}}{(X_p-X_c)m_{31} + (Y_p-Y_c)m_{32} + (Z_p-Z_c)m_{33}}$$

(ii) DLT with additional parameters:

$$x_p + \Delta x_p = \frac{L_1 X_p + L_2 Y_p + L_3 Z_p + L_4}{L_9 X_p + L_{10} Y_p + L_{11} Z_p + 1} \qquad (5.2)$$

$$y_p + \Delta y_p = \frac{L_5 X_p + L_6 Y_p + L_7 Z_p + L_8}{L_9 X_p + L_{10} Y_p + L_{11} Z_p + 1}$$

Traditionally the compensation terms for systematic errors are composed of polynomial functions of the radial distance to express distortions such as radial lens distortion, affine distortion, and decentering distortion. Murai et al. (1984) provide a listing of some of the published compensation terms, together with a comparison of results achieved with each.

The difficulty with polynomial functions is that when applying them, symmetry is assumed in the error distribution, and thus the systematic errors are only partially removed while even larger errors may be produced in areas which are poorly controlled (El-Hakim and Faig, 1977). As a result the use of spherical harmonics has been developed at the University of New Brunswick to model the combined effects of systematic errors and has been incorporated into the GEBAT family of program packages (El-Hakim, 1982).

5.8 Comparison of Mathematical Models

In evaluating the experimental data for the calibration of the reflector antenna the three software packages investigated provided different solutions for the collinearity condition. The direct linear transformation with data snooping is the only non-iterative solution. Since the collinearity equations are non-linear in the bundle adjustment, they need to be linearized by Taylor expansion at an

approximate value which leads to an iterative solution. The various mathematical models used in each program for the compensation of systematic effects are now compared.

5.8.1 Program UNBASC2

The program UNBASC2 employs the photo-variant mode of analytical self-calibration and is ideally suited for non-metric evaluations of this nature. The modified collinearity equations (5.1) are employed with additional parameters to correct for lens distortions, film deformation and affinity, along with the elements of interior orientation. All of these parameters are computed for each individual photograph involved in the solution. The following polynomials are used to correct for:

a. Radial Lens Distortion:

$$dr_x = (x-x_o)(k_1r^2+k_2r^4+k_3r^6) \tag{5.3}$$

$$dr_y = (y-y_o)(k_1r^2+k_2r^4+k_3r^6) \tag{5.4}$$

b. Decentering Lens Distortion (tangential and assymetric radial lens distortion):

$$dp_x = p_1\,[r^2 + 2(x-x_o)^2] + 2p_2(x-x_o)(y-y_o) \tag{5.5}$$

$$dp_y = p_2\,[r^2 + 2(y-y_o)^2] + 2p_1(x-x_o)(y-y_o) \tag{5.6}$$

c. Affinity (film distortion):

$$dq_x = A(y-y_o) \tag{5.7}$$

$$dq_y = B(y-y_o) \tag{5.8}$$

where

x_o, y_o are coordinates of the principal point;

k_1, k_2, k_3 are parameters of radial symmetric lens distortion;

p_1, p_2 are the parameters of decentering lens distortion;

A,B are the parameters of affine film deformation;

x,y are image coordinates of the photo point; and

$r^2 = (x-x_o)^2 + (y-y_o)^2$ [radial distance].

These additional parameters: k_1, k_2, k_3, p_1, p_2, A and B plus the three basic interior orientation parameters (x_o,y_o and c), six exterior orientation parameters (X_C,Y_C,Z_C,ω,ϕ,κ) and the three object point unknowns (X_p,Y_p and Z_p) constitute the unknowns in the mathematical model of self-calibration employed in the program UNBASC2 (Moniwa, 1972 and 1977). More recently, considerations for constraining all distortion parameters to a system of harmonic functions has been investigated by Moniwa in the program CMPASC3. Preliminary test results show an improvement of approximately 40 percent over the polynomial formulations (Moniwa, 1981).

5.8.2 Program GEBAT-V

The program GEBAT-V is a combined photogrammetric and geodetic self-calibrating bundle adjustment program designed for close-range non-metric applications. Derived from the general GEBAT system (El-Hakim, 1982), the geodetic observations are restricted to spatial distances and height differences. In addition, gross error detection is applied using Baarda's data snooping approach. Along with the adjustment results provided in the standard bundle adjustment solution, a variance-covariance matrix and error ellipsoid for each adjusted object point are provided.

The modified collinearity equations (5.1) are employed as the photogrammetric mathematical model. The two geodetic observation equations are:

a. Slope Distance, S_{ij}:

$$V_{S_{ij}} = C_1(dX_j - dX_i) + C_2(dY_j - dY_i) + C_3(dZ_j - dZ_i) + (S_c - S_o) \qquad (5.9)$$

where

$$C_1 = (X_j - X_i)/S = \Delta X/S$$
$$C_2 = (Y_j - Y_i)/S = \Delta Y/S \qquad (5.10)$$
$$C_3 = (Z_j - Z_i)/S = \Delta Z/S$$

where S_c is computed as $[(\Delta X)^2 + (\Delta Y)^2 + (\Delta Z)^2]^{\frac{1}{2}}$ using approximate coordinates X,Y,Z of points i and j, and S_o is the observed value.

b. Elevation Differences, ΔH_{ij}:

$$V_{\Delta H_{ij}} = (Z_j - Z_i) - \Delta h_o \qquad (5.11)$$

In GEBAT-V the additional parameters do not explicitly contain distortion parameters commonly found in bundle solutions (e.g. UNBASC2), but the correction terms in the collinearity equations (5.1) are replaced by:

$$dV_x = (x_A - x_o) \cdot T \qquad (5.12)$$

$$dV_y = (y_A - y_o) \cdot T \qquad (5.13)$$

with T being the harmonic function;

$$T = a_{00} + a_{11}\cos\lambda + b_{11}\sin\lambda + a_{20}r + a_{22}r\cos 2\lambda + b_{22}r\sin 2\lambda + a_{31}r^2\cos\lambda + b_{31}r^2\cos\lambda + a_{33}r^2\cos 3\lambda + b_{33}r^2\sin 3\lambda + \ldots \qquad (5.14)$$

where

$$\lambda = \tan^{-1}\left[\frac{y - y_o}{x - x_o}\right]$$

$$r = [(x - x_o)^2 + (y - y_o)^2]^{\frac{1}{2}}$$

5.8.3. Program DLT with Data Snooping

The program DLT is a modification of the Direct Linear

Transformation approach developed at the University of Illinois (Abdel-Aziz and Karara, 1971, 1973; Karara and Abdel-Aziz, 1974). The program is an extension to that published by Marzan and Karara (1975) and was developed by Chen (1985) as part of investigations of a three-phase modular adjustment scheme.

In the DLT solution a capability for correction of systematic errors follows the traditional method using the following polynomials:

$$\Delta x = (x-x_o)\ (k_1 r^2 + k_2 r^4 + k_3 r^6) + p_1\ [r^2 + 2(x-x_o)^2] + 2p_2\ (y-y_o)(x-x_o) \qquad (5.15)$$

$$\Delta y = (y-y_o)\ (k_1 r^2 + k_2 r^4 + k_3 r^6) + 2p_1\ (x-x_o)(y-y_o) + p_2\ [r^2 + 2(y-y_o)^2] \qquad (5.16)$$

Table 5.1 illustrates the various data reduction modes (correction of systematic errors) possible when utilizing the DLT. Therefore the number of parameters of interior orientation can be stipulated by the user just as in UNBASC2. It has been found however, on the basis of experimental investigations (Karara and Abdel-Aziz, 1974) that the term k_1 need only be taken into account in modelling lens distortion and film deformations. In developing a modular adjustment scheme, Chen (1985) has incorporated a data snooping routine in the DLT similar to that used in GEBAT-V for blunder detection, localization and subsequent elimination. Since using blunder detection in GEBAT-V is very time-consuming and expensive the approach of eliminating large blunders using the DLT first is a more economical and efficient way to arrive at a solution. Also, any approximations needed in GEBAT-V are calculated

CORRECTION OF SYSTEMATIC ERRORS IN THE DLT SOLUTION			
Systematic Errors Corrected	Unknowns in DLT Solution	Number of Unknowns	Minimum Number of Spatial Control Points
Linear components of film deformation, lens distortion and comparator errors	L_1 to L_{11}	11	6
Linear components as above and symmetrical lens distortion (first term only)	L_1 to L_{11} k_1	12	6
Linear components as above and symmetrical lens distortion (first three terms only)	L_1 to L_{11} k_1, k_2, k_3	14	7
Linear components as above symmetrical lens distortion (first three terms) and asymmetrical lens distortion	L_1 to L_{11} k_1, k_2, k_3 P_1, P_2	16	8

Table 5.1: Correction of Systematic Errors in the DLT Solution (Source: Atkinson, 1980)

at the same time. This approach has been evaluated in this report.

5.9 Data Reduction by Photogrammetry

The photogrammetric data reduction was completed using the Computing Centre facilities at the University of New Brunswick. Currently the computing system consists of an IBM 3090-180 with vector facility. It has 32 megabytes of memory and executes floating point instructions at a scalar rate of 17 million per second. The vector rate is up to 5 times faster. Evaluating bundle adjustment programs on such a system may be misleading since most industries would not have access to such computational power. However, for the purpose of this study the mainframe computer at UNB was the most readily available.

5.9.1 Analytical Evaluation Using UNBASC2

In the mathematical formulation used in UNBASC2, the fact that some of the parameters are strongly correlated is a disadvantage. This sometimes results in an ill-conditioned system of normal equations. Appendix II lists these correlations between the parameters as found by Moniwa (1977). As a result, these correlations must be considered when assigning an iteration segmentation. The program is quite flexible beyond this difficulty and the user can remove or add any desired parameters from the mathematical model by so specifying in the input.

The following iteration segmentation was found to be the most effective in achieving convergency in this project.

Iteration Segmentation	Iterations
XC,YC,KP,X,Y	(1)
XC,PH,X,Y	(1)
XC,OM,Y,Z	(1)
XC,YC,ZC,OM,PH,KP	(4)
XC,YC,ZC,OM,PH,KP,X,Y,Z	(5)
XC,YC,ZC,OM,PH,KP,X,Y,Z,AFF	(3)
XC,YC,ZC,OM,PH,KP,X,Y,Z,X0,Y0,PD,AFF	(5)
XC,YC,ZC,OM,PH,KP,X,Y,Z,X0,Y0,PD,AFF,RAD	(5)
XC,YC,ZC,OM,PH,KP,X,Y,Z,X0,YO,PD,AFF,RAD,DEC	(7)

where

XC,YC,ZC	are Perspective Centre Coordinates
OM,PH,KP	are Tilt, Tip and Swing Rotations
X,Y,Z	are Object Space Coordinates
X0,Y0	are Principal Point Coordinates
PD	is the Principal Distance
RAD	are Radial Lens Distortion Parameters
DEC	are Decentering Distortion Parameters
AFF	are Affine Distortion Parameters

Therefore, two points must be remembered when selecting an iteration sequence for UNBASC2. First, iteration steps should not contain parameters which are highly correlated until the solution converges. Also each step should be allowed sufficient convergence before proceeding onto the next. Generally, good results can be obtained with the minimum two planimetric and three vertical control points but optimum results are obtained with reduced control when control points are selected at four corners surrounding the object.

5.9.2 Analytical Evaluation Using GEBAT-V

The program package GEBAT-V has a number of advantages over other bundle adjustment solutions for non-metric evaluations in industrial applications. These include the direct incorporation of geodetic observations, the capability to perform error propagation upon completion of the adjustment through the generation of error ellipsoid

information, and the blunder detection capabilities by data snooping. However, the major disadvantage found with GEBAT-V is the need for a vast number of initial approximations at the initial point of linearization. This precludes GEBAT-V from being used as a stand-alone data reduction scheme for non-metric imagery. With the assistance of a direct linear transformation program to generate such initial approximations this problem is solved. In this study both the use of spatial distances and data snooping were evaluated. Of the twenty points selected on the invar rods at least one third were singled out in the data snooping results. This was due to the fact that these points appeared on the outer edges of the photographs and were not as easy to point to in the comparator as the computer generated targets. Another difficulty with the program GEBAT-V in its present configuration is that it is only capable of handling four photographs and a maximum of 80 object points. Both of these can be altered, as was required in this evaluation, by changing various statements in the Fortran source code. However, a large increase in points might not be possible depending on limitations of the computer system used. For numerous object points or extremely complex objects, a breakdown into several solutions may be more feasible than increasing these limits.

5.9.3 Analytical Evaluation Using DLT

The program package DLT with data snooping was modified to handle all 320 points in the evaluation of the reflector antenna. It was also solved using the four possible schemes illustrated in Table 5.1. The only difficulty is that the selection of control points alluded to earlier is quite critical. The accuracy of the DLT solution is expected

to be slightly lower than that of bundle solutions. Chen (1985) points out the following reasons for this:

a. Some of the 11 coefficients, which are considered as independent of each other are actually not;

b. Coordinates of non-control image points play no role in the determination of the projective transformation parameters and additional parameters;

c. In the resection stage, coordinates of control points are treated as fixed.

Therefore the errors in the object-space control point coordinates are absorbed in the 11 coefficients and the additional parameters. In compensating for these difficulties the DLT with data snooping incorporates a number of innovations. First, data snooping schemes for both resection and intersection are provided. The only difficulty in the existing program is that the critical value for data snooping is hard-coded into the program. Secondly, the orientation parameters are calculated for each photograph for subsequent use in GEBAT-V. Finally iterations are introduced into the DLT solution to improve the accuracy. The primary advantage of the DLT solution is the considerable saving in computational time realized.

5.10 Data Acquisition Using Electronic Theodolites

The measurement of the reflector antenna using electronic theodolites involves data acquisition and reduction simultaneously. In this practical application four data reduction systems have been developed at UNB. This involved the development of software packages for each of the following microcomputers:

a. the MacIntosh PC;

b. the Epson HX-20;

c. the Hewlett-Packard HP71B; and

d. the Radio Shack TRS80

For all the systems, software was needed to support communications with the Kern E-2 theodolite. Then in the operational mode, a package first had to be developed to check the theodolite vertical index errors and horizontal collimation errors. A second set of routines were needed for computing the scale for the local X,Y,Z system. Next, mutually collimating software was prepared for the measurement of individual points on the antenna surface. Finally, various means of data transfer to the IBM 3090/VF mainframe computer were examined for further analysis of the reflector. This research, conducted by the engineering surveying group at UNB, supported the notion of interfacing relatively inexpensive computers to electronic theodolites. The subsequent point mensuration was conducted by each member of the group using the various personalized software packages.

CHAPTER 6

EVALUATION OF RESULTS

The analytical reduction of data is perhaps the most time consuming and yet important aspect of a project. In industrial applications involving virtually hundreds of object points this process is lengthened and can be prone to blunders if care is not taken and checks completed. The use of photogrammetry enables a more flexible approach to completing this object point densification problem at the expense of additional intermediate steps away from the project site. The utilization of elaborate analytical photogrammetric solutions can be a time consuming process where the results may not be available for several days. Conversely, the use of electronic theodolites provides immediate results with the difficulty of requiring both the object and theodolites to be stationary for long periods of time. In this chapter an evaluation of results is presented with an elaboration on the advantages and shortcomings of each method.

6.1 Close-Range Photogrammetry

With the necessary control points and files containing all the observed photo coordinates it was then possible to investigate the three available solutions. The program UNBASC2 was attempted first as it required no additional approximations for a solution. With knowledge of the camera station positions and orientations, GEBAT-V was next examined. Finally the Direct Linear Transformation with data snooping was brought on-line and utilized. This is not necessarily the order of evaluation which would have been chosen had the author been experienced in all

three programs at the outset.

6.1.1 Results with UNBASC2

The program UNBASC2 has great potential for non-metric applications of this nature. However, the selection of parameters for each iteration is often difficult due to the intercorrelations between them. Often times the user finds difficulty dealing with an ill-conditioned system of equations and can expend much computational effort in arriving at a proper solution. With the particular data at hand it was found that two of the control points away from the antenna surface caused problems in attaining convergency. With these two points eliminated (points 318 and 319) a solution could be found. Another important aspect when using any bundle adjustment program is the appropriate selection of weights for both control and photo coordinates. This was particularly the case when using UNBASC2.

Various indicators are useful to ensure that the adjustment is converging to a proper solution when using UNBASC2. The first indicator can be the comparison of the derived principal distance with that known for the camera a-priori. The proper assignment of weights is critical in this respect. The next step is to check the residuals of the photo point coordinates to see if any obvious outliers can be detected. These points can be eliminated and the program rerun. In a similar fashion the residual parallaxes at the object points can be compared to determine the quality of the adjusted object point positions.

In Tables 6.1, 6.2 and 6.3 various results of computations with differing additional parameters are listed for the program UNBASC2. For

Number of Control (used) H - V	(check) H - V	Calibration Parameters	Residuals at Image Points [rms in mm] (x)	(y)	Residual Parallaxes at Object Points [rms in mm] (X)	(Y)	(Z)	Residuals Check Points [rms in mm] (X)	(Y)	(Z)	# of Unk	# of Iter	Total CPU (sec)	CPU sec per It.
23 - 23	0 - 0	-	0.005	0.006	0.289	0.387	0.147	-	-	-	1020	15	17.02	1.13
23 - 23	0 - 0	x_o, y_o, c	0.003	0.003	0.209	0.202	0.101	-	-	-	1032	17	26.52	1.56
23 - 23	0 - 0	x_o, y_o, c k_1, k_2, k_3	0.003	0.003	0.173	0.185	0.083	-	-	-	1044	25	44.04	1.76
23 - 23	0 - 0	x_o, y_o, c p_1, p_2	0.003	0.003	0.196	0.193	0.096	-	-	-	1040	25	43.30	1.73
23 - 23	0 - 0	x_o, y_o, c A, B	0.003	0.003	0.194	0.188	0.090	-	-	-	1040	21	40.82	1.94
23 - 23	0 - 0	x_o, y_o, c k_1, k_2, k_3 p_1, p_2	0.002	0.003	0.163	0.176	0.079	-	-	-	1052	31	65.42	2.11
23 - 23	0 - 0	x_o, y_o, c p_1, p_2 A, B	0.003	0.003	0.190	0.186	0.088	-	-	-	1048	28	62.63	2.24
23 - 23	0 - 0	x_o, y_o, c k_1, k_2, k_3 A, B	0.002	0.003	0.160	0.178	0.079	-	-	-	1052	29	59.26	2.04
23 - 23	0 - 0	x_o, y_o, c k_1, k_2, k_3 p_1, p_2, A, B	0.002	0.003	0.158	0.176	0.078	-	-	-	1060	35	84.67	2.42

Table 6.1 Comparison of Adjustment Results with UNBASC2 using Different Calibration Parameters (23 H - 23 V Control Points)

Number of Control (used) H - V	(check) H - V	Calibration Parameters	Residuals at Image Points [rms in mm] (x)	(y)	Residual Parallaxes at Object Points [rms in mm] (X)	(Y)	(Z)	Residuals Check Points [rms in mm] (X)	(Y)	(Z)	# of Unk	# of Iter	Total CPU (sec)	CPU sec per It.
15 - 15	8 - 8	-	0.004	0.006	0.280	0.380	0.144	0.760	0.712	1.209	1020	23	28.23	1.23
15 - 15	8 - 8	x_o, y_o, c	0.003	0.003	0.206	0.201	0.101	0.531	0.371	0.743	1032	33	42.48	1.29
15 - 15	8 - 8	x_o, y_o, c k_1, k_2, k_3	0.003	0.003	0.171	0.186	0.084	0.534	0.301	0.470	1044	40	61.64	1.54
15 - 15	8 - 8	x_o, y_o, c p_1, p_2	0.003	0.003	0.192	0.191	0.095	0.472	0.396	0.910	1040	42	60.82	1.45
15 - 15	8 - 8	x_o, y_o, c A, B	0.003	0.003	0.193	0.189	0.090	0.747	0.670	0.763	1040	36	58.14	1.62
15 - 15	8 - 8	x_o, y_o, c k_1, k_2, k_3 p_1, p_2	0.002	0.003	0.159	0.176	0.079	0.500	0.322	0.500	1052	48	84.53	1.76
15 - 15	8 - 8	x_o, y_o, c p_1, p_2 A, B	0.003	0.003	0.187	0.189	0.088	0.796	0.725	0.729	1048	44	81.11	1.84
15 - 15	8 - 8	x_o, y_o, c k_1, k_2, k_3 A, B	0.002	0.003	0.159	0.179	0.078	0.529	0.511	0.641	1052	46	77.54	1.69
15 - 15	8 - 8	x_o, y_o, c k_1, k_2, k_3 p_1, p_2, A, B	0.002	0.003	0.156	0.178	0.077	0.604	0.610	0.488	1060	53	106.31	2.01

Table 6.2 Comparison of Adjustment Results with UNBASC2 using Different Calibration Parameters (15 H - 15 V Control Points)

Number of Control (used) H - V	(check) H - V	Calibration Parameters	Residuals at Image Points [rms in mm] (x)	(y)	Residual Parallaxes at Object Points [rms in mm] (X)	(Y)	(Z)	Residuals Check Points [rms in mm] (X)	(Y)	(Z)	# of Unk	# of Iter	Total CPU (sec)	CPU sec per It.
12 - 12	11 - 11	-	0.005	0.006	0.295	0.394	0.151	0.861	0.795	0.911	1020	25	30.16	1.21
12 - 12	11 - 11	x_o, y_o, c	0.003	0.003	0.205	0.200	0.100	0.583	0.327	0.731	1032	49	50.24	1.03
12 - 12	11 - 11	x_o, y_o, c k_1, k_2, k_3	0.003	0.003	0.170	0.185	0.083	0.461	0.249	0.453	1044	57	69.76	1.22
12 - 12	11 - 11	x_o, y_o, c p_1, p_2	0.003	0.003	0.190	0.191	0.094	0.490	0.328	0.743	1040	65	89.25	1.37
12 - 12	11 - 11	x_o, y_o, c A, B	0.003	0.003	0.195	0.188	0.090	0.977	0.625	0.889	1040	54	62.20	1.15
12 - 12	11 - 11	x_o, y_o, c k_1, k_2, k_3 p_1, p_2	0.002	0.003	0.162	0.180	0.079	0.707	0.454	0.713	1052	63	92.20	1.46
12 - 12	11 - 11	x_o, y_o, c p_1, p_2 A, B	0.003	0.003	0.188	0.188	0.085	1.079	0.621	0.900	1048	61	82.43	1.35
12 - 12	11 - 11	x_o, y_o, c k_1, k_2, k_3 A, B	0.002	0.003	0.162	0.180	0.079	0.707	0.454	0.713	1052	65	97.10	1.49
12 - 12	11 - 11	x_o, y_o, c k_1, k_2, k_3 p_1, p_2, A, B	0.002	0.003	0.158	0.178	0.077	0.774	0.489	0.661	1060	67	109.61	1.64

Table 6.3 Comparison of Adjustment Results with UNBASC2 using Different Calibration Parameters (12 H - 12 V Control Points)

this project, the minimum control possible for a solution using UNBASC2 was found to be 12 full control points. The reason for this is that since blunder detection capabilities are not available, the solution contains a number of weakly determined photo coordinates which only became evident after studying the results using GEBAT-V.

6.1.2 Results with GEBAT-V

The program GEBAT-V, as alluded to earlier, is quite satisfactory for use in conjunction with non-metric imagery provided initial approximations are known a-priori. The solution is generally attained with far fewer iterations than UNBASC2 due to the addition of these close approximations. The selection of weights for the various observations and parameters of GEBAT-V is more versatile than with UNBASC2. To reduce computational time initial approximations for object space coordinates were provided to GEBAT-V as input. It was found difficult to achieve a solution for so many object points without these approximations. No approximate values are needed for the additional parameters since the program always assumes zeros as initial values for these. In addition it was found suitable to introduce the additional parameters after three iterations only.

Table 6.4 illustrates the results of computations achieved under different conditions using GEBAT-V. The blunder detection capability of the program pointed to some 35 rejections of photo coordinates on initial submission. In the data snooping approach, the standardized residual, which is the residual divided by its own standard deviation, is tested for gross errors. Therefore it is assumed in the program that the standardized residual w_i of the observation

Number of Control (used) H - V	(check) H - V	Calibration Parameters	Residuals at Image Points [rms in mm] (x)	(y)	Residuals Check Points [rms in mm] (X)	(Y)	(Z)	# of Iter	Total CPU (sec)	CPU sec per It.
Full Control										
22 - 22	1 - 1	-	0.0040	0.0041	0.256	0.216	0.557	3	30.06	10.0
22 - 22	1 - 1	All Harmonics	0.0035	0.0036	0.101	0.105	0.316	7	66.07	9.4
Full Control with Rejected Outliers Removed										
22 - 22	1 - 1	-	0.0027	0.0031	0.217	0.115	0.161	3	27.59	9.2
22 - 22	1 - 1	All Harmonics	0.0025	0.0028	0.209	0.101	0.121	7	64.48	9.2
15 - 15	8 - 8	-	0.0040	0.0041	0.225	0.240	0.357	4	39.14	9.8
15 - 15	8 - 8	All Harmonics	0.0034	0.0032	0.219	0.295	0.397	8	85.47	10.7
10 - 10	13 - 13	-	0.0039	0.0041	0.279	0.373	0.444	4	42.16	10.5
10 - 10	13 - 13	All Harmonics	0.0033	0.0032	0.227	0.341	0.373	8	84.89	10.6
5 - 5	18 - 18	-	0.0039	0.0040	0.258	0.409	0.629	4	42.19	10.5
5 - 5	18 - 18	All Harmonics	0.0033	0.0031	0.234	0.387	0.569	8	84.67	10.6
3 - 3	20 - 20	-	0.0038	0.0040	0.462	0.452	0.557	4	42.21	10.6
3 - 3	20 - 20	All Harmonics	0.0033	0.0031	0.554	0.473	0.526	8	84.67	10.6

Table 6.4 Comparison of Adjustment Results with GEBAT-V using Different Calibration Parameters and Various Control Configuration

$$w_i = v_i/\sigma_{v_i} \quad = v_i/(\sigma_o \sqrt{q_i})$$

is a standardized normally distributed variable.

Here q_i is the diagonal element i of matrix Q_{vv} which must be computed. Q_{vv} is found as $Q_{\ell\ell}-AN^{-1}A^T$ where $Q_{\ell\ell}$ is the weight cofactor matrix of the observations, A is the first design matrix and N is the normal equation matrix of the unknowns. In the statistical test, the null hypothesis, H_o, that no gross-error exists in observation ℓ_i is rejected if

$$|w_i| > C$$

where C is critical value chosen for a specific confidence level by the user. As a guide El-Hakim (1982) recommends the value of C be chosen between 3.0 and 4.05 for large populations and between 2.0 and 3.0 for small populations. Here C is chosen as 4.1 based on recommendations made by Baarda (El-Hakim, 1984).

6.1.3 Results with the DLT

The Direct Linear Transformation solution was run for the four photograph configuration chosen for this project with varying numbers of control points. Tests were conducted for each situation using the 11-,12-,14- and 16-unknown solution capability of the DLT (see Table 5.1). With each solution a data snooping evaluation was possible both at the resection and intersection stages of the computations. It became quite evident that although the DLT solution yielded slightly less accurate results, its saving in computational time made it more attractive. In selecting control points for the reduced control

situations, care was taken to ensure the best possible distribution in all 3 dimensions. The results of all combinations of solutions are listed in Table 6.5. It can be seen that the 12-unknown solutions tended to be better in all cases, and that when the 16-unknown solution was attempted it yielded the poorest results.

Number of Full Control Points	Unknowns in DLT Solution	Residuals at Object Points (rms in mm) (X)	(Y)	(Z)	(POS)	Total CPU (sec)
25	16	21.5	2.9	119.0	121.0	6.48
25	14	0.2	0.3	1.3	1.3	5.84
25	12	0.1	0.1	0.3	0.3	5.72
25	11	0.2	0.2	0.5	0.6	5.66
20	16	4.1	2.5	19.1	19.7	5.92
20	14	0.2	0.4	2.1	2.1	5.78
20	12	0.1	0.1	0.3	0.3	5.67
20	11	0.2	0.2	0.5	0.6	5.61
15	16	9.5	5.2	38.9	40.4	5.74
15	14	0.2	0.4	0.9	1.0	5.65
15	12	0.1	0.1	0.3	0.4	5.61
15	11	0.1	0.2	0.4	0.5	5.51
10	16	37.4	20.2	116.7	124.2	5.93
10	14	1.3	2.0	12.9	13.1	5.63
10	12	0.1	0.1	0.2	0.2	5.55
10	11	0.1	0.1	0.2	0.2	5.49

Table 6.5: Comparison of Adjustment Results with DLT using Different Unknowns and Various Control Configurations

6.1.4 Comparison of Three Photogrammetric Approaches

To compare the three available photogrammetric approaches used in this evaluation it is necessary to examine the results for accuracies attained, requirements for control points and the computational time needed for each. Examination of the preceeding tables leads to various considerations for using each in industrial photogrammetry.

The main merit of the DLT is that both fiducial marks and initial approximations are not needed to obtain a solution. Due to its simplistic formulation and non-iterative nature much less computer time is required than for the simultaneous bundle solution. This allows the DLT to be considered for use on microcomputers. On the other hand, the requirement for more control points, particularly if highly accurate results are desired, makes the DLT solution less desirable in some applications. However, even when the simultaneous bundle solutions failed to converge the DLT provided results which can be useful in certain instances. In this project the DLT solution provided surprisingly good results.

Conversely, the simultaneous bundle solutions are particularly more useful in precision industrial surveys since less information is lost resulting in higher accuracy. Theoretically, fewer control points are needed to arrive at a solution and it is possible to incorporate geodetic observations into the solution. The primary disadvantage of the bundle solution found here is that good initial values for unknowns are necessary, otherwise the system fails to converge to the proper solution.

Since the DLT and bundle solution both have advantages and disadvantages, it would be best in a practical situation to combine the

merits of each into one package for industrial surveys. It would be advisable to investigate a DLT solution before attempting a simultaneous bundle adjustment to reduce the required computer time for the overall solution.

As a further evaluation of the three programs a comparison of check distances against adjusted distances for a number of points on the levelling rods is useful. Table 6.6 lists these comparative values by program. Here it was found that large errors resulting in numerous check point rejections enabled fewer check distances for the bundle solutions. The DLT seemingly provides better results, however this is due to the nature of the transformation solution involved.

When these spatial distances were used to supplement the control in the program GEBAT-V the solution was not able to converge. Therefore it was decided from these results not to attempt to use the spatial distances in the final solution.

6.2 Gross-Error Detection in Photogrammetry

In photogrammetric solutions least squares estimators for unknown parameters are generally used. These estimators are defined such that they minimize the weighted sum of the squared residuals. It is generally assumed that the residuals are random variables with zero mean and therefore the condition of least squares enforces this criterion. The least squares estimators are very susceptible to gross-errors in observed data as a result. The difficulty arises when there is more than one gross-error in an adjustment since the location of these errors by an analysis of the residuals may be impossible.

FROM	TO	KNOWN DIST. (mm)	ADJ. DIST. UNBASC2 (mm)	ADJ. DIST. GEBAT-V (mm)	ADJ. DIST. DLT (mm)
400	401	300.0	-	-	299.88
400	402	600.0	599.06	598.85	599.38
401	402	300.0	-	-	299.50
402	403	200.0	-	-	200.92
403	404	300.0	-	-	299.91
405	406	300.0	295.64	294.93	299.76
405	406	300.0	-	-	299.76
405	407	600.0	567.99	562.74	599.76
406	407	300.0	301.95	-	299.81
408	409	300.0	-	-	299.55
408	410	600.0	-	-	600.08
409	410	300.0	299.85	299.03	300.47
409	411	600.0	-	-	600.14
410	411	300.0	299.54	298.45	299.69
412	413	300.0	294.39	293.17	298.94
413	414	200.0	197.39	197.03	199.86
412	414	500.0	-	-	498.80
415	416	300.0	297.64	237.77	299.57
416	417	300.0	300.01	300.13	301.07
417	418	300.0	-	-	300.15
417	419	600.0	599.62	598.81	599.30
418	419	300.0	-	-	299.15

Table 6.6: Comparison of Check Distances versus Adjusted Distances

Assuming every possible precaution has been taken at the data acquisition stage to minimize these gross-errors it is left to perform rigorous statistical testing for the detection of smaller errors during the adjustment. In two of the software packages utilized, Baarda's data snooping approach was used to detect these errors.

The elimination of gross-errors must occur singly by eliminating the largest undetectable blunder. The difficulty in eliminating photo coordinate observations found is that often the remaining observations to an object point are less than three since few photographs were used. To maintain reliability it is desirable to have a minimum of three intersecting rays at each object point. In this project GEBAT-V was found to detect more gross-errors than the DLT with Data Snooping. The Direct Linear Transformation tended to be less informative in this respect, however it was still found useful in pointing out large blunders.

6.3 Achievable Accuracies Using Non-Metric Imagery

In essence it has been shown that any amateur camera can be used in a close-range photogrammetric evaluation, provided sufficient object space control is available and an appropriate analytical data reduction scheme is followed. However, of interest here is just how accurate data reduction using non-metric imagery can be. As shown, the 0.5 mm accuracy desired in this project is achievable using all three solutions. It would be possible to improve these results if an optimum configuration of the imaging geometry were selected along with a combination of multiple target settings, multiple targets to define an object point and multiple frames at each station. Depending on the

amount of this additional effort and time taken, it is estimated that RMS accuracies to 0.2 mm should be possible using non-metric imagery.

6.4 Precision Close-Range Surveying

The use of precision surveying with electronic theodolites is undoubtedly the most accurate method for the point-by-point evaluation of an object at close range. The measurement of the parabolic satellite weather reflector using this method yielded 5 separate sets of antenna coordinates. Although each antenna point was found in real-time with a rigorous error propagation providing the standard deviations of the x, y and z coordinates the overall measurement of the antenna was found to require 7 to 10 hours to complete on the average requiring two surveyors.

Three different techniques were attempted by the various programmers to perform initial vertical index error, horizontal collimation error and scaling of the baseline between the theodolites. The most time efficient method was developed using collimation checks and scaling by the simultaneously pointing of each theodolite upon one another. Another method attempted was the theodolite pointing to a subtense bar which was set perpendicular to its line of sight. This technique seemed quite time consuming and required a subtense bar to be available for the measurement and not simply any known spatial distance. Finally, the bundle adjustment described in Section 3.5 was attempted by one programmer. The bundle solution was found to be quite time consuming to perform and seemed to require considerable variation in height between the elevation of the stable points selected. The time needed to perform this initialization of the two theodolites was found

to take an average of 30 to 45 minutes depending on the degree of sophistication of the microcomputer used.

At this stage most of the systems required a further 10 minutes to create data files needed for the object points to be measured. The measuring procedure for individual object points could then be attempted.

The different microcomputers tested proved to offer various advantages and disadvantages. Due to the limited readout capability of the Epson HX-20, Radio Shack TRS 80, and the Hewlett Packard HP71B models much time was lost in programming and operating the system. However, since these systems can operate without AC power they offer the advantage of being compatible for field operations. Each of the above systems can be expanded with additional peripherals enabling quicker operational capabilities. The MacIntosh computer offers the advantage of full screen text and graphics capabilities although it is less robust for field usage. Post data acquisition analysis, such as surface fitting, is possible using the MacIntosh including the graphical display of the results. This makes it most suitable in an indoor industrial setting for an overall evaluation.

6.4.1 Comparison of Results

The direct comparison of antenna object coordinates as determined by separate theodolite measurements is not possible unless known coordinates are available on the antenna. Then the transformation of each set of coordinates to this datum would provide one method for comparison. In testing the different systems it is possible to examine the computed spatial distances between the theodolites. When this was

done it was found that differences as large as 10 mm were detected. This difference will of course provide a scaling error to all antenna object points. A second way to compare results is to proceed with the surface fitting and subsequent evaluation. The transformed coordinates of the paraboloid in its standard form would still be meaningless for comparison purposes but the derived focal lengths of the best fitting paraboloids for each set of measurements would give a good indication of the accuracy of antenna measurements.

6.4.2 Achievable Accuracies

The achievable accuracies when using precision electronic theodolites at ranges of less than 10 metres was defined earlier as being in the range of 0.05 mm. This value in practice must be rigorously evaluated using comprehensive error propagation calculations at all stages of the measurement. Numerous influences however, affect the outcome of results when a large number of points are to be observed. The same operator should perform the measurements at each theodolite throughout the evaluation or else pointing errors may become large. Due to the time period involved, operator exhaustion may be a source of errors in an extended observation session. Therefore while individual point accuracies may be high, overall the RMS accuracy of 3-dimensional spatial positioning may be somewhat reduced to the range of 0.05 to 0.1 mm.

6.5 Compatibility of Results for Further Processing

Since the final computed coordinates using all three photogrammetric solutions were available on the IBM 3090 mainframe

computer it was a relatively simple task to create data files for further analysis on this system. The results from surveying however had to be transferred from the cassette tapes and floppy diskettes of the microcomputers where they were acquired to the computer to be used for subsequent analysis. This step required additional software development and access to a modem for data transmission. In the case of the Epson HX-20, data transmission was impossible altogether and manual input of all antenna coordinates was required. Manual input is blunder prone and should be avoided at all costs when dealing with large quantities of data. In practice it would be desirable to perform all computations on one computer system and have data access via modem from external sources, such as data gathered from electronic theodolites.

CHAPTER 7

DATA ANALYSIS AND DISPLAY OF RESULTS

In surveying engineering, surface fitting plays an important role in the analysis, interpretation, and correlation of experimental data with models transformed from fundamental mathematical principles. This is particularly true in the analysis of deformations in geometric objects of known shape. In evaluating the shape of a structure such as an antenna, the coordinates of all points determined on the surface must be converted first into data which can be directly utilized. In this chapter a presentation of the techniques used in analyzing geometrical objects will be given. Using these methods the data gathered in this study can then be reduced to commonly accepted geometrical forms.

7.1 Surface Fitting Techniques

Given a set of observations, it is desirable to summarize the data by fitting it to a "model" of some form which depends on adjustable parameters. It is often the case where such modelling is a kind of constrained interpolation, where the data is fitted to a function whose form is known or suspected prior to the fitting. The approach used is generally to adjust the parameters of the model so that a minimization of some function occurs, yielding best-fit parameters. Therefore such an adjustment process is a minimization problem and the most generally accepted technique used to solve problems of this nature is the use of Least Squares as the Maximum Likelihood Estimator. In order to provide a meaningful modelling of the experimental data a fitting procedure must be developed to provide:

a. estimates of parameters;

b. error estimates of the parameters; and

c. a statistical measure of goodness-of-fit.

The problem in dealing with surfaces such as antenna reflectors involves finding the equation of a second degree surface that best fits the measured coordinates. To approach this problem in the most general sense, the origin and angular altitude of the surface are presumed unknown to provide flexibility to the measurement procedure. Therefore the general quadratic equation can be used to perform the modelling:

$$Ax^2 + By^2 + Cz^2 + Dxy + Exz + Fyz + Gx + Hy + Iz + K = 0 \qquad (7.1)$$

The outcome of surface classification using the quadratic equation leads to one of a number of surfaces which can be subsequently reduced to their more commonly accepted standard forms through a manipulation of the final parameters. By utilizing the method of least squares a solution is obtained taking advantage of the high redundancy of observations measured on the surface. Appendix IV provides a discussion of the procedure involved in fitting data to quadratic surfaces using the combined method of least squares adjustment.

Owing to the difficulty of dealing with non-linear problems of this nature in adjustment calculus, many authors have alluded to some problems and possible solutions (Pope, 1972; Bopp et al., 1977; Vanicek and Krakiwsky, 1982 and Fiedler et al., 1986). The problems arise from replacing a non-linear model by its linear approximation. The unknown parameters tend to be highly correlated and both the observations and unknowns are non-linear in the mathematical model.

For the analysis of the reflector antenna at hand a surface fitting program was first developed based on the general quadratic form (Appendix IV). The usefulness of such a program is its potential application to the fitting of a number of surfaces with minimum alterations to the source code. A solution to this problem was found attainable provided close approximations were given for the point of initial linearization. Since the quadratic form can describe one of a number of possible surfaces, one runs the risk of finding that the surface of best fit is in fact not the surface expected. This happened to be the case here, where a circular paraboloid was the design surface known a-priori and an ellipsoid was found to best describe the data provided.

An alternate method of surface fitting was needed to ensure a circular paraboloid was the model fitted. This was performed in a second program developed by the author as a constrained form of surface interpolation. Appendix V describes the differences in this method from the first solution. The advantage of this method is that the parameters desired for the calibration of the reflector surface are directly attainable with the various rotation components computed as nuisance parameters.

7.1.1 Description of the Adjustment

Due to the intercorrelation of the antenna parameters in both surface fitting programs some method was needed to arrive at suitable initial approximations for the parameters sought. In the constrained paraboloidal interpolation case these approximations were easier to estimate since their values represented physical quantities. It was found particularly effective to treat the centroid of the paraboloid and

approximate focal length as fixed for an initial solution to estimate the rotation angles (direction cosines). With this completed, the solution converged more readily. Due to the number of points the surface fitting programs were developed with 50 points and later tested with 75 points. Little difference was noted in the estimated parameters between these two solutions. Computationally it took 2 min 45 sec of CPU time to complete the solution with 50 points and 4 min 15 sec of CPU time to complete the adjustment with 75 points. When one iteration of the combined adjustment was attempted using all the points measured, the algorithm developed consumed 22 min of CPU time.

The primary cause for such long execution times was the fact that for each iteration of the least squares solution three matrix inversion operations are required. Matrix inversion is an N^3 operation where N is the number of antenna points and for large problems is time consuming. It was found that solving for P^{-1} and M^{-1} (see Appendix V) explicitly saved valuable computer time since these are essentially diagonal matrices. Once the direction cosines were computed all original coordinates were simply transformed using these adjusted parameters prior to subsequent analysis.

7.1.2 Determination of Critical Reflector Calibration Parameters

To determine the two reflector calibration parameters of interest, the best fitting paraboloid centroid and focal length, slightly different procedures are followed for each of the two solutions presented. When using the quadratic form the rotations and translations are implicit in the adjusted parameters and therefore solving for these

quantities requires some post-adjustment manipulation of the parameters. The use of eigenvalues and eigenvectors is most appropriate and the author's modified version of subroutine EIGEN3 (Arsenault, 1982) was investigated for this purpose.

For the fitting of a circular paraboloid directly by constrained paraboloidal interpolation the desired parameters are immediately known. For this study, the centroid of best fit was found to be located at the point:

$$X_o = 1859.87 \text{ mm}$$

$$Y_o = 3262.91 \text{ mm}$$

$$Z_o = 971.97 \text{ mm}$$

The paraboloidal focal length of best fit was found to be 449.97 mm. Since the surface design characteristics are unknown it is difficult to compare this focal length against its design value.

7.1.3 Determination of Reflector Irregularities

The problem of determining irregularities on the reflector surface is made more difficult without any knowledge of the reflector's exact design parameters. If the design focal length was known it could be held fixed in the adjustment and the goodness-of-fit of the paraboloid would provide some measure of irregularities on the surface. A second method of surface evaluation involves the use of least squares collocation. Here the observations are treated as being composed of two components, ie. statistically dependent components [reflector irregularities (signal)] and statistically independent components [measurement error (noise)]. The relationship between these components in a least squares adjustment is

$$\ell = AX + n + s \tag{7.2}$$

where the term s is the signal and n is the matrix of observational errors. By the theory of collocation the desired signal is given by

$$\hat{s}_p = - C_{s_p s} B_s^T M (A_\delta + W) \tag{7.3}$$

where $C_{s_p s}$ is a covariance matrix for the cross-correlation between the points of prediction (where signal is to be predicted) and the observation points. It is the covariance among all the signal components which mediates the prediction, by relating s to s_p (Vanicek and Krakiwsky, 1982).

The requested prediction of the signal can be made as part of the adjustment or after it. However, it is evident that such a technique relies on the ability to adjust simultaneously all of the data involved in determining the signal. Here it is impractical to adjust all observed points on the antenna surface to begin with. Therefore least-squares collocation using all points is also not practical and is only useful in adjusting relatively small numbers of observations. With all of these difficulties in mind it was then found useful to adjust all points on the antenna surface in separate adjustments of seventy-five points. Then by checking the RMS of the residuals found, some measure of surface deviation could be predicted. For each adjustment a random distribution of residuals was found with RMS values generally ranging from 0.8 to 1.25 mm. By separating measurement errors of 0.5 mm from these values, it is possible to attribute surface deviations of approximately 0.3 mm to 0.75 mm to the reflector.

Irregularities can also be thought of as normal departures of the

true points on the reflector from the best fitted surface. In order to determine these, the residuals from the fit have to be used to compute the normal departure, n, at each point as,

$$n = \sqrt{V_x^2 + V_y^2 + V_z^2} \tag{7.4}$$

where V_x, V_y and V_z are the residuals with respect to each coordinate. These resultant departures can also be plotted using contour curves or with a three dimensional grid showing the surface topography at an exaggerated scale.

7.1.4. Maximum Achievable Frequency

The maximum achievable frequency may be obtained by examining the regularity of the reflector. Bearing in mind that the reflector is designed to operate in the S-Band of microwaves (wavelengths λ = 15 cm to λ = 7.5 cm) maximum surface roughness cannot exceed 2.67 mm. The RMS surface roughness, now known approximately for the whole reflector, can be applied to Ruze's formula defined earlier for this purpose. Based on the maximum RMS surface roughness determined, 0.75 mm, the maximum resolvable wavelength can be computed as, λ_{max} = 2.1 cm. This corresponds to a frequency which falls within the Ku-band of microwaves (12.4 GHz to 18 GHz).

Microwaves are generally used for satellite communications since they are less susceptible to the noise temperature of the sky and man-made noise. Therefore operating this antenna at higher frequencies as recommended here may enhance the operation of the receiver. Possibly this antenna reflector can be used to receive other than satellite weather information.

7.2 Graphic Display of Reflector Surface

In recent years rapid advances in computer graphics have enabled scientists and engineers to quickly view the results of their work. The analysis of images formed on CRTs or subsequently on printed output allows the discovery of various trends which may otherwise be masked by the volume of data. In surveying engineering, there is no set method for performing this task and it is left to the engineer to select representations which best illustrate the problem. Computer graphics which are capable of interactive control through the use of keyboards, function keypads, joysticks and lightpens are the most useful for creating images quickly.

The choice of a computer graphics package will naturally depend on its availability, but ideally it should be based on the same computer as the program packages used for data reduction. At the University of New Brunswick numerous computer graphics packages are available on the IBM 3090/VF mainframe computer which interact using different programming languages. One in particular, SAS/GRAPH, is useful for 3-dimensional representations of data and has been selected for representing the antenna surface. Other graphics packages such as CAD systems like UNIGRAPHICS and MOVIE.BYU are available on separate computer installations as well and have been used in various photogrammetric studies at UNB (Reedijk, 1985 and Krolikowsky, 1986).

7.2.1 Description of Software

SAS/GRAPH is the graphics software developed by SAS (Statistical Analysis System) capable of displaying data in the form of colour plots on CRTs and hardcopy devices. Besides its availability, other reasons

for its selection were:

a. Plots are created with relatively few statements;

b. The graphics software output can be displayed on IBM 3279 colour graphics terminals available at UNB;

c. The graphics software provides extensive title and footnote annotation;

d. The software is well documented;

e. Files of antenna coordinates are easily read by SAS/GRAPH programs for rapid display of plots;

f. Extensive data management and replay capabilities allow the quick review of catalogued plots stored on disk; and

g. Colour display, both on a graphic terminal and as hardcopy plots makes the results easier to understand.

7.2.2 Representation of Surface

The rapid display of SAS/GRAPH output made it possible to monitor the data reduction process. With the raw antenna coordinates measured by either photogrammetry or surveying, the viewing of a scatter plot of coordinates (Figure 7.1) ensured a right-handed system was enforced prior to adjustment of the circular paraboloid. When the adjustment was completed it was possible to view the paraboloidal shape a number of ways to ensure the reflector surface coordinates were in fact in their standard form. Figures 7.2 and 7.3 represent these results.

With the knowledge of the paraboloid in its standard form it is possible to generate an ideal paraboloid with simply the knowledge of the focal length using equation 7.5.

$$X^2 + Y^2 = 4fZ \qquad (7.5)$$

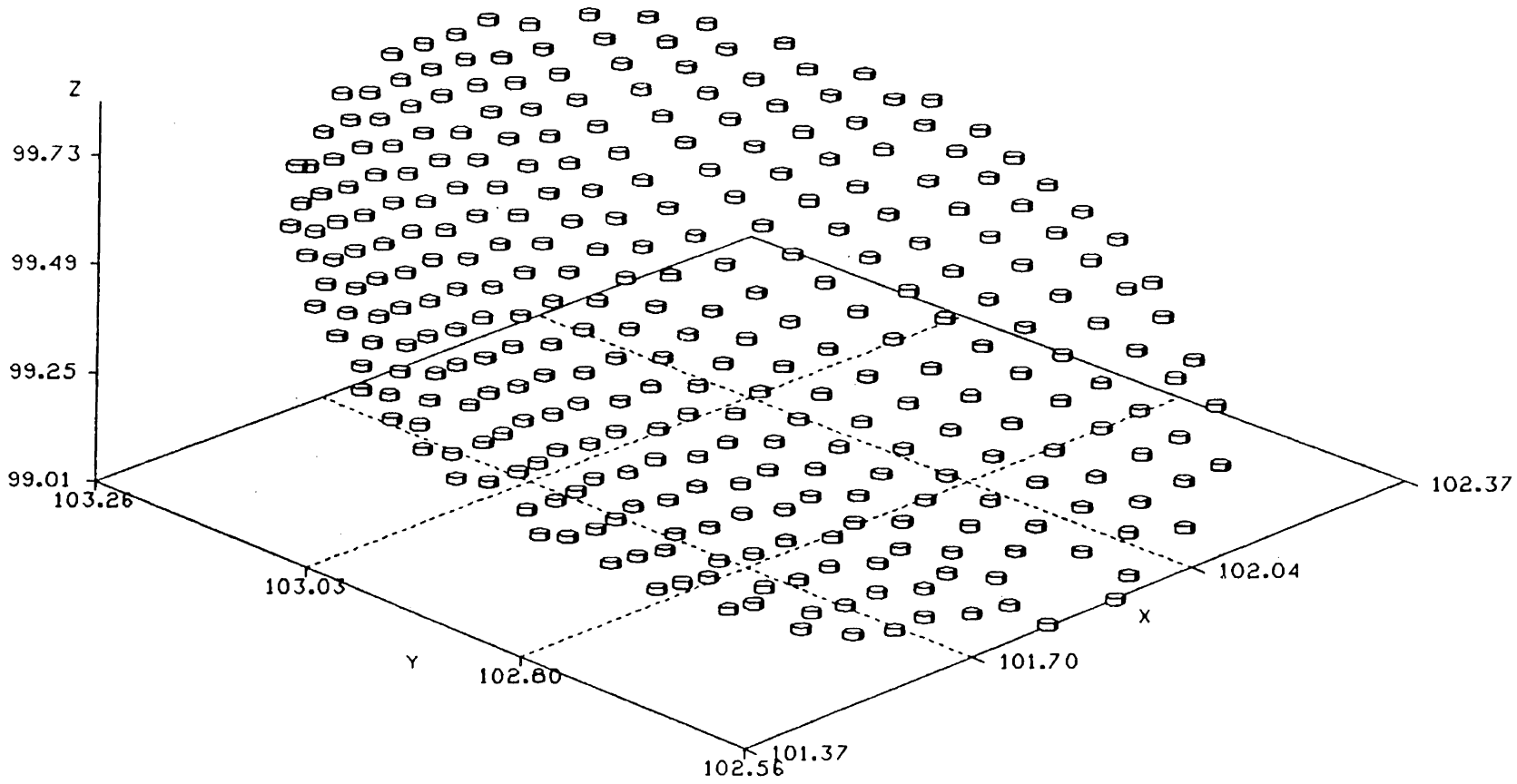

FIGURE 7.1: SCATTER PLOT OF POINTS ROTATED
45 DEGREES AND TILTED 45 DEGREES

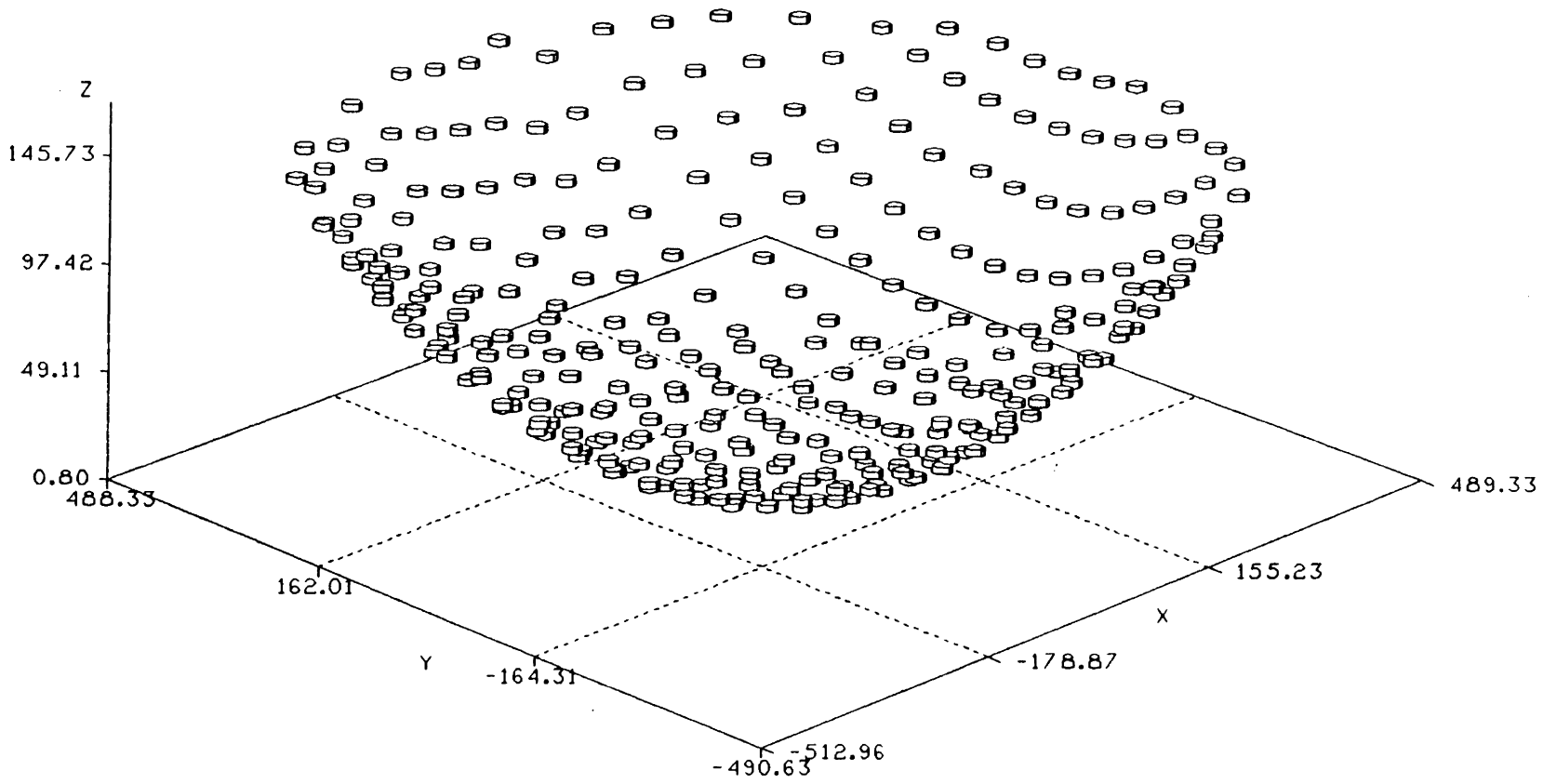

FIGURE 7.2 SCATTER PLOT OF ANTENNA POINTS FOR A PARABOLOID IN ITS STANDARD FORM ROTATED 45 DEGREES AND TILTED 45 DEGREES

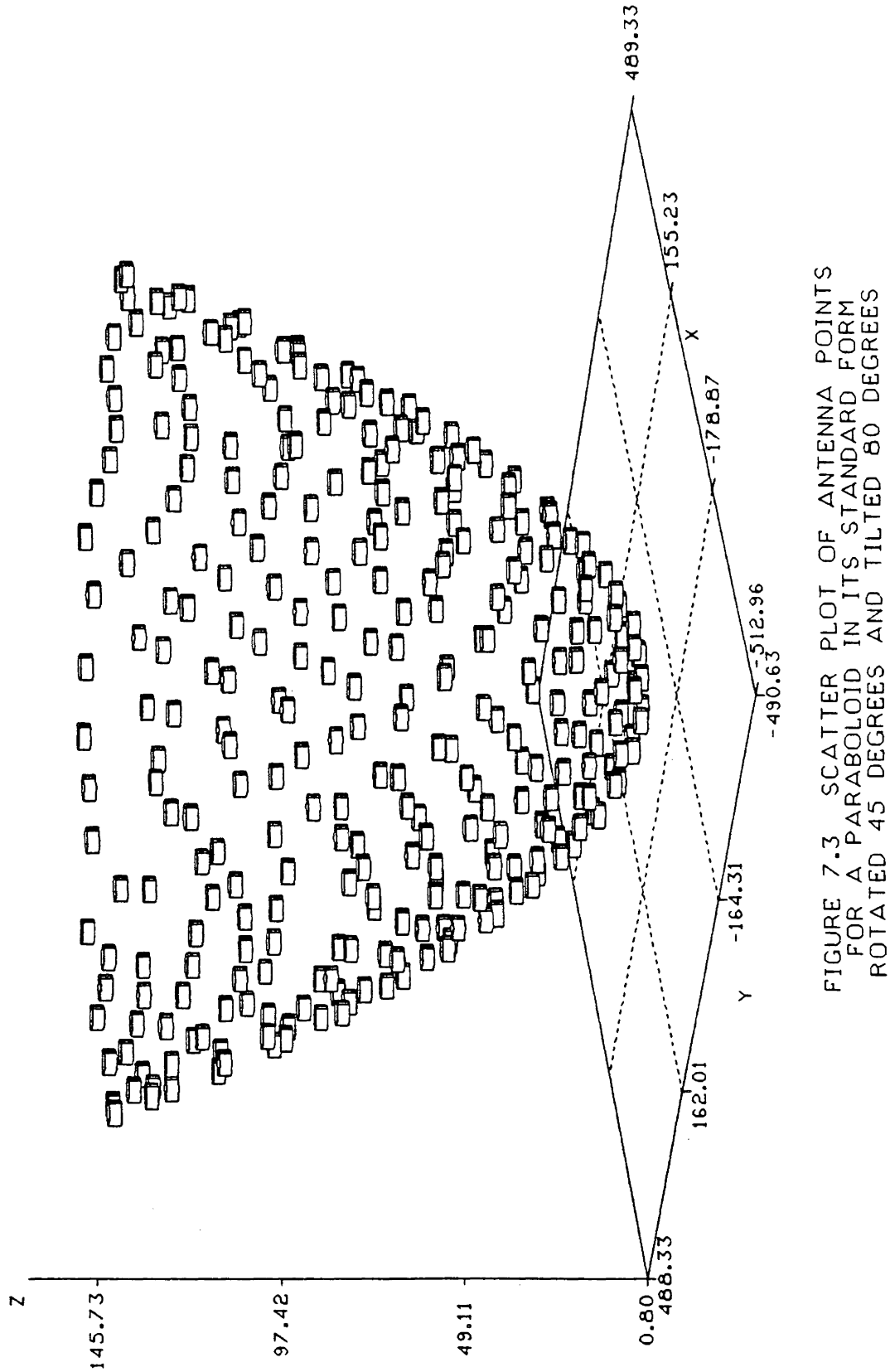

FIGURE 7.3 SCATTER PLOT OF ANTENNA POINTS
FOR A PARABOLOID IN ITS STANDARD FORM
ROTATED 45 DEGREES AND TILTED 80 DEGREES

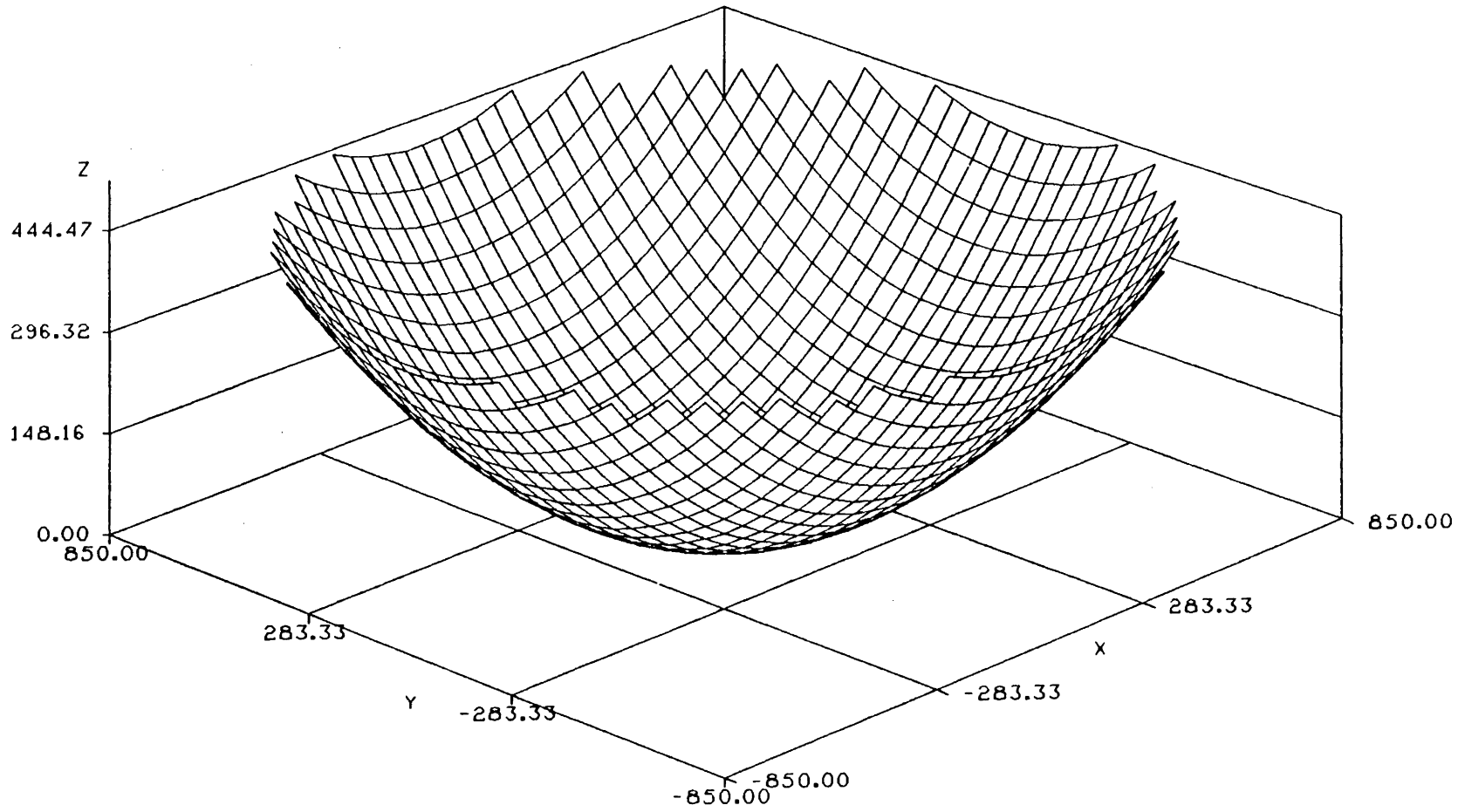

FIGURE 7.4 COMPUTER GENERATED ANTENNA SURFACE
BASED ON A PARABOLOID
WITH FOCAL LENGTH 449.97 MM

A plot of this shape is shown in Figure 7.4. An alternate method of representing surfaces, given a number of data points, is through the use of various interpolation procedures. In the SAS/GRAPH software a number of procedures require that data be provided in the form of a rectangular grid. For example, to create contour plots this is the case. Therefore the interpolation procedure interpolates a function of two variables onto a rectangular grid. For this purpose SAS/GRAPH utilizes a modification of the bivariate interpolation developed by Akima in 1978 (SAS/GRAPH User's Guide, 1985). Two options available are the use of either a partial spline or spline interpolation. In either a bivariate spline is fit to the nearest neighbours and used to estimate the needed grid point elevations.

It is recommended that the spline be used only for fewer than 100 points or else the resultant plot is expensive in terms of CPU time. Therefore, the spline interpolation provides a greater degree of smoothness of the final interpolated function. Figure 7.5 illustrates a spline interpolation of the reflector surface coordinates. It is also possible to perform an interpolation of the residuals of the reflector surface which resulted from the surface fitting. This resultant plot is found in Figure 7.6.

Finally to provide an indication of the trends of surface deviations contour plots based on the above mentioned interpolated grids were studied. Figure 7.7 represents a contour plot of the antenna surface shape. As expected this yields a series of concentric circles. Meanwhile Figure 7.8 represents a contour plot of surface deviations derived from residuals found in the surface fitting results. An examination of these residuals indicates that no truly significant deviations exist on the antenna.

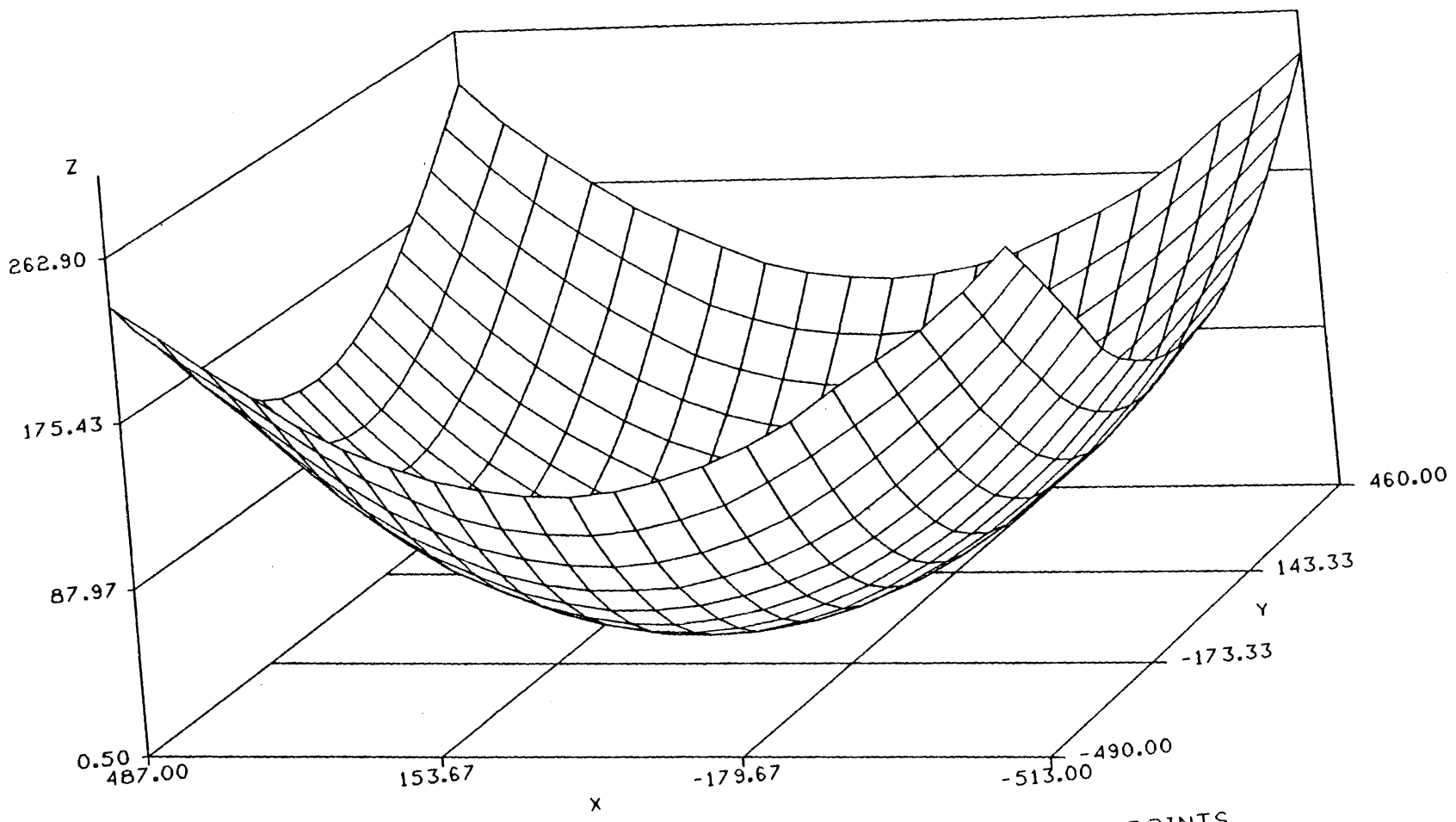

FIGURE 7.5: GRID GENERATION OF ANTENNA POINTS USING SPLINE INTERPOLATION

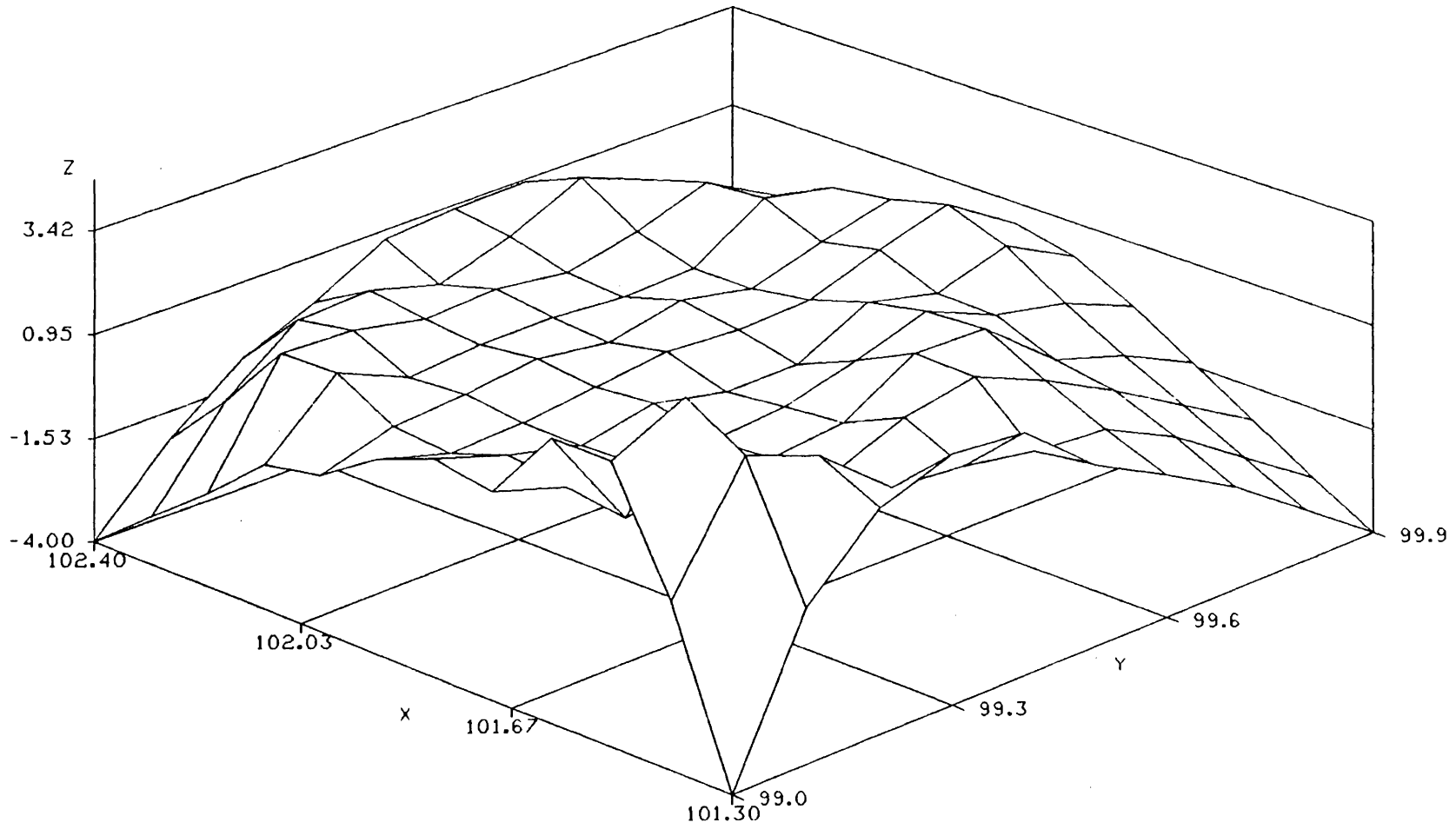

FIGURE 7.6 SPLINE INTERPOLATION OF ANTENNA NORMAL RESIDUALS AFTER ADJUSTMENT

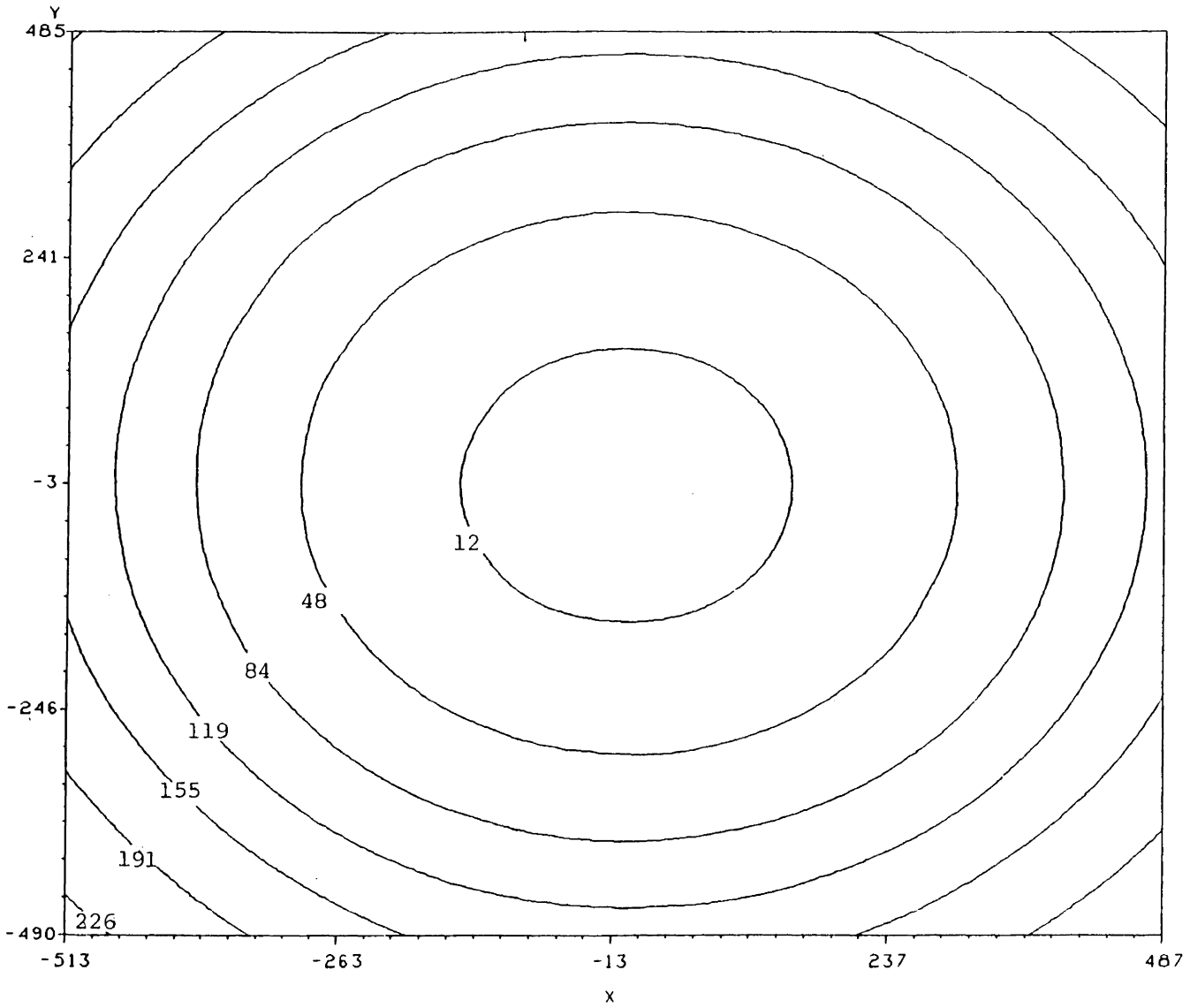

FIGURE 7.7 CONTOUR PLOT OF SPLINE INTERPOLATED ANTENNA POINTS IN STANDARD FORM

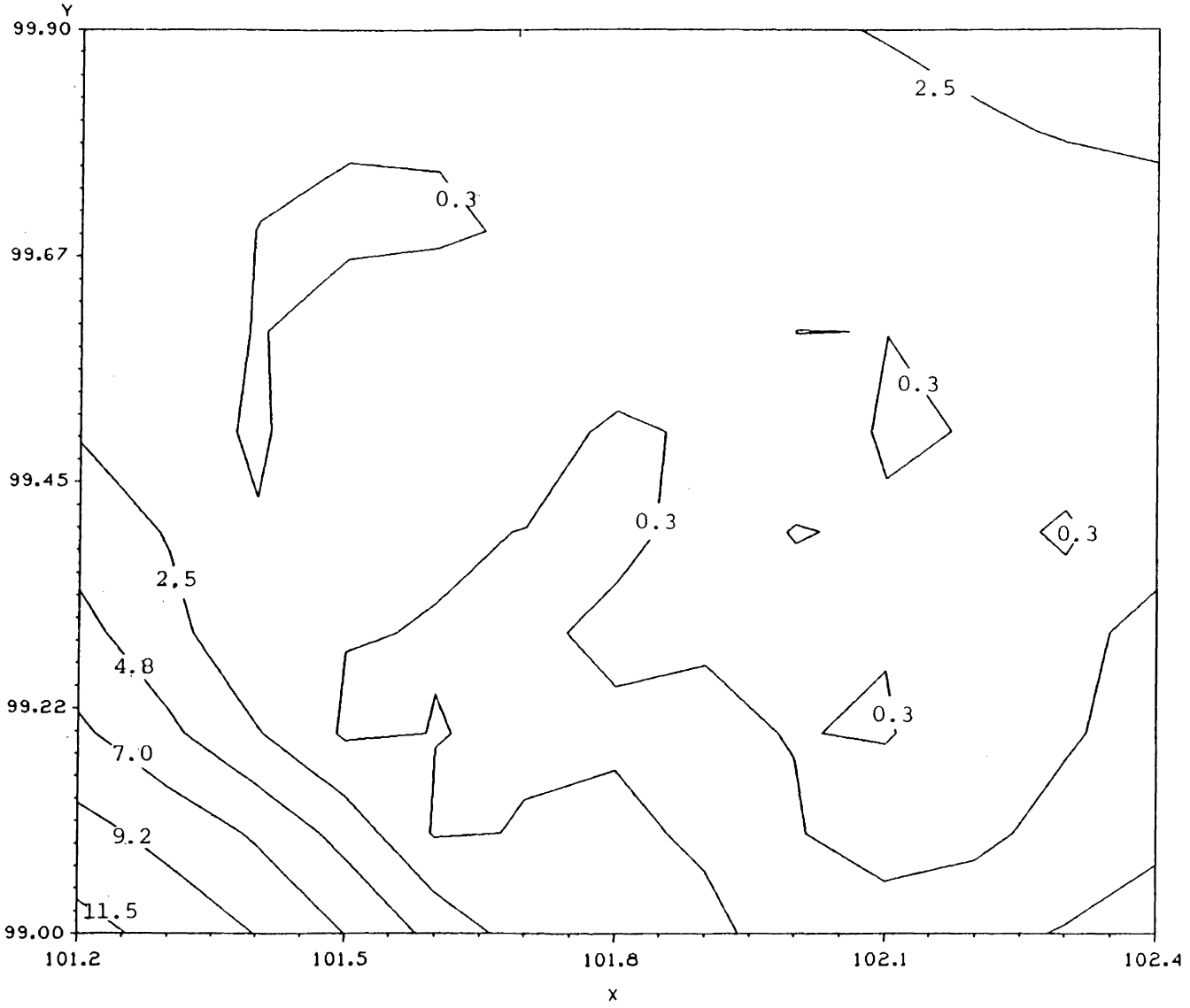

FIGURE 7.8 CONTOUR PLOT OF SPLINE INTERPOLATED ANTENNA NORMAL DEVIATIONS

7.3 Integrated Analysis For Reflector Calibration

In the broad field of surveying engineering the analysis of deformations has often evolved with separate monitoring techniques examining basically the same deformations or movements. Therefore in recent years there has been an interest amongst photogrammetrists, surveyors, and often scientists in integrating all results into a single analysis. With reference to reflector antenna analysis it is possible to consider an integrated analysis in two ways.

Firstly, using photogrammetry it is possible to integrate geodetic information into the simultaneous bundle adjustment solution in the form of spatial distances and height differences. A second technique is to integrate both photogrammetric and geodetic antenna coordinates into the surface fitting, provided different weights are assigned to the two sets of observations. Since both methods of measuring the antenna provided all the points on the antenna for the surface fitting an integrated analysis was not used here.

CHAPTER 8

COMPARISON OF TWO MEASURING APPROACHES

From the outset of this project the main goal has been to test the suitability of non-metric analytical photogrammetry for performing the task of reflector antenna calibration. Although both methods described have advantages and disadvantages, both close-range photogrammetry and precision surveying with electronic theodolites have proven capable of providing the required object points to study the antenna. The initial accuracy specification of 0.5 mm RMS has also been achieved using either method. In this chapter three fundamental considerations will be evaluated to compare close-range photogrammetry and precision surveying with electronic theodolites for future potential antenna calibration studies. These are estimates of achievable accuracies, required equipment, and an evaluation of time requirements to complete the project.

8.1 Achievable Accuracy

It is well known that the achievable accuracy of any photogrammetric solution depends on the control used in the data reduction. However to ensure similar results have been obtained it would be best to compute, using all three photogrammetric solutions, new object space coordinates based on control points taken from the multiple theodolite solutions. This was not possible, however a comparison of photogrammetric results is found in Appendix VI. A conclusive proof of the achievable accuracy can be found if the surface is completely known, however this is not the case in this project. As discussed earlier it

is anticipated that with large numbers of object points, object instability or operator exhaustion would detract from the best possible accuracy of 0.05 mm using electronic theodolites. In this case it is then quite possible that a non-metric photogrammetric analysis would yield similar results as conventional surveying. This is particularly true due to the remeasurement capability available to photogrammetry. A photograph is after all an analog medium on which the object is captured indefinitely for subsequent analysis.

The methods of enhancing accuracy in photogrammetry are through the use of multiple image settings, multiple exposures at a camera station and the use of multiple exposure stations. As long as a manually operated comparator is relied upon for image coordinate measurements it is quite probable that none of these three techniques would be adopted in industry. However, due to the development of robotic photogrammetric monocomparators, these methods will potentially become more viable. This is particularly true if retroreflective object targets and scanners are used to detect individual points.

8.2 Equipment Requirements

Considering that the objectives of industrial close-range measurement are to achieve object space coordinates in the quickest and most efficient way, the cost of equipment should be of lesser concern if tremendous savings in time are possible and repeated applications performed. In industry the setting-out of components or quality control of finished products have attracted surveying and photogrammetric techniques frequently due to their rapid output capabilities. Instrumentation for both close-range photogrammetry and surveying with

electronic theodolites is quite costly, however it has been shown in this report that readily available microcomputers and non-metric cameras can be used effectively at great savings.

In the use of electronic theodolites, perhaps a less expensive solution is found. In non-metric close-range photogrammetry elaborate bundle adjustment programs which run most efficiently on large computers add to the cost as does the expense of owning and maintaining a stereocomparater such as the Zeiss PSK-2. It has been shown however that the DLT solution, which is more satisfactory for microcomputer operation, is capable of yielding extremely good results for reflector antenna calibration purposes.

8.3 Evaluation of Time Requirements

Another element, besides equipment costs, which adds to the expense of close-range object mensuration is the time required to arrive at a solution. This includes both the costs of personnel and computing time necessary for data acquisition, reduction and analysis. Here it is reasonable to assume that the data analysis time requirements are the same for all methods as it involves the study of the final computed object space coordinates and surface fitting.

For surveying with electronic theodolites it has been shown that a considerable saving in time is realized at the data acquisition stage. If only a manual measurement procedure is available to the photogrammetrist on a comparator or analytical plotter, then the method would need 50% more time than the conventional surveying approach. It would be advisable to seek more automated methods. Should a robotic monocomparator be too expensive then software could be developed for any

analytical plotter to revisit measured points and provide multiple measurements quickly. This method was developed at UNB by Armenakis and Faig (1986).

At the data reduction stage, photogrammetry also has the difficulty of requiring lengthy periods of time for computations particularly if data snooping is used. It was found here to be useful to employ a direct linear transformation first to provide initial approximations for bundle solutions. Much time can be spent in sorting and positioning photo coordinates and control points in all appropriate fields needed by the photogrammetric adjustments. In practice the necessary utility programs to perform this task could be prepared to accelerate the solutions. Table 8.1 provides a comparison of time required in this particular project for data acquisition and reduction.

From the above data it becomes readily apparent that close-range surveying as performed in this project is more time and effort efficient than close-range photogrammetry. In future studies it would be possible to reduce the time requirements if newer equipment were investigated such as the use of servo-theodolites equipped with CCD cameras and rapid image analysis and data reduction systems such as the STARS system developed by Brown as described in Chapter 2.

Schedule of Time Comparison		
Events	Surveying with Electronic Theodolites	Photogrammetry
1. Object Preparation	2 hrs	2 hrs
2. Acquisition of 25 Control Points		
(i) Angle Measurement	-	2 hrs
(ii) Reduction of Coordinates	-	1 hr
3. Multiple Theodolite Initialization	0.75 hrs	-
4. Antenna Measurement using Theodolites (2 persons)	20 man hours	-
5. Obtain 4 photos of Antenna and Film Development	-	2 hrs
6. Object Measurement on Zeiss PSK Stereocomparator (4 photos x 10 hrs/photo)	-	40 hrs
7. Data Transfer to IBM 3090/VF Mainframe	2 hrs	-
8. Preparation and Photogrammetric Bundle Solution	-	4 hrs
Total Time	24.75 hrs	51 hrs

Table 8.1: Schedule of Time Comparison between Close-Range Surveying with Theodolites and Close-Range Photogrammetry.

CHAPTER 9

RECOMMENDATIONS AND CONCLUDING REMARKS

Based on the results obtained in this study both close-range photogrammetry and precision surveying with electronic theodolites can be concluded as suitable methods for effectively calibrating reflector antennas. It has been shown that decisions can be made about the operational capabilities of antennas up to the Ku-band of microwaves using these methods. A greater appreciation however is now possible of the instrumental costs and time requirements needed to complete a study of this nature. Therefore, a number of recommendations can be made regarding the implementation of close-range photogrammetry in an industrial environment.

9.1 Recommendations for Industrial Close-Range Photogrammetry

The following recommendations, based on the results of this reflector antenna study, can be noted when considering close-range photogrammetry for industry.

a. The importance of thoroughly conducting a preanalysis prior to commencing a photogrammetric survey cannot be over emphasized. Therefore some consideration towards developing an interactive computer graphics network design package should be made. This would be useful in control point selection and camera station positioning.

b. It has become evident from this study that the Direct Linear Transformation with data snooping can be a valuable program for use

in medium to high accuracy surveys. It would be recommended for data reduction particularly if only a microcomputer is available for use. In this case it would also be advantageous to examine ways to optimize the use of bundle adjustment programs on smaller computers.

c. The importance of the proper selection of control points has been illustrated in this study. Adequate variation in all three dimensions must be ensured. The usefulness of incorporating spatial distances and height differences into close-range photogrammetric solutions as control was found difficult to test in this study. The difficulty here lay in the inability to point to a specific spot on the invar strip in two or three sets with some measure of reliability. Alternate methods of providing such control in the evaluation of surfaces should be evaluated.

d. Should additional large format non-metric cameras be available for close-range evaluations they should be considered for use to provide better accuracies. Small amateur cameras may prove unsatisfactory for larger antennas.

e. When performing the data reduction of a large number of object points, which is usually the case in antenna surface evaluations, it may be more suitable to perform photogrammetric solutions in smaller batches.

f. When considering the analysis of deformations on the surface of reflector antennas it may prove more cost beneficial altogether to consider other techniques such as microwave holography. However, this technology is new and may not be affordable or available to smaller antenna installations.

g. For the day-to-day measurement of antennas under manufacture a turnkey system such as STARS would be the most suitable so that engineers with little photogrammetric knowledge could arrive at usable results quickly.

9.2 Conclusion

Non-metric cameras offer the photogrammetrist the versatility necessary to evaluate complex shapes, such as antenna reflectors, in an industrial setting. They are capable of extremely high accuracies at the expense of rigorous analytical self-calibration solutions. It has been shown however that the Direct Linear Transformation solution is also a useful data reduction method particularly with the availability of data snooping for the detection of gross-errors. The decision as to which type of data reduction scheme to use will depend on the available control and computational capabilities of the industry. In general, reflector antennas which operate at wavelengths larger than the Ku-band can be calibrated using non-metric analytical photogrammetry.

APPENDIX I

BASIC SPECTRUM OF RADIO AND MICROWAVES

(Source: Wright, 1978, p. 65)

BASIC SPECTRUM OF
RADIO AND MICROWAVES

Wavelengths are given
for C=300,000 km/s

	λ		frequency
------	30,000 m	----------	10 KHz
		V.L.F. Very Low Frequency	
	20,000 m	----------	15 KHz
	10,000 m	----------	30 KHz
		L.F. Low Frequency	
	1,000 m	----------	300 KHz
Radio Waves		Medium Frequency Medium Waves	
	100 m	----------	3 MHz
		H.F. High Frequency	
	10 m	----------	30 MHz
		V.H.F. Very High Frequency	
	1 m	----------	300 MHz
		U.H.F. Ultra High Frequency	
---------	30 cm	----------	1 GHz
		L-band	
	15 cm	----------	2 GHz
		S-band	
	7.5 cm	----------	4 GHz
Microwaves		C-band	
	3.7 cm	----------	8.2 GHz
		X-band	
	2.4 cm	----------	12.4 GHz
		Ku-band	
	1.7 cm	----------	18 GHz
---------	1 cm	----------	30 GHz
	1 mm	----------	300 GHz

APPENDIX II

CHARACTERISTICS OF THE KERN E-2

PRECISION ELECTRONIC THEODOLITE

Characteristics of Kern E-2 Electronic Theodolite	
Manufacturer	Kern, Switzerland
Telescope	
Magnification	32X
Objective Aperture	45mm
Shortest Sighting Distance	1.7m
Field of View	1°20'
Angle Measurement	
Circle Code	Incremental
Number of graduation lines	20,000
Diameter of graduated circles	71mm
Max Slew Rate	2.5 rps
Automatic Vertical Circle Compensator	
Type	Fluid
Working Accuracy	$<\pm$ 0.3"
Centering Time	$\simeq$ 3 sec.
Range	$\pm$ 2/5'
Compensation Error	$<$ 5% of vertical axis inclination
Displays	
7 segment - liquid crystal display (LCD)	
Angle Values	
Period of updating the display	$\simeq$ 0.33 sec.
Smallest value displayed	1"
Mean Square Error of a directional measured in two positions	$\pm$ 0.3"
Mean Square error of the vertical angle measured in two positions, including the compensator	$\pm$ 1"
Data Storage	
Device	R32/48
Type	Solid-State
Keyboard	Numeric & Functions
Display	15 digit, partially alphanumeric, LED
Weight of Theodolite	8.7kg

(Source: Cooper, 1982, p. 249 and Kern E-2 Instruction Manual)

APPENDIX III

CORRELATION VALUES IN PERCENT FOR ALL PARAMETERS IN UNBASC2 (from, Moniwa 1977)

	X_c	Y_c	Z_c	ω	ϕ	κ	x_o	y_o	c	k_1	k_2	k_3	p_1	p_2	A	B
X_c	100															
Y_c	35	100														
Z_c	87	39	100													
ω	2	6	3	100												
ϕ	20	8	19	1	100											
κ	1	3	1	98	4	100										
x_o	14	7	18	0	99	3	100									
y_o	0	5	1	99	2	99	1	100								
c	87	38	98	4	19	2	17	1	100							
k_1	1	4	1	2	0	2	0	3	19	100						
k_2	1	5	1	3	0	3	1	3	18	98	100					
k_3	0	6	3	3	0	4	1	4	18	95	99	100				
p_1	8	2	5	1	89	2	93	2	5	1	2	2	100			
p_2	3	8	4	93	2	92	1	92	4	1	1	2	0	100		
A	5	34	4	7	17	20	17	10	4	1	1	0	23	8	100	
B	21	0	5	18	3	18	7	18	9	4	4	4	6	24	0	100

Correlation Values in Percent for all Parameters in UNBASC2

APPENDIX IV

SURFACE FITTING OF A PARABOLOID USING THE QUADRATIC FORM AND THE METHOD OF LEAST SQUARES

APPENDIX IV

SURFACE FITTING OF A PARABOLOID USING THE METHOD OF LEAST SQUARES

Quadric surfaces such as circular paraboloids can be mathematically defined by the most general polynomial equation of the second degree in x,y and z. This equation takes the form:

$$Ax^2 + By^2 + Cz^2 + Dxy + Exz + Fyz + Gx + Hy + Iz + K = 0 \qquad \text{(IV.1)}$$

Here the ten coefficients A,B,C,D,E,F,G,H,I and K are real numbers and represent the unknown parameters which can best be solved for using the combined case of the least squares adjustment (Wells and Krakiwsky, 1971). Generally, K, the constant term is selected as 1 or -1 to simplify this relationship. Rewritten, the above equation is often expressed in matrix form as:

$$(x \;\; y \;\; z) \begin{pmatrix} A & D/2 & E/2 \\ D/2 & B & F/2 \\ E/2 & F/2 & C \end{pmatrix} \begin{pmatrix} x \\ y \\ z \end{pmatrix} + (G \;\; H \;\; I) \begin{pmatrix} x \\ y \\ z \end{pmatrix} + 1 = 0 \qquad \text{(IV.2)}$$

or

$$X^T \quad \bar{A} \quad X + C^T \quad X + 1 = 0 \qquad \text{(IV.3)}$$

where

$X^T\bar{A}X$ gives the second degree terms

C^TX gives the first degree terms

K=1 is the constant or zero degree term

By introducing the appropriate rotations and translations to the observed antenna coordinates the resulting quadratic form (Eqn. IV.1) can be reduced to the more commonly accepted and desirable standard form

of a circular paraboloid, that being:

$$\frac{x^2}{a^2} + \frac{y^2}{a^2} + \frac{z}{c} = 0 \qquad \text{(IV.4)}$$

or simply,

$$x^2 + y^2 = 4fz \qquad \text{(IV.5)}$$

where f is the paraboloidal focal length.

I. LEAST SQUARES APPROXIMATION OF UNKNOWN PARAMETERS

The general quadratic equation acts as the basic observation equation for the least squares approximation of the unknown parameters:

$$V_i = Ax^2 + By^2 + Cz^2 + Dxy + Exz + Fyz + Gx + Hy + Iz + 1 \qquad \text{(IV.6)}$$

Such a mathematical model expresses the relationship between two vectors, the solution vector $\bar{X}$ and the observation vector $\bar{L}$ and takes the general form:

$$F\ (\bar{X},\bar{L}) = 0 \qquad \text{(IV.7)}$$

which is known as the mathematical model for the combined method. The vector function F represents n equations relating 3n observations with u unknowns. Therefore the method of least squares can be applied when $3n + u > n > u$. Here, (n-u) dictates the degrees of freedom, however this model is non-linear and must be linearized through the use of their Taylor's series linear approximations. Expansion takes place about the initial approximation to the solution vector (X°), and the measured antenna coordinates of the observation vector (L).

For the case of the combined method linearization yields:

$$F\ (\bar{X},\bar{L}) = F(X^\circ,L) + \left.\frac{\partial F}{\partial \bar{X}}\right|_{X^\circ,L} \delta + \left.\frac{\partial F}{\partial \bar{L}}\right|_{X^\circ,L} V \qquad \text{(IV.8)}$$

or in its more common matrix form as:

$$A\,\delta + BV + W = 0 \qquad \text{(IV.9)}$$

where

$${}_{n}W_{1} = F(X^{\circ},L) \qquad \text{[Misclosure Vector]}$$

$${}_{n}A_{9} = \left.\frac{\partial F}{\partial \bar{X}}\right|_{X^{\circ},L} \qquad \text{[First Design Matrix]}$$

$$= \left.\left(\frac{\partial F_i}{\partial A}, \frac{\partial F_i}{\partial B}, \frac{\partial F_i}{\partial C}, \frac{\partial F_i}{\partial D}, \frac{\partial F_i}{\partial E}, \frac{\partial F_i}{\partial F}, \frac{\partial F_i}{\partial G}, \frac{\partial F_i}{\partial H}, \frac{\partial F_i}{\partial I}\right)\right|_{X^{\circ},L}$$

$${}_{n}B_{3n} = \left.\frac{\partial F}{\partial L}\right|_{X^{\circ},L} \qquad \text{[Second Design Matrix]}$$

$$= \left.\left(\frac{\partial F_i}{\partial x_i}, \frac{\partial F_i}{\partial y_i}, \frac{\partial F_i}{\partial z_i}\right)\right|_{X^{\circ},L}$$

${}_{9}\delta_{1}$ = Vector of Corrections

${}_{3n}V_{1}$ = Residuals whose weighted square sum is to be minimized

The least squares solution for $\bar{X}$ yields the correction vector using the following matrix equation:

$$\delta = -\,[A^{T}(BP_{v}B^{T})^{-1}A]^{-1}\;A^{T}(BP_{v}B^{T})^{-1}W \qquad \text{(IV.10)}$$

$$\delta = -\,[A^{T}M^{-1}A]^{-1}\;A^{T}M^{-1}W \qquad \text{(IV.11)}$$

Finally, the weight matrix, ${}_{3n}Pv_{3n}$ is selected such that the weights of each coordinate component are based on the variance of the observations:

$$P_{v_{i,j}} = \frac{1}{\sigma x^{2}}\,, \quad P_{v_{i+1,j+1}} = \frac{1}{\sigma y^{2}}\,, \quad P_{v_{i+2,j+2}} = \frac{1}{\sigma z^{2}}$$

Examining the individual matrix elements:

$$ {}_{n}A_{9} = \begin{bmatrix} x_i^2 & y_i^2 & z_i^2 & x_iy_i & x_iz_i & y_iz_i & x_i & y_i & z_i \\ \vdots & \vdots & \vdots & \vdots & \vdots & \vdots & \vdots & \vdots & \vdots \\ x_n^2 & y_n^2 & z_n^2 & x_ny_n & x_nz_n & y_nz_n & x_n & y_n & z_n \end{bmatrix} $$

$$ {}_{n}B_{3n} = \begin{bmatrix} \alpha_i & \beta_i & \gamma_i & 0 & 0 & 0 & \cdots & 0 & 0 & 0 \\ 0 & 0 & 0 & \alpha_2 & \beta_2 & \gamma_2 & \cdots & 0 & 0 & 0 \\ \vdots & \vdots & \vdots & \vdots & \vdots & \vdots & & \vdots & \vdots & \vdots \\ 0 & 0 & 0 & 0 & 0 & 0 & \cdots & \alpha_n & \beta_n & \gamma_n \end{bmatrix} $$

where

$$ \alpha_i = 2Ax_i + Dy_i + Ez_i + G $$

$$ \beta_i = 2By_i + Dx_i + Fz_i + H $$

$$ \gamma_i = 2Cz_i + Ex_i + Fy_i + I $$

$$ {}_{n}W_{1} = \begin{bmatrix} Ax_1^2+By_1^2+Cz_1^2+Dx_1y_1+Ex_1z_1+Fy_1z_1+Gx_1+Hy_1+Iz_1+1 \\ \vdots \\ Ax_i^2+By_i^2+Cz_i^2+Dx_iy_i+Ex_iz_i+Fy_iz_i+Gx_i+Hy_i+Iz_i+1 \end{bmatrix} $$

For the parabolic antenna under consideration the values of the

nine parameters were determined using the program SURFACE to be:

A = 0.00005361
B = 0.00003828
C = 0.00003740
D = -0.00001545
E = -0.00000029
F = 0.00000026
G = -0.01092117
H = -0.00471830
I = -0.00419106
K = 1.00000000

II. REDUCTION OF GENERAL QUADRATIC EQUATION TO STANDARD FORM

By a suitable change of coordinates involving a rotation and translation of axes, but no scale change, the above parameters describing the general form can now be reduced to standard form as shown in Equation IV.5. The first step is to translate the coordinate axes. This can be done by completing the square to find the translation constants. From the relationship:

$$ax^2 + bx = a\left(x^2 + \frac{bx}{a} + \frac{b^2}{4a^2}\right) - \frac{b^2}{4a}$$

$$= a\left(x + \frac{b}{2a}\right)^2 - \frac{b^2}{4a}$$

From the least squares adjustment it should become evident that:

$A \simeq 0$, and $B \simeq C \neq 0$ if the surface is to represent a circular paraboloid. It is evident from the values above that the surface of best fit is an ellipsoid.

Therefore the translation components become:

$$\left(\frac{G}{2A}, \frac{H}{2B}, \frac{I}{2C}\right)$$

This also describes the centroid of the paraboloid of best fit. It is possible to translate the observed coordinates by these components to reposition the origin of the axis system.

The next step is to rotate the coordinate axes so that they are

parallel to the axes of the paraboloid in its standard form. Since the current direction of the axes are dictated by the second degree terms $X^T\overline{A}X$, where $\overline{A}$ is the coefficient matrix for the quadratic, then the use of eigenvalues and eigenvectors is appropriate.

Let $$Q = X^T\overline{A}X \tag{IV.12}$$

It is necessary to perform the rotations such that:

$$Q = \hat{X}^T B \hat{X} \tag{IV.13}$$

where $\hat{X}^T = (\hat{x},\hat{y},\hat{z})$; The antenna coordinates expressed in terms of observed coordinates appropriately rotated.

and $B = \begin{pmatrix} \lambda_1 & 0 & 0 \\ 0 & \lambda_2 & 0 \\ 0 & 0 & \lambda_3 \end{pmatrix}$; $\lambda_1,\lambda_2,\lambda_3$ are eigenvalues.

Further;

$$\hat{X} = \overline{P}^T X \tag{IV.14}$$

and

$$B = \overline{P}^T \overline{A}\ \overline{P} \tag{IV.15}$$

where $\overline{P} = (u_1\ u_2\ u_3)$; the matrix of eigenvectors.

To solve for the eigenvalues:

$$f(\lambda) = |A - \lambda I| = 0 \tag{IV.16}$$

we expand it to

$$f(\lambda) = \begin{vmatrix} a_{11} - \lambda & a_{12} & a_{13} \\ a_{21} & a_{22} - \lambda & a_{23} \\ a_{31} & a_{32} & a_{33} - \lambda \end{vmatrix} = 0 \tag{IV.17}$$

This leads to a cubic equation in λ.

$$f(\lambda) = -(\lambda^3 + a\lambda^2 + b\lambda + c) = 0 \tag{IV.18}$$

and the roots are:

$$\lambda_1 = 22.620451$$

$$\lambda_2 = 52.550762$$

$$\lambda_3 = 53.416731$$

Next solve for the eigenvectors such that:

$$(A - \lambda_i I)\overline{P}_i = 0, \qquad i = 1,3 \tag{IV.19}$$

Here, $\overline{P}_i$ is a column of $\overline{P}$ denoting one eigenvector. Theoretically $(A-\lambda I)$ is singular. However, its singularity depends on the value of λ. Therefore once $\overline{P}$ is known an evaluation must take place to ensure a reflection of the surface is not represented.

$$\overline{P} = \det\{\overline{P}\} = +1.0000.$$

Having solved for the eigenvalues and eigenvectors it is now possible to express the surface in terms of:

$$\hat{X}^T B\hat{X} + C\overline{P}\hat{X} + (K) = 0 \tag{IV.20}$$

Recall $K = 1$ and $\hat{X} = \overline{P}^T X$.

The classification of the best fitting surface is now possible. The eigenvalues are checked for sign and magnitude. Here an ellipsoid is found to be the best fitting surface.

APPENDIX V

SURFACE FITTING OF A PARABOLOID

BY CONSTRAINING THE PARABOLOIDAL FUNCTION

APPENDIX V

SURFACE FITTING OF A PARABOLOID BY CONSTRAINING THE PARABOLOIDAL FUNCTION

As an alternative method of fitting data to a surface, knowledge about the surface a-priori is used in the adjustment. It is known that the reflector represents a circular paraboloid which, in its standard form would be defined by the equation:

$$(X')^2 + (Y')^2 = 4f(Z') \qquad (V.1)$$

where f = focal length of the paraboloid.

However, since this surface is measured at an arbitrary angle and position in space it is necessary to incorporate into this equation rotation and translation components. This is done with the following transformation equations:

$$\begin{aligned} X' &= \ell_1 (x-x_o) + m_1 (y-y_o) + n_1 (z-z_o) \\ Y' &= \ell_2 (x-x_o) + m_2 (y-y_o) + n_2 (z-z_o) \\ Z' &= \ell_3 (x-x_o) + m_3 (y-y_o) + n_3 (z-z_o) \end{aligned} \qquad (V.2)$$

where

- X', Y', Z' : are coordinates for the paraboloid in standard form
- x, y, z : are observed coordinates
- x_o, y_o, z_o : are translation components
- ℓ_i, m_i, n_i : are direction cosines describing rotation angles

Equation (V.1) is expanded to become:

$$F(X',Y',Z') = [\ell_1 (x-x_o) + m_1 (y-y_o) + n_1 (z-z_o)]^2 + [\ell_2 (x-x_o) + m_2 (y-y_o) + n_2 (z-z_o)]^2 - 4f [\ell_3 (x-x_o) + m_3 (y-y_o) + n_3 (z-z_o)] = 0 \quad (V.3)$$

This equation can be greatly simplified by selecting an appropriate axis system for the paraboloid in its standard form. Assuming the X'-axis is parallel to the x-axis then:

$$\ell_1 = 1$$

$$m_1 = 0$$

$$n_1 = 0$$

$$\ell_2 = 0$$

$$\ell_3 = 0$$

Therefore the mathematical model used in the adjustment becomes:

$$V_i = (x_i-x_o)^2 + [m_2 (y_i-y_o) + n_2 (z_i-z_o)]^2 - 4f [m_3 (y_i-y_o) + n_3 (z_i-z_o)] \quad (V.4)$$

The number of unknowns is reduced to 8. Considering the combined adjustment solution described in Appendix IV the solution here is similar except for the following partial derivatives:

$$A_{i,1} = \frac{\partial F}{\partial m_2} = 2[m_2(y-y_o) + n_2(Z-Z_o)]\ (y-y_o)$$

$$A_{i,2} = \frac{\partial F}{\partial n_2} = 2[m_2(y-y_o) + n_2(z-z_o)]\ (z-z_o)$$

$$A_{i,3} = \frac{\partial F}{\partial m_3} = -4f(y-y_o)$$

$$A_{i,4} = \frac{\partial F}{\partial n_3} = -4f(z-z_o)$$

$$A_{i,5} = \frac{\partial F}{\partial x_o} = -2(x-x_o)$$

$$A_{i,6} = \frac{\partial F}{\partial y_o} = 2[m_2(y-y_o) + n_2\ (z-z_o)]\ (-m_2) + 4fm_3$$

$$A_{i,7} = \frac{\partial F}{\partial z_o} = 2[m_2(y-y_o) + n_2(z-z_o)]\ (-n_2) + 4fn3$$

$$A_{i,8} = \frac{\partial F}{\partial f} = -4[m_3(y-y_o) + n_3\ (z-z_o)]$$

$$B_{i,3i-2} = \frac{\partial F}{\partial x} = 2(x-x_o)$$

$$B_{i,3i-1} = \frac{\partial F}{\partial y} = 2[m_2(y-y_o) + n_2\ (z-z_o)]\ (m_2)\ -4fm_3$$

$$B_{i,3i} = \frac{\partial F}{\partial z} = 2[m_2(y-y_o) + n_2\ (z-z_o)]\ (n_2)\ -4fn_3$$

APPENDIX VI

COMPARISON OF X, Y AND Z COORDINATES

COMPARISON OF X,Y AND Z COORDINATES AS DETERMINED USING UNBASC2, GEBAT-V AND DLT WITH DATA SNOOPING

	(UNBASC2)			(GEBAT-V - UNBASC2)			(DLTSNP - UNBASC2)		
POINT	X (MM)	Y (MM)	Z (MM)	DX (MM)	DY (MM)	DZ (MM)	DX (MM)	DY (MM)	DZ (MM)
1	1492.35	3295.35	1073.38	0.03	0.00	-0.14	0.23	-0.04	-0.42
2	1491.97	3262.43	1110.95	0.04	-0.02	-0.19	0.15	0.15	-0.10
3	1492.79	3231.84	1151.00	0.05	-0.02	-0.22	0.10	-0.09	-0.43
4	1494.59	3202.76	1192.00	0.06	-0.02	-0.23	0.12	-0.07	-0.57
5	1497.86	3176.06	1234.22	0.07	-0.02	-0.25	-0.01	-0.30	-0.53
6	1501.99	3151.66	1277.81	0.07	-0.00	-0.24	-0.07	-0.09	-0.76
7	1507.36	3129.97	1322.41	0.07	0.02	-0.26	-0.30	-0.16	-0.22
8	1530.11	3615.83	841.38	0.21	0.21	-0.02	0.15	0.13	0.00
9	1527.92	3569.34	859.87	0.15	0.20	0.01	0.08	0.03	0.25
10	1526.78	3524.38	881.58	0.09	0.18	-0.01	0.05	0.18	0.33
11	1527.20	3480.58	905.95	0.04	0.15	-0.02	0.21	-0.03	-0.24
12	1528.47	3437.40	931.09	0.00	0.10	-0.03	0.07	-0.11	-0.01
13	1531.21	3395.70	959.52	-0.02	0.06	-0.04	0.18	-0.12	-0.33
14	1535.03	3355.43	989.66	-0.03	0.01	-0.06	0.21	0.09	-0.15
15	1536.74	3314.21	1026.16	-0.03	-0.03	-0.09	0.14	-0.18	-0.31
16	1536.84	3279.16	1061.67	-0.02	-0.06	-0.12	0.09	-0.17	0.01
17	1537.63	3245.85	1099.36	-0.01	-0.08	-0.15	0.04	-0.16	-0.08
18	1539.68	3214.77	1138.87	0.01	-0.08	-0.17	0.10	-0.02	-0.27
19	1542.40	3185.65	1179.48	0.02	-0.08	-0.18	0.13	0.02	-0.55
20	1546.17	3155.87	1227.99	0.04	-0.07	-0.18	0.05	0.02	-0.59
21	1548.65	3132.04	1272.00	0.05	-0.05	-0.18	-0.12	-0.22	-0.61
22	1552.50	3111.19	1317.29	0.06	-0.02	-0.19	-0.02	-0.18	-0.53
23	1556.88	3092.00	1363.02	0.08	0.01	-0.16	-0.09	-0.13	-0.36
24	1583.85	3645.02	809.49	0.16	0.21	-0.03	0.17	0.14	0.14
25	1580.64	3598.19	826.75	0.00	0.01	-0.00	0.18	-0.04	0.54
26	1578.47	3552.06	846.54	0.04	0.20	-0.02	0.17	0.04	-0.26
27	1576.89	3506.93	868.27	-0.01	0.16	-0.02	0.07	0.03	0.47
28	1576.97	3463.70	892.90	-0.05	0.12	-0.01	0.18	0.02	0.11
29	1577.73	3420.60	919.48	0.00	-0.01	0.00	0.07	0.13	-0.04
30	1579.28	3379.29	948.39	-0.09	0.01	-0.03	0.20	-0.01	0.23
31	1581.89	3339.90	979.10	-0.09	-0.04	-0.05	0.15	-0.10	0.11
32	1585.32	3301.87	1011.63	-0.08	-0.09	-0.07	0.04	-0.31	-0.10
33	1589.97	3265.60	1045.76	-0.07	-0.12	-0.08	0.14	-0.07	-0.07
34	1587.47	3233.83	1083.78	-0.00	-0.00	-0.00	0.13	0.07	0.33
35	1587.76	3203.18	1123.66	-0.03	-0.14	-0.13	0.06	-0.08	-0.19
36	1589.16	3174.45	1164.67	-0.00	-0.14	-0.13	-0.05	0.00	-0.22
37	1591.60	3148.22	1206.89	0.02	-0.12	-0.14	-0.05	-0.14	-0.40
38	1594.96	3123.89	1250.70	0.03	-0.10	-0.12	-0.12	-0.11	-0.02
39	1598.73	3101.23	1295.70	-0.01	-0.01	0.00	-0.24	0.24	-0.66
40	1604.01	3082.17	1341.24	0.06	-0.03	-0.09	0.62	-0.12	-0.16
41	1606.20	3067.97	1382.32	0.07	0.01	-0.06	0.13	-0.21	0.11
42	1639.42	3672.41	784.50	0.12	0.22	-0.07	0.06	0.17	0.26
43	1635.99	3624.33	799.41	0.05	0.23	-0.07	0.27	0.16	0.12
44	1633.35	3577.36	817.73	-0.01	0.22	-0.07	0.17	-0.03	0.44
45	1631.65	3531.68	837.70	-0.06	0.19	-0.06	0.15	-0.08	-0.13
46	1630.42	3486.49	860.40	-0.09	0.14	-0.03	0.31	-0.01	-0.11
47	1630.15	3443.08	885.43	-0.12	0.09	-0.03	0.07	-0.26	0.26
48	1630.66	3400.67	912.51	-0.14	0.02	-0.03	0.04	-0.22	0.00
49	1631.99	3359.61	941.15	-0.13	-0.05	-0.05	0.05	-0.24	0.07
50	1634.20	3320.23	972.33	-0.13	-0.11	-0.06	0.15	-0.08	0.15

COMPARISON OF X,Y AND Z COORDINATES AS DETERMINED USING UNBASC2, GEBAT-V AND DLT WITH DATA SNOOPING

	(UNBASC2)			(GEBAT-V - UNBASC2)			(DLTSNP - UNBASC2)		
POINT	X (MM)	Y (MM)	Z (MM)	DX (MM)	DY (MM)	DZ (MM)	DX (MM)	DY (MM)	DZ (MM)
51	1637.18	3282.72	1005.66	-0.11	-0.15	-0.07	0.19	-0.16	-0.46
52	1640.96	3247.19	1040.67	-0.09	-0.18	-0.08	0.11	-0.01	-0.08
53	1640.91	3214.37	1080.66	-0.06	-0.20	-0.09	0.11	0.02	-0.14
54	1641.81	3184.18	1120.65	-0.03	-0.19	-0.10	0.04	-0.06	-0.30
55	1643.53	3156.09	1162.06	-0.01	-0.18	-0.09	0.02	-0.07	-0.29
56	1645.93	3130.04	1204.72	0.01	-0.16	-0.09	0.06	-0.06	-0.28
57	1649.05	3106.31	1248.75	0.02	-0.13	-0.07	0.02	-0.07	-0.35
58	1652.17	3085.25	1293.73	0.04	-0.09	-0.06	-0.01	0.12	-0.21
59	1656.34	3066.07	1339.88	0.05	-0.06	-0.04	-0.07	-0.08	-0.54
60	1661.35	3049.75	1386.79	0.07	-0.01	-0.01	-0.04	0.02	-0.34
61	1699.46	3708.07	760.91	0.10	0.21	-0.11	0.24	0.21	0.01
62	1696.39	3659.75	773.06	0.04	0.24	-0.12	0.18	0.19	0.29
63	1693.82	3612.13	788.77	-0.01	0.24	-0.13	0.18	0.04	-0.18
64	1691.54	3565.24	806.05	-0.07	0.22	-0.12	0.10	0.02	0.39
65	1689.61	3519.25	826.73	-0.11	0.18	-0.10	0.06	-0.08	0.49
66	1687.88	3474.46	849.85	-0.14	0.12	-0.09	0.06	-0.07	0.11
67	1686.65	3430.77	874.32	-0.16	0.06	-0.06	0.04	-0.13	0.40
68	1686.14	3388.70	902.03	-0.16	-0.02	-0.03	0.15	-0.19	-0.16
69	1685.93	3347.74	931.51	-0.16	-0.10	-0.05	0.08	-0.16	-0.36
70	1686.72	3308.54	963.56	-0.14	-0.16	-0.06	0.09	-0.12	0.10
71	1688.45	3271.67	997.07	-0.11	-0.20	-0.07	0.09	-0.02	-0.08
72	1690.74	3236.47	1032.99	-0.08	-0.23	-0.08	0.09	-0.23	-0.31
73	1693.89	3203.71	1070.65	-0.06	-0.24	-0.08	0.02	-0.08	-0.29
74	1697.68	3173.46	1110.60	-0.03	-0.23	-0.07	0.01	-0.08	-0.09
75	1702.03	3145.05	1151.68	-0.01	-0.22	-0.06	-0.02	-0.12	-0.17
76	1706.52	3118.12	1196.25	0.00	-0.19	-0.05	-0.10	-0.07	-0.14
77	1708.22	3095.00	1241.15	0.02	-0.16	-0.02	-0.01	0.01	-0.25
78	1710.07	3073.81	1285.85	0.04	-0.12	-0.01	0.06	-0.05	-0.39
79	1712.65	3055.31	1333.09	0.05	-0.07	0.02	-0.14	-0.09	-0.38
80	1715.99	3039.04	1379.46	0.06	-0.02	0.05	-0.02	-0.03	-0.21
81	1745.62	3684.29	758.39	0.04	0.24	-0.17	0.24	0.25	-0.10
82	1743.14	3636.12	771.85	-0.01	0.25	-0.18	0.17	0.05	-0.07
83	1741.48	3588.66	787.90	0.00	-0.01	0.00	-0.05	0.04	0.09
84	1739.86	3542.27	806.68	-0.10	0.21	-0.18	0.12	-0.16	-0.15
85	1738.94	3496.57	827.87	-0.14	0.16	-0.14	0.07	-0.30	-0.21
86	1738.13	3451.49	851.43	-0.17	0.09	-0.10	0.17	-0.08	-0.11
87	1737.61	3408.05	877.11	-0.17	0.01	-0.07	0.21	-0.09	-0.36
88	1737.79	3366.10	904.61	-0.17	-0.08	-0.04	0.11	-0.06	-0.39
89	1738.67	3326.15	934.91	-0.15	-0.15	-0.06	0.21	-0.16	-0.47
90	1740.06	3287.65	967.19	-0.12	-0.22	-0.08	0.09	-0.14	0.07
91	1741.93	3251.14	1001.99	-0.09	-0.25	-0.09	-0.14	-0.03	0.20
92	1744.74	3216.96	1039.03	-0.06	-0.26	-0.06	0.04	-0.09	-0.08
93	1747.77	3184.99	1077.62	0.00	0.00	0.00	-0.15	-0.25	-0.39
94	1751.23	3155.67	1118.16	-0.02	-0.25	-0.04	-0.03	-0.14	-0.22
95	1755.06	3128.52	1160.74	-0.01	-0.22	-0.02	0.15	0.12	-0.33
96	1759.42	3103.63	1204.38	0.01	-0.19	-0.01	0.12	0.12	-0.15
97	1763.59	3079.39	1251.65	0.00	-0.01	0.00	-0.05	0.31	-0.09
98	1764.81	3059.52	1297.84	0.04	-0.11	0.03	-0.02	0.03	-0.31
99	1766.59	3042.07	1344.40	0.05	-0.06	0.06	-0.04	-0.00	-0.14
100	1768.58	3027.03	1392.16	0.06	-0.01	0.11	0.04	0.11	-0.18

COMPARISON OF X,Y AND Z COORDINATES AS DETERMINED USING UNBASC2, GEBAT-V AND DLT WITH DATA SNOOPING

	(UNBASC2)			(GEBAT-V - UNBASC2)			(DLTSNP - UNBASC2)		
POINT	X (MM)	Y (MM)	Z (MM)	DX (MM)	DY (MM)	DZ (MM)	DX (MM)	DY (MM)	DZ (MM)
101	1801.49	3729.07	741.68	0.05	0.21	-0.19	-0.02	0.24	0.39
102	1799.92	3680.19	753.32	0.01	0.25	-0.22	0.10	0.29	0.19
103	1798.62	3631.96	766.15	-0.03	0.25	-0.23	-0.12	-0.14	0.34
104	1797.32	3584.26	782.00	-0.07	0.24	-0.24	0.84	-0.77	6.63
105	1796.40	3537.97	801.27	-0.10	0.21	-0.23	0.08	-0.05	-0.06
106	1795.89	3491.97	821.56	-0.12	0.15	-0.19	0.05	-0.11	-0.16
107	1795.64	3447.25	844.98	-0.14	0.08	-0.13	0.01	-0.05	0.46
108	1795.66	3403.88	869.99	-0.15	-0.00	-0.09	0.03	-0.06	0.04
109	1795.93	3362.06	897.57	-0.00	-0.00	0.00	0.03	-0.13	-0.29
110	1796.64	3321.50	927.80	-0.13	-0.18	-0.05	-0.02	-0.08	0.15
111	1797.92	3283.18	961.17	-0.10	-0.24	-0.08	0.10	-0.18	-0.21
112	1799.26	3246.73	995.05	-0.07	-0.27	-0.08	-0.12	-0.13	0.16
113	1800.93	3213.00	1032.04	-0.05	-0.28	-0.06	-0.01	-0.01	0.05
114	1802.15	3181.05	1070.78	-0.03	-0.27	-0.05	0.02	-0.02	-0.21
115	1803.91	3151.83	1111.78	-0.02	-0.25	-0.03	-0.03	-0.01	-0.18
116	1805.43	3125.10	1154.35	-0.00	-0.22	-0.00	0.03	0.07	-0.40
117	1807.45	3100.64	1198.16	0.01	-0.19	0.01	0.05	-0.03	-0.37
118	1809.49	3078.06	1242.51	0.02	-0.16	0.02	-0.07	-0.05	-0.22
119	1811.94	3057.47	1288.76	0.03	-0.12	0.04	0.03	0.01	-0.34
120	1814.99	3039.72	1334.80	0.05	-0.07	0.08	0.11	0.12	-0.17
121	1852.41	3725.07	740.30	0.01	0.21	-0.20	0.04	0.14	0.53
122	1850.78	3676.23	751.32	-0.01	0.24	-0.25	0.02	0.02	0.09
123	1849.17	3627.90	764.31	-0.03	0.25	-0.28	-0.08	0.01	0.23
124	1848.30	3581.84	787.21	-0.06	0.22	-0.27	0.08	-0.08	0.30
125	1848.04	3515.71	806.82	-0.08	0.18	-0.26	0.01	-0.12	0.30
126	1848.17	3470.14	828.91	-0.10	0.11	-0.22	-0.02	-0.14	-0.30
127	1848.25	3425.80	852.13	-0.10	0.03	-0.15	-0.03	-0.14	0.33
128	1848.74	3383.33	878.83	-0.11	-0.05	-0.08	-0.20	-0.19	0.40
129	1848.92	3341.98	907.61	-0.10	-0.13	-0.04	-0.06	-0.20	-0.22
130	1849.53	3302.51	939.12	-0.09	-0.20	-0.06	-0.10	-0.13	-0.10
131	1850.36	3265.34	972.93	-0.00	-0.00	-0.00	0.03	-0.10	0.10
132	1850.93	3230.52	1008.76	-0.05	-0.27	-0.06	-0.02	-0.17	-0.32
133	1852.03	3196.97	1046.07	-0.04	-0.27	-0.06	0.00	0.05	-0.43
134	1852.75	3166.21	1086.02	-0.02	-0.25	-0.03	0.15	-0.01	-0.36
135	1853.54	3138.00	1127.26	-0.01	-0.23	-0.01	0.10	-0.05	-0.37
136	1854.72	3112.13	1170.34	-0.00	-0.21	0.00	-0.07	-0.08	-0.21
137	1855.86	3088.95	1214.87	0.01	-0.18	0.02	0.12	0.02	-0.49
138	1856.89	3067.56	1260.13	0.02	-0.13	0.06	-0.19	0.05	-0.01
139	1854.36	3045.52	1313.12	0.03	-0.09	0.08	0.01	0.17	-0.29
140	1852.23	3029.21	1360.48	0.05	-0.04	0.11	0.26	0.13	-0.07
141	1902.41	3721.28	740.94	-0.00	0.20	-0.23	-0.13	0.20	0.61
142	1902.53	3672.25	751.87	-0.02	0.23	-0.25	-0.05	0.15	0.06
143	1902.78	3623.73	765.34	-0.02	0.24	-0.29	0.02	0.08	0.07
144	1903.07	3576.13	781.38	-0.03	0.22	-0.30	-0.03	-0.05	0.16
145	1903.47	3529.72	800.68	-0.04	0.18	-0.27	-0.12	-0.15	0.13
146	1904.15	3483.82	821.68	-0.04	0.12	-0.25	-0.00	-0.02	-0.01
147	1904.53	3439.18	844.82	-0.04	0.04	-0.19	-0.08	-0.15	0.36
148	1905.23	3396.11	870.46	-0.04	-0.04	-0.12	-0.03	-0.16	-0.07
149	1905.66	3354.66	898.33	-0.05	-0.12	-0.06	-0.11	-0.23	-0.20
150	1906.46	3314.22	928.90	-0.06	-0.18	-0.03	-0.07	-0.13	-0.11

COMPARISON OF X,Y AND Z COORDINATES AS DETERMINED USING UNBASC2, GEBAT-V AND DLT WITH DATA SNOOPING

	(UNBASC2)			(GEBAT-V - UNBASC2)			(DLTSNP - UNBASC2)		
POINT	X (MM)	Y (MM)	Z (MM)	DX (MM)	DY (MM)	DZ (MM)	DX (MM)	DY (MM)	DZ (MM)
151	1906.90	3276.39	961.96	-0.06	-0.23	-0.05	0.02	-0.12	-0.26
152	1907.19	3240.45	996.85	-0.05	-0.25	-0.07	-0.21	-0.12	-0.01
153	1907.79	3206.52	1033.84	-0.05	-0.25	-0.05	-0.06	0.04	-0.20
154	1908.01	3174.93	1073.73	-0.03	-0.24	-0.03	-0.06	-0.03	0.15
155	1908.87	3146.26	1114.71	-0.02	-0.22	-0.00	0.03	-0.04	-0.22
156	1909.17	3119.39	1157.20	-0.01	-0.20	0.02	-0.01	-0.08	-0.15
157	1910.12	3095.18	1201.37	-0.00	-0.16	0.04	0.04	0.00	-0.23
158	1910.73	3073.26	1246.31	0.01	-0.13	0.06	0.06	0.04	-0.52
159	1911.20	3053.54	1292.64	0.03	-0.09	0.09	0.13	0.19	-0.58
160	1911.74	3035.87	1339.37	0.04	-0.04	0.13	0.07	-0.03	-0.33
161	1950.22	3657.21	757.90	-0.02	0.22	-0.27	-0.08	-0.05	0.32
162	1951.48	3609.40	772.73	-0.02	0.22	-0.28	-0.04	-0.10	0.05
163	1952.74	3561.87	790.10	-0.00	-0.01	0.00	-0.13	0.06	-0.16
164	1953.79	3515.85	809.65	-0.01	0.14	-0.27	-0.19	-0.14	0.53
165	1954.88	3470.40	831.23	-0.00	0.08	-0.21	-0.20	-0.07	0.21
166	1955.86	3425.98	855.67	0.00	-0.01	-0.16	-0.11	-0.21	0.25
167	1956.53	3383.44	881.80	-0.01	-0.09	-0.09	-0.16	-0.15	0.16
168	1956.93	3342.40	911.25	-0.02	-0.16	-0.05	-0.10	-0.14	-0.12
169	1957.16	3302.96	942.07	-0.04	-0.21	-0.05	-0.16	-0.16	0.23
170	1959.50	3255.98	985.54	-0.06	-0.25	-0.04	-0.20	-0.06	0.16
171	1961.29	3221.52	1021.92	-0.06	-0.23	-0.01	-0.12	0.02	0.13
172	1962.43	3189.56	1060.50	0.00	-0.00	-0.00	-0.17	0.17	0.38
173	1963.60	3159.88	1100.73	-0.04	-0.20	0.03	-0.24	-0.16	0.11
174	1964.49	3132.38	1142.77	-0.03	-0.18	0.04	-0.07	0.06	-0.24
175	1965.61	3107.27	1186.12	-0.02	-0.15	0.07	0.00	0.06	-0.40
176	1966.15	3084.53	1231.07	-0.00	0.00	-0.00	0.11	-0.11	-0.04
177	1966.92	3063.57	1276.31	0.01	-0.07	0.10	0.10	0.18	-0.34
178	1967.27	3045.58	1323.39	0.02	-0.03	0.14	0.12	0.19	-0.07
179	1967.37	3028.92	1371.07	0.04	0.02	0.17	0.28	-0.05	-0.07
180	1967.77	3015.74	1418.68	0.10	0.05	0.19	0.07	-0.00	0.12
181	2000.51	3701.41	752.32	-0.05	0.18	-0.23	0.04	0.16	0.25
182	2004.37	3652.92	764.80	-0.03	0.19	-0.25	-0.19	0.01	0.39
183	2007.90	3605.36	780.49	-0.01	0.18	-0.26	-0.01	0.05	-0.15
184	2011.30	3558.58	798.20	0.01	0.15	-0.24	-0.00	-0.14	-0.08
185	2014.16	3512.74	819.32	0.02	0.11	-0.22	-0.12	-0.16	0.22
186	2016.83	3467.69	841.51	0.03	0.04	-0.18	-0.08	-0.12	0.24
187	2019.01	3423.84	866.08	0.02	-0.03	-0.11	-0.10	-0.10	0.28
188	2020.47	3381.60	893.26	-0.00	-0.01	0.00	-0.03	0.10	-0.22
189	2021.34	3341.23	922.65	-0.01	-0.17	-0.06	-0.08	-0.12	-0.10
190	2022.13	3302.24	954.90	-0.04	-0.21	-0.03	-0.14	-0.10	0.04
191	2022.49	3265.19	989.16	-0.06	-0.22	-0.01	-0.11	-0.10	0.08
192	2021.56	3229.29	1026.34	-0.07	-0.21	0.04	-0.32	0.03	0.37
193	2024.52	3197.44	1064.60	-0.07	-0.19	0.06	-0.16	-0.09	-0.09
194	2027.42	3167.70	1104.97	-0.06	-0.17	0.08	-0.15	-0.08	-0.02
195	2029.62	3140.35	1147.03	-0.05	-0.14	0.09	0.03	-0.01	-0.58
196	2031.05	3115.12	1190.32	-0.04	-0.11	0.10	-0.06	0.15	0.14
197	2032.02	3092.26	1235.05	-0.03	-0.07	0.12	-0.29	-0.07	0.32
198	2032.48	3071.09	1280.38	-0.01	-0.03	0.14	-0.13	0.05	0.25
199	2033.03	3053.23	1326.92	0.03	0.00	0.11	0.18	0.22	-0.04
200	2032.45	3036.87	1374.78	0.06	0.05	0.14	0.12	0.02	0.13

COMPARISON OF X,Y AND Z COORDINATES AS DETERMINED USING UNBASC2, GEBAT-V AND DLT WITH DATA SNOOPING

	(UNBASC2)			(GEBAT-V - UNBASC2)			(DLTSNP - UNBASC2)		
POINT	X (MM)	Y (MM)	Z (MM)	DX (MM)	DY (MM)	DZ (MM)	DX (MM)	DY (MM)	DZ (MM)
201	2073.78	3697.14	766.51	-0.09	0.14	-0.19	0.12	0.26	-0.16
202	2078.67	3648.97	779.71	-0.06	0.15	-0.21	-0.06	0.04	0.24
203	2083.16	3601.80	796.41	-0.03	0.14	-0.21	-0.04	0.17	0.05
204	2087.10	3555.63	815.45	-0.01	0.11	-0.19	-0.00	-0.13	-0.17
205	2090.31	3510.05	836.69	0.01	0.07	-0.16	-0.19	-0.04	0.22
206	2092.91	3465.47	860.21	0.01	0.01	-0.11	-0.08	-0.15	0.19
207	2094.91	3422.36	886.03	0.01	-0.05	-0.10	-0.12	-0.15	-0.12
208	2096.10	3380.70	913.39	-0.00	-0.11	-0.05	-0.26	-0.08	0.05
209	2096.44	3341.04	943.64	-0.03	-0.15	-0.02	-0.16	-0.01	0.19
210	2096.18	3301.47	976.70	-0.05	-0.17	0.00	-0.26	-0.06	0.12
211	2095.88	3265.12	1011.88	-0.06	-0.18	0.04	-0.11	-0.06	-0.07
212	2094.75	3230.84	1048.33	-0.07	-0.18	0.07	-0.27	-0.11	0.09
213	2093.13	3198.74	1086.78	-0.08	-0.15	0.09	-0.21	-0.06	-0.07
214	2091.68	3168.08	1128.35	-0.08	-0.13	0.11	-0.13	0.14	-0.16
215	2091.51	3141.03	1170.51	-0.07	-0.09	0.12	-0.12	0.09	-0.08
216	2090.55	3115.69	1214.60	-0.05	-0.05	0.13	-0.03	0.07	0.02
217	2089.10	3093.18	1259.50	-0.04	-0.01	0.13	-0.24	0.18	0.23
218	2086.87	3072.86	1305.34	-0.03	0.04	0.18	-0.34	0.01	0.51
219	2085.01	3055.16	1352.11	0.03	0.06	0.12	0.10	0.10	0.18
220	2082.36	3039.31	1399.24	0.07	0.11	0.15	0.47	0.41	0.23
221	2135.34	3674.84	788.03	-0.12	0.11	-0.17	0.16	0.25	0.10
222	2141.08	3627.48	804.51	-0.09	0.12	-0.17	0.03	0.03	-0.18
223	2146.40	3580.81	822.57	0.00	0.01	-0.00	-0.11	0.05	0.37
224	2150.66	3535.38	843.61	-0.03	0.07	-0.16	0.03	0.15	-0.06
225	2154.43	3491.10	866.23	-0.02	0.03	-0.12	-0.03	-0.19	-0.12
226	2157.03	3447.29	891.73	-0.02	-0.01	-0.08	-0.07	0.07	0.38
227	2159.08	3405.41	919.58	-0.02	-0.06	-0.06	-0.01	-0.03	0.06
228	2160.51	3365.25	948.83	-0.04	-0.10	-0.02	-0.23	-0.09	0.03
229	2161.07	3326.46	980.98	-0.06	-0.12	0.00	-0.04	0.06	-0.01
230	2160.73	3289.28	1015.23	-0.07	-0.14	0.02	-0.11	-0.13	-0.01
231	2159.49	3248.38	1057.23	-0.08	-0.13	0.06	-0.20	0.02	-0.10
232	2160.04	3216.95	1096.22	-0.09	-0.11	0.06	-0.25	0.02	0.22
233	2160.00	3186.67	1136.06	-0.10	-0.08	0.11	-0.02	0.20	0.17
234	2159.09	3158.80	1177.34	-0.09	-0.06	0.10	-0.08	-0.10	-0.06
235	2157.05	3132.99	1220.43	-0.09	-0.02	0.12	-0.35	-0.15	0.56
236	2154.24	3110.16	1265.44	0.21	-0.05	-0.23	0.25	-0.13	-0.29
237	2151.31	3088.68	1309.92	-0.02	0.06	0.09	0.01	-0.29	0.03
238	2146.62	3070.52	1356.15	0.01	0.11	0.11	0.14	-0.09	0.13
239	2190.68	3649.34	813.98	-0.17	0.09	-0.14	0.07	0.19	-0.00
240	2196.28	3602.82	832.19	-0.13	0.09	-0.12	-0.08	0.11	0.29
241	2203.51	3549.04	857.62	-0.10	0.06	-0.12	0.01	0.12	0.14
242	2207.83	3504.80	880.74	-0.07	0.04	-0.10	0.07	-0.04	-0.45
243	2211.46	3461.62	906.14	-0.07	0.00	-0.09	0.03	0.04	-0.39
244	2214.19	3419.91	933.70	-0.00	0.00	-0.00	-0.03	0.06	0.27
245	2216.14	3379.10	963.15	-0.07	-0.06	-0.03	-0.28	0.02	0.10
246	2216.98	3340.56	995.79	-0.08	-0.08	-0.01	-0.12	-0.13	0.15
247	2216.83	3303.46	1029.84	-0.09	-0.09	0.01	-0.26	-0.14	0.13
248	2216.13	3268.30	1065.86	-0.11	-0.09	0.04	-0.30	-0.06	0.32
249	2215.75	3235.78	1104.05	-0.00	0.01	-0.01	0.18	-0.10	-0.06
250	2214.64	3204.95	1144.54	-0.11	-0.04	0.06	0.01	-0.01	-0.02

COMPARISON OF X,Y AND Z COORDINATES AS DETERMINED USING UNBASC2, GEBAT-V AND DLT WITH DATA SNOOPING

	(UNBASC2)			(GEBAT-V - UNBASC2)			(DLTSNP - UNBASC2)		
POINT	X (MM)	Y (MM)	Z (MM)	DX (MM)	DY (MM)	DZ (MM)	DX (MM)	DY (MM)	DZ (MM)
251	2212.43	3176.42	1185.41	-0.11	-0.01	0.08	-0.15	0.06	0.19
252	2209.09	3150.30	1228.65	-0.10	0.02	0.09	0.04	-0.11	-0.11
253	2204.59	3125.95	1272.47	-0.05	0.06	0.02	-0.20	-0.25	0.17
254	2200.30	3104.54	1316.10	-0.03	0.10	0.05	0.19	-0.02	0.15
255	2193.66	3084.41	1362.70	0.01	0.00	0.00	-0.22	0.01	-0.08
256	2252.78	3604.01	856.38	-0.21	0.07	-0.10	0.10	0.16	-0.11
257	2257.70	3558.82	877.97	-0.18	0.06	-0.11	0.02	0.07	0.07
258	2262.18	3514.56	901.04	-0.15	0.04	-0.08	-0.06	-0.03	-0.17
259	2265.23	3471.82	927.24	-0.13	0.02	-0.09	0.05	-0.04	-0.15
260	2267.30	3429.81	955.21	-0.13	-0.00	-0.07	-0.14	-0.18	0.12
261	2278.85	3383.73	996.15	-0.14	-0.02	-0.04	-0.31	0.01	0.25
262	2279.30	3345.80	1029.09	-0.13	-0.03	-0.05	0.07	0.07	-0.07
263	2278.28	3308.95	1063.36	-0.14	-0.03	-0.03	-0.14	-0.22	0.24
264	2276.38	3274.48	1099.62	-0.14	-0.02	-0.00	-0.04	-0.10	-0.12
265	2274.73	3240.03	1141.01	-0.14	-0.00	0.00	0.08	-0.02	-0.09
266	2274.02	3210.72	1181.85	-0.14	0.03	0.01	-0.13	0.14	0.50
267	2271.79	3183.58	1223.88	-0.09	0.05	-0.08	0.13	0.17	0.15
268	2268.21	3158.62	1266.88	-0.06	0.09	-0.08	0.23	0.13	0.19
269	2264.10	3135.12	1311.61	0.00	0.00	0.01	-0.03	-0.02	-0.01
270	2305.10	3547.09	908.30	-0.24	0.05	-0.11	0.08	0.15	-0.05
271	2312.83	3505.51	935.00	-0.23	0.04	-0.10	-0.04	0.10	-0.34
272	2319.45	3464.79	964.00	-0.21	0.04	-0.09	-0.04	0.05	0.02
273	2325.03	3425.60	994.32	-0.20	0.03	-0.09	-0.14	-0.07	0.27
274	2329.01	3387.38	1026.74	-0.20	0.02	-0.08	-0.22	0.13	0.08
275	2331.27	3350.65	1061.82	-0.19	0.02	-0.07	0.02	0.16	-0.01
276	2332.29	3315.99	1097.38	-0.19	0.03	-0.07	0.07	0.03	0.09
277	2331.97	3283.13	1135.06	-0.13	0.04	-0.18	0.06	0.05	0.03
278	2329.74	3251.47	1174.28	-0.12	0.07	-0.17	-0.09	-0.07	0.11
279	2326.54	3221.91	1215.59	-0.10	0.09	-0.18	0.12	-0.07	0.11
280	2359.06	3456.26	996.44	-0.27	0.05	-0.11	0.09	0.18	0.21
281	2364.06	3416.60	1030.16	-0.26	0.05	-0.12	0.01	0.05	-0.37
282	2367.43	3379.87	1064.15	-0.25	0.06	-0.10	-0.07	0.00	0.09
283	2370.05	3344.91	1099.98	-0.17	0.07	-0.25	0.13	-0.01	-0.09
284	2370.89	3311.23	1137.05	-0.17	0.08	-0.25	0.13	0.15	0.08
285	1368.91	3445.02	1029.98	0.01	0.01	-0.00	-0.17	-0.12	-0.23
286	1368.59	3407.38	1063.31	0.32	0.19	-0.21	-0.02	0.15	-0.26
287	1368.82	3370.72	1097.27	0.29	0.18	-0.26	-0.11	0.09	-0.15
288	1370.24	3335.37	1133.19	0.26	0.17	-0.30	-0.00	0.08	-0.48
289	1418.78	3528.06	941.38	0.34	0.20	-0.06	-0.01	0.16	0.07
290	1416.06	3485.90	968.01	0.29	0.19	-0.08	0.17	0.14	-0.24
291	1414.42	3444.96	996.61	0.25	0.17	-0.09	-0.01	0.03	-0.14
292	1414.48	3405.07	1027.11	0.21	0.15	-0.14	0.02	0.15	-0.04
293	1415.43	3366.74	1059.80	0.19	0.13	-0.16	0.00	0.13	-0.20
294	1417.93	3330.29	1094.20	0.17	0.11	-0.21	0.02	-0.03	-0.40
295	1422.25	3295.09	1129.97	0.15	0.09	-0.24	-0.05	-0.02	-0.43
296	1427.67	3261.91	1167.09	0.14	0.07	-0.27	-0.04	0.00	-0.53
297	1434.67	3230.83	1205.55	0.13	0.06	-0.31	-0.10	0.03	-0.41
298	1443.08	3201.84	1245.43	0.12	0.06	-0.32	-0.16	0.02	-0.27
299	1452.88	3174.62	1286.74	0.11	0.06	-0.33	-0.17	-0.14	-0.35
300	1483.08	3609.89	865.03	0.00	0.01	-0.00	0.00	-0.01	0.35

COMPARISON OF X,Y AND Z COORDINATES AS DETERMINED USING UNBASC2, GEBAT-V AND DLT WITH DATA SNOOPING

	(UNBASC2)			(GEBAT-V - UNBASC2)			(DLTSNP - UNBASC2)		
POINT	X (MM)	Y (MM)	Z (MM)	DX (MM)	DY (MM)	DZ (MM)	DX (MM)	DY (MM)	DZ (MM)
301	1479.40	3564.35	886.60	0.24	0.20	-0.01	-0.06	0.07	0.55
302	1476.97	3519.70	909.45	0.19	0.18	-0.01	-0.02	0.14	0.35
303	1475.97	3476.51	934.75	0.14	0.16	-0.01	0.16	0.06	0.05
304	1476.11	3434.28	962.31	0.10	0.13	-0.05	0.09	0.01	-0.32
305	1477.57	3393.47	992.03	0.07	0.09	-0.06	0.09	0.04	-0.18
306	1480.18	3354.24	1023.46	0.06	0.06	-0.10	0.21	-0.01	-0.40
307	1562.02	3659.52	812.88	0.23	0.20	-0.00	-0.01	0.21	0.57
308	1952.77	3728.65	741.11	-0.03	0.18	-0.22	0.01	0.21	0.27
309	2342.80	3502.49	955.55	-0.00	0.00	-0.00	-0.06	0.01	0.22
310	2354.15	3260.60	1185.58	-0.20	0.10	-0.08	0.10	0.22	0.23
311	2302.06	3178.33	1264.08	-0.14	0.12	0.01	0.30	0.01	0.07
312	1918.52	3008.15	1437.29	0.11	0.04	0.19	0.11	-0.15	-0.03
314	1818.28	3010.64	1435.75	0.11	0.00	0.16	0.02	-0.18	-0.12
316	1817.78	3020.66	1397.49	0.10	-0.03	0.12	-0.03	0.00	-0.13
317	1393.47	3259.87	1205.80	0.19	0.12	-0.36	-0.26	0.01	-0.13
400	1180.04	2596.74	1150.32	2.38	0.31	0.59	0.73	-1.26	1.00
402	1200.90	3195.38	1159.01	0.87	0.16	0.02	0.11	-0.92	-1.09
405	1229.08	3929.10	1136.84	1.60	0.33	-0.71	-2.59	3.26	-1.14
406	1242.97	4224.40	1138.13	2.24	-0.40	-1.15	-4.21	7.54	-0.55
407	1335.37	4463.23	1298.11	-7.25	1.81	-19.52	-4.83	0.98	-12.43
409	1692.17	4034.08	680.19	0.79	-0.90	1.12	-0.05	1.20	0.50
410	1991.90	4036.53	672.18	-0.03	-1.02	1.12	0.55	1.62	-0.13
411	2291.33	4039.05	664.27	-1.10	-1.57	1.63	0.71	1.32	0.09
412	2518.11	4369.12	1114.39	-1.08	-1.47	-2.20	6.19	9.81	-3.55
413	2527.09	4074.90	1118.53	-0.94	-0.21	-0.48	4.24	5.25	-1.66
414	2532.70	3877.60	1120.95	-0.74	0.16	-0.73	2.93	2.70	-1.80
415	2534.40	3794.08	1144.89	-0.60	0.30	-0.92	2.57	2.44	-1.14
416	2541.68	3496.53	1146.59	-0.57	0.17	-0.78	1.27	0.43	-0.45
417	2549.05	3196.61	1146.89	-0.99	0.05	-0.01	0.29	-0.56	-0.08
418	2555.45	2896.54	1147.69	-1.52	0.31	0.99	-0.64	-0.63	0.65
419	2560.86	2597.10	1147.62	-1.87	0.86	2.31	-0.87	-0.27	2.33

REFERENCES

Abdel-Aziz, Y.I. (1973). "Lens Distortion and Close Range". Photogrammetric Engineering. Vol. 39, No. 6, pp. 611-615.

Abdel-Aziz, Y.I. (1974). "Expected Accuracy of Convergent Photos". Photogrammetric Engineering and Remote Sensing. Vol. 40, No. 7, pp.1341-1346.

Abdel-Aziz, Y.I. (1978). "Applications of Photogrammetric Techniques of Building Construction". Photogrammetric Engineering and Remote Sensing, Vol. 45, No. 2, 1979.

Abdel-Aziz, Y.I. (1982). "The Accuracy of Control Points for Close Range Photogrammetry". International Archives of Photogrammetry, Vol. 24, Part V/1, 1982.

Abdel-Aziz, Y.I. and Karara, H.M. (1971). "Direct Linear Transformation from Comparator Coordinates into Object Space Coordinates in Close-Range Photogrammetry". Proceedings of the ASP/UI Symposium on Close-Range Photogrammetry, Urbana, Illinois, 1971.

Abdel-Aziz, Y.I. and Karara, H.M. (1973). "Photogrammetric Potential of Non-Metric Cameras". Civil Engineering Studies, Photogrammetric Series No. 36, University of Illinois, Urbana, Illinois, U.S.A., 1973.

Ackermann, F., Ebner, H. and Klein, H. (1973). "Block Triangulation with Independent Models". Photogrammetric Engineering, Vol. 39, No. 8, pp. 967-981.

Adams, L.P. (1981). "The Use of Non-Metric Cameras in Short-Range Photogrammetry". Photogrammetria, 36 (1981), pp. 51-60.

American Society of Photogrammetry (1980). Manual of Photogrammetry, Published by the American Society of Photogrammetry, Falls Church, Va., 4th edition.

American Society of Photogrammetry (1985). Close-Range Photogrammetry and Surveying: State-of-the-Art, Published by the American Society of Photogrammetry, Falls Church, Va.

Anderson, L.J. and Groth, L.H. (1963). "Reflector Surface Deviations in Large Parabolic Antennas". IEEE Transactions on Antennas and Propagation, Vol. AP-II, No. 2, March 1963. pp. 148-152.

Armenakis, C., (1983). "Subsidence Determination by Aerial Photogrammetry". Technical Report No. 93, Department of Surveying Engineering, University of New Brunswick.

Armenakis, C. and Faig, W. (1986). "On-Line Data Acquisition for Multi-Temporal Photography Using the Analytical Plotter OMI AP-2C, Proceedings of the XXIV International Congress of the International Society of Photogrammetry. Rio de Janeiro, Commission V., Vol. XXVI-V, June, 1986.

Arsenault, T. (1982). "Computer Program Library User's Guide." Technical Report No. 86, Department of Surveying Engineering, University of New Brunswick.

Atkinson, K.B. (Ed.) (1980). "Developments in Close-Range Photogrammetry". Applied Science Publishers Ltd., London.

Ayeni, O.O. (1982). "Phototriangulation: A Review and Bibliography". Photogrammetric Engineering and Remote Sensing. Vol. 48, No. 11, November 1982, pp. 1733-1759.

Barnard, W.E. (1983). "Accuracy Improvement in Close-Range Non-Metric Photogrammetry Through the Use of Multiple Exposure Photography". Undergraduate Technical Report, Division of Surveying Engineering, University of Calgary, Calgary, Alberta, Canada.

Bennett, J.C., Anderson, A.P., McInnes, P.A. and Whitaker, A.J.T. (1976). "Microwave Holographic Metrology of Large Reflector Antennas". IEEE Transactions on Antennas and Propagation, Vol. AP-24, No. 3, May, 1976, pp. 295-303.

Blachut, T.J., Chrzanowski, A. and Saastamoinen, J.H. (1979). Urban Surveying and Mapping, Springer-Verlag, New York, U.S.A.

Bopp, H. and Krauss, H. (1977). "A Simple and Rapidly Converging Orientation and Calibration Method for Non-Topographic Applications". Proceedings of the American Society of Photogrammetry Fall Technical Meeting, 1977, pp. 425-432.

Bopp, H. and Krauss, H. (1978). "An Orientation and Calibration Method for Non-Topographic Applications". Photogrammetric Engineering and Remote Sensing". Vol. 44, No. 9, pp. 1191-1196.

Bopp, H., Krauss, H. and Preuss, H.D. (1977). "Photogrammetric Control Survey of a Large Cooling Tower". Proceedings of the American Society of Photogrammetry Fall Technical Meeting, 1977, pp. 433-439.

Brown, D.C. (1971). "Close Range Camera Calibration". Photogrammetric Engineering. Vol. 37, No. 8, pp. 855-866.

Brown, D.C. (1982). "STARS, A Turnkey System for Close-Range Photogrammetry". International Archives of Photogrammetry, Vol. 24, Part V/1; pp. 68-89.

Brown, D.C. (1985). "Adaptation of the Bundle Method for Triangulation of Observations made by Digital Theodolites". Proceedings of the Conference of Southern African Surveyors, 1985, Paper No. 43, 18 pages.

Chen, Liang-Chien (1985). "A Selection Scheme for Non-Metric Close-Range Photogrammetric Systems". Ph.D. Dissertation, Department of Civil Engineering, University of Illinois at Urbana-Champaign.

Chrzanowski, A. (1974-1977). "Preanalysis and Design of Surveying Projects". Northpoint (Journal of the Survey Technicians and Technologists of Ontario), Vol. 11, 1974; Vol. 12, 1975; Vol. 13, 1976; Vol. 14, 1977.

Chrzanowski, A. (1977). "Design and Error Analysis of Surveying Projects", Lecture Notes No. 47, University of New Brunswick, 1977.

Cooper, M.A.R. (1982). 2nd Ed. Modern Theodolites and Levels. Granada Publishing Limited, London.

Daniel, C. and Wood, F. (1980). Fitting Equations to Data, John Wiley, New York.

De Vengoechea, F.P. (1965). "Radar Antenna Calibration Using Half-Base Convergent Photogrammetry", Photogrammetric Engineering, Vol. 31, No. 1, pp. 91-95.

Elghazali, M.S. and Hasson, M.M. (1986). "Performance of Surface Fitting Algorithms Using Fictitious Double Fourier Data". Presented Paper Proceedings of 1986 ASPRS-ACSM Fall Convention. Anchorage, Alaska, September 28 - October 3, 1986.

El-Hakim, S.F. (1979). "Potentials and Limitations of Photogrammetry for Precision Surveying". Ph.D. Dissertation, Department of Surveying Engineering, University of New Brunswick, Fredericton, New Brunswick, Canada.

El-Hakim, S.F. (1982). The General Bundle Adjustment Triangulation (GEBAT) System - Theory and Applications. Photogrammetric Research, National Research Council of Canada. 47 pages.

El-Hakim, S.F. (1984). "Precision Photogrammetry for Microwave Antenna Manufacturing", Presented Paper Proceedings of the XXV International Congress of the International Society of Photogrammetry. Ottawa, Commission V.

El-Hakim, S.F. (1986). "A Real-Time System for Object Measurement with CCD Cameras". Proceedings of the Symposium Real-Time Photogrammetry - A New Challenge, Vol. 26, Part 5, Ottawa, Canada, June 1986, pp. 465-472.

El-Hakim, S.F. and Faig, W. (1977). "Compensation of Systematic Image Errors using Spherical Harmonics", Proceedings of the American Society of Photogrammetry Fall Technical Meeting, Little Rock, 1977.

El-Hakim, S.F. and Faig, W. (1981). "A Combined Adjustment of Geodetic and Photogrammetric Observations". Photogrammetric Engineering and Remote Sensing, Vol. 47, No. 1, pp. 93-99.

El-Hakim, S.F. and Ziemann, H. (1984). "A Step-by-Step Strategy for Gross-Error Detection", Photogrammetric Engineering and Remote Sensing, Vol. 50, No. 6, pp. 713-718.

El-Hakim, S.F., Moniwa, H. and Faig, W. (1979). "Analytical and Semi-Analytical Photogrammetric Programs - Theory and User's Manual". Technical Report No. 64, Department of Surveying Engineering, University of New Brunswick.

Erlandson, J.P. and Veress, S.A. (1975). "Monitoring Deformations of Structures". Photogrammetric Engineering and Remote Sensing, Vol. 41, No. 11, pp. 1375-1384.

Faig, W. (1972A). "Design, Construction and Geodetic Coordination of Close-Range Photogrammetric Test Field", Civil Engineering Studies, Photogrammetric Series No. 32. University of Illinois, Urbana, Illinois, U.S.A., 1972.

Faig, W. (1972B). "Single Camera Approaches in Close-Range Photogrammetry". Proceedings of the 38th Annual Meeting of the American Society of Photogrammetry, Washington, D.C., pp. 1-8.

Faig, W. (1975). "Calibration of Close-Range Photogrammetric System Mathematical Formulation". XIII Congress of the International Society for Photogrammetry, Commission V, Helsinki, 1976, also published in Photogrammetric Engineering and Remote Sensing, Vol. 41, No. 12, pp. 1479-1486.

Faig, W., (1976A). "Aerotriangulation". Lecture Notes No. 40, Department of Surveying Engineering, University of New Brunswick.

Faig, W. (1976B). "Photogrammetric Potentials of Non-Metric Cameras". Photogrammetric Engineering and Remote Sensing, Vol. 42, No. 1, pp. 47-49.

Faig, W. (1981). Close-Range Precision Photogrammetry for Industrial Purposes". Photogrammetria. Vol. 36 (1981), pp. 183-191.

Faig, W., (1984). "Aerial Triangulation and Adjustment". Workshop Notes, School of Surveying, University of New South Wales.

Faig, W. (1987). Ch. 6 - Non-Metric and Semi-Metric Cameras: Data Reduction, Handbook of Non-Topographic Photogrammetry, (In Press). American Society of Photogrammetry, Falls Church, Va., 2nd edition.

Faig, W. and El-Hakim, S.F. (1982). "The Use of Distances as Object Space Control in Close-Range Photogrammetry". International Archives of Photogrammetry, Vol. 24, Part V/1, York.

Faig, W. and Moniwa, H. (1973). "Convergent Photos for Close Range". Photogrammetric Engineering and Remote Sensing, Vol. 40, pp. 605-610.

Faig, W. and Shih, T.Y. (1986). "Critical Configuration of Object Space Control for the Direct Linear Transformation". International Archives of Photogrammetry and Remote Sensing, Vol 26, Part 5, pp. 23-29.

Feedback Weather Satelite Receiver WSR513 Instruction Manual, Vol. 3, S-Band Adaptor W5R515, Feedback Instruments Limited, Crowborough, England, 1984.

Fiedler, T., Petrovic, S., Lapaine, M. and Jandric-Sare, M. (1986). "Computer Aided Modelling of a Complex 3-D Object" Proceedings of the Symposium Real-Time Photogrammetry - A New Challenge, Vol. 26, Part 5, Ottawa, Canada, June 1986, pp. 465-472.

Forrest, R.B. (1966). "Radio Reflector Calibration", Photogrammetric Engineering. Vol. 32, No. 1, pp. 109-112.

Fraser, C.S. (1980). "Multiple Focal Length Setting Self-Calibration of Close-Range Metric Cameras", Photogrammetric Engineering and Remote Sensing. Vol. 46, No. 9., pp. 1161-1171.

Fraser, C.S. (1981). "Accuracy Aspects of Multiple Focal Length Setting Self-Calibration Applied to Non-Metric Cameras". Photogrammetria. Vol. 36 (1981), pp. 121-132.

Fraser, C.S. (1982A). "On the Use of Non-Metric Cameras in Analytical Photogrammetry". The Canadian Surveyor, Vol. 36, No. 3, pp. 259-279.

Fraser, C.S. (1982B). "Optimization of Precision in Close-Range Photogrammetry. Photogrammetric Engineering and Remote Sensing, Vol. 48, No. 4, pp. 561-570.

Fraser, C.S. (1984). "Network Design Considerations for Non-Topographic Photogrammetry", Photogrammetric Engineering and Remote Sensing. Vol. 50, No. 8, August 1984, pp. 1115-1126.

Fraser, C.S. (1986). "Microwave Antenna Measurement". Photogrammetric Engineering and Remote Sensing. Vol. 50, No. 10. October 1986, pp. 1627-1635.

Fraser, C.S. (1987). "Limiting Error Propagation in Network Design". Photogrammetric Engineering and Remote Sensing. Vol. 53, No. 5, May 1987, pp. 487-493.

Fuchs, H. and Leberl H. (1984). "Universal Analytical Plotter Software for Photographs with Perspective Geometry (CRISP)". International Archives of Photogrammetry and Remote Sensing. Vol. 25, A5, pp. 308-314.

Ghosh, S.K. (1975). Phototriangulation. Lexington Books, D.C. Heath and Company.

Goslee, J.W., Hinson, W.F. and Kennefick, J.F. (1984). "Measurement of Electrostatically Formed Antennas using Photogrammetry and Theodolites". Technical Papers 1984 ACSM-ASPRS Annual Convention, Vol. 3, pp. 424-433.

Gottwald, R. and Berner, W. (1987). "The New KERN 'System for Positioning and Automated Coordinate Evaluation' - Advanced Technology for Automated 3-D Coordinate Determination". Technical Papers 1987 ACSM-ASPRS Annual Convention, Vol. 3, pp. 260-266.

Grafarend, E. (1974) "Optimization of Geodetic Networks", Boll. Geod. Sci. Aff. 33 (1974), pp. 351-406.

Gustafson, P.C. and Brown, J.D. (1985). "Interactive Photogrammetric Design on a Microcomputer". Presented Paper, ACSM-ASP Annual Convention, Washington, D.C.

Karara, H.M. (1972). "Simple Cameras for Close-Range Applications". Photogrammetric Engineering. Vol. 38, No. 5, May, 1972, pp. 447-451.

Karara, H.M. (1975). "Industrial Photogrammetry". Proceedings of the 1975 Symposium on Close-Range Photogrammetric Systems, ASP, Champaign, Illinois, July 28 - August 1, 1975, pp. 97-141.

Karara, H.M. (Ed.), (1979). Handbook of Non-Topographic Photogrammetry, American Society of Photogrammetry, Falls Church, Va., U.S.A.

Karara, H.M. and Abdel-Aziz, Y.I. (1974). "Accuracy Aspects of Non-Metric Imageries". Photogrammetric Engineering. Vol. 40, No. 9, 1974, pp. 1107-1117.

Kenefick, J.F. (1977). "Applications of Photogrammetry in Shipbuilding". Photogrammetric Engineering and Remote Sensing. Vol. 43, No. 9, September, 1977, pp. 1169-1175.

Krolikowsky, M. (1986). "The Utlization of Computer Graphics in Close-Range Photogrammetry". M.Sc.E. Thesis, Department of Surveying Engineering, University of New Brunswick.

Kruck, E. (1984). "BINGO: A Program for Bundle Adjustment for Engineering Applications, Possibilities, Facilities and Practical Results". International Archives of Photogrammetry. Vol. 25, A5, pp. 471-480.

Lardelli, A. (1984). ECDS1 - An Electronic Coordinate Determination System for Industrial Applications, Aarau, Kern and Co., Ltd.

Larsson, R. (1983). Simultaneous Photogrammetric and Geodetic Adjustment. - Algorithms and Data Structures. Department of Photogrammetry, Royal Institute of Technology, Stockholm, 99 pages.

Love, A.W. (1976). "Some Highlights of Reflector Antenna Development" Radio Science, Vol. 11, No. 8, pp. 671-684. Aug-Sep. 1976.

MacRitchie, S.C. (1977). "Object Space Control and the Direct Linear Transformation Model". M.Sc.E. Thesis, Department of Surveying Engineering, University of New Brunswick, Fredericton, New Brunswick, Canada.

Marks, G.W. (1963). "Geometric Calibration of Antennas by Photogrammetry". Photogrammetric Engineering, Vol. 29, No. 4, pp. 589-593.

Marzan, G.T. and Karara, H.M. (1975). "A Computer Program for Direct Linear Transformation Solution of the Collinearity Condition and Some Applications of It". Proceedings of the Symposium on Close-Range Photogrammetric Systems. American Society of Photogrammetry, Falls Church, Virginia, pp. 420-476.

Mayer, C.E., Davis, J.H., Peters, W.L. and Vogel, W.J. (1983). "A Holographic Surface Measurement of the Texas 4.9 m. Antenna at 86 GHz". IEEE Transactions on Instrumentation and Measurement. Vol. IM-32, No. 1, March 1983, pp. 102-109.

Methley, B.D.F. (1986). Computational Models in Surveying and Photogrammetry. Blackie & Son, Ltd., Glasgow, Great Britain.

Meyer, R. (1973)."The Present State in Industrial Photogrammetry", Surveying News, No. 17, 1973.

Mikhail, E.M. and Gracie, G. (1981). Analysis and Adjustment of Survey Measurements, Van Nostrand Reinhold Company, New York, U.S.A.

Milliken, G.A. (1979). "Photogrammetric Evaluation of Spherical Tank Component Deformations". M.Eng. Report, Department of Surveying Engineering, University of New Brunswick, Fredericton, New Brunswick, Canada.

Mohammed-Karim, M. (1981). "Diagrammatic Approach to Solve Least-Squares Adjustment and Collocation Problems". Technical Report No. 83. Department of Surveying Engineering, University of New Brunswick, Fredericton, New Brunswick, Canada.

Moniwa, H. (1972). "Analytical Camera Calibration for Close-Range Photogrammetry". M.Sc.E. Thesis, Department of Surveying Engineering, University of New Brunswick, Fredericton, New Brunswick, Canada.

Moniwa, H. (1977). "Analytical Photogrammetric System with Self-Calibration and its Applications". Ph.D. Dissertation, Department of Surveying Engineering, University of New Brunswick, Fredericton, New Brunswick, Canada.

Moniwa, H. (1981). "The Concept of "Photo-Variant" Self-Calibration and its Application in Block Adjustments with Bundles". Photogrammetria. Vol. 36 (1981), pp. 11-29.

Murai, S., Matsuoka, R. and Okuda, T. (1984). "A Standard on Analytical Calibration for Non-Metric Camera and Accuracy of Three Dimensional Measurement". International Archives of Photogrammetry and Remote Sensing, 25 (A5), pp. 570-579.

Nickerson, B.G. (1978). "A-Priori Estimation of Variance for Surveying Observables". Technical Report No. 57. Department of Surveying Engineering, University of New Brunswick. Fredericton, New Brunswick, Canada.

Ni-Chuiv, N. (1979). "Differential Geometry for Surveying Engineers". Department of Mathematics and Statistics Lecture Notes No. 5, 2nd ed., University of New Brunswick, Fredericton, New Brunswick, Canada.

Ockert, D.L. (1959). "A Photogrammetric Radio Telescope Calibration". Photogrammetric Engineering; Vol. 25, No. 3, pp. 386-395.

Oderinlo, C.O. (1980). "A More Economical and Efficient Approach to Analytical Aerial Triangulation with Self-Calibration". M.Sc.E. Thesis, Department of Surveying Engineering, University of New Brunswick, Fredericton, New Brunswick, Canada.

Oldfield, S. (1985). "Photogrammetric Determination of the Form of a 10 m Diameter Radio Antenna". International Archives of Photogrammetry and Remote Sensing, Vol. XXV, Part A-5, pp. 590-594.

Oren, W., Pushor, R. and Ruland, R. (1987). "Incorporation of the Kern ECDS-PC Software into A Project Oriented Software Environment". Technical Papers 1987 ACSM-ASPRS Annual Convention, Vol. 3, pp. 88-94.

Paiva, J.V.R. (1987). "Understanding Electronic Theodolites and Tacheometers". Technical Papers 1987 ACSM-ASPRS Annual Convention, Vol. 3, pp. 267-277.

Papo, H. (1982). "Free Net Analysis in Close-Range Photogrammetry". Photogrammetric Engineering and Remote Sensing, Vol. 48, No. 4, pp. 571-576.

Parekh, Sharad (1980). "On the Solution of Best Fit Paraboloid as Applied to Shape Dual Reflector Antennas". IEEE Transactions on Antennas and Propagation, Vol. AP-28, No. 4, July 1980. pp. 560-562.

Pope, A.J. (1972). "Some Pitfalls to be Avoided in the Iterative Adjustment of Non-Linear Problems". Proceedings of the 38th Annual Meeting of ASP, Washington, D.C., March, 1972. pp. 449-477.

Pope, A.J. (1976). "The Statistics of Residuals and the Detection of Outliers". NOOA Technical Report NOS 65 NGS1, Rockville, Md., May, 1976.

Rahmat-Samii, Y. (1979). "Useful Coordinate Transformations for Antenna Applications". IEEE Transactions on Antennas and Propagation, Vol. AP-27, No. 4, July 1979. pp. 571-574.

Reedijk, W.H.C. (1985). "The Implementation of Close-Range Photogrammetry for the Determination of the Spatial Coordinates of a Football Helmet". Undergraduate Technical Report I, No. 506, Department of Surveying Engineering, University of New Brunswick, Fredericton, New Brunswick, Canada.

Ruze, J. (1966). "Antenna Tolerance Theory - A Review, Proceedings of the IEEE, Vol. 54, No. 4, April, 1966, pp. 633-640.

SAS/GRAPH User's Guide, Version 5 Edition, SAS Institute Inc., Cary, North Carolina, 1985.

Shaffer, D.B. (1986). "Holographic Measurements of Surface Distortions in Reflector Antennas". Presented Paper Proceedings of the Deformations Measurements Workshop PEDS II. ACSM, MIT, Boston, Massachusetts, U.S.A., October 31 - November 1, 1986.

Trinder, J.C. (1972). "Systematic Errors in Pointing Observations". Photogrammetria, Vol. 28, No. 2, 1972, pp. 61-70.

Vanicek, P. and Krakiwsky, E.J. (1982) Geodesy: The Concepts, North-Holland Publishing Company, Amsterdam, Holland.

Wester-Ebbinghaus, W. (1985). "Bundeltriangulation mit gemeinsamer Ausgleichung photogrammetrischer and geodatischer Beobachtungen. Zeitschrift fur Vermessungswesen, 110/3; pp. 101-111.

Wolf, P.R. (1983). Elements of Photogrammetry, McGraw-Hill Book Company, New York, U.S.A., 2nd edition.

Wong, K.W. and Elphingstone, G. (1972). "Aerotriangulation by SAPGO". Photogrammetric Engineering. Vol. 38, No. 8, pp. 779-790.

Wright, J.S. (1978). Radio Aids Theory. (Hydrography II Course Notes). Canadian Hydrographic Service. Department of Fisheries and Oceans, Ottawa, Ontario.

Zarghamee, M.S. (1967). "On Antenna Tolerance Theory". IEEE Transactions on Antennas and Propagation, Vol. AP-15, No. 6, November, 1967. pp. 777-781.

Zhou, G. and Roberts, T. (1987). "Camera Calibration for Kern E2-S Automatic Theodolite". Technical Papers 1987 ACSM-ASPRS Annual Convention, Vol. 3, pp. 278-286.